NATIONAL TECHNICAL UNIVERSITY OF ATHENS
Faculty of Civil Engineering
Institute of Steel Structures

Bending behavior of concrete slabs with cast – in channels

MSC THESIS

Evangelos G. Zafeiratos

Supervisors: Ioannis Vayias, Panagiotis Spyridis

Athens, October 2021

EMK ME 2021/07

Ζαφειράτος Ε. Γ. (2021).
Μελέτη της συμπεριφοράς πλακών σκυροδέματος με εγκιβωτισμένα μεταλλικά κανάλια
Διπλωματική Εργασία ΕΜΚ ΜΕ 2021/07
Εργαστήριο Μεταλλικών Κατασκευών, Εθνικό Μετσόβιο Πολυτεχνείο, Αθήνα.

Zafeiratos E. G. (2011).
Behavior of concrete slabs with cast – in channels
Diploma Thesis EMK ME 2021/07
Institute of Steel Structures, National Technical University of Athens, Greece

Contents

NATIONAL TECHNICAL UNIVERSITY OF ATHENS
FACULTY OF CIVIL ENGINEERING
INSTITUTE OF STEEL STRUCTURES

MSC THESIS
EMK ME 2021/07

Behavior of concrete slabs with cast – in channels

Zafeiratos E. G. (Supervisors: Vayias I., Spyridis P.)

Abstract

Cast-in channels are an efficient and easy way to install adjustable connections to hang heavy loads in tunnels, buildings, bridges and other structures. These steel parts collaborate with concrete with the use of shear bolts, forming a composite section. Except from supporting heavy loads, cast-in channels can increase the bending capacity of the section.

In this study, using the theory of composite structures, the possible positive effects in the bending behavior of the section will be investigated for many types of steel sections, the effective width that is achieved depending on the shear connection used will be defined and other parameters about the influence of these parameters on the behavior of the section will be examined.

The investigation will examine the problem analytically using the knowledge for the behavior of composite sections from EC-4 and computationally with finite element analysis. Different steel sections will be checked for concrete height of 300mm and bolt distances. The hanging loads will be the weights of typical equipment and structures, such as jetfans in a road tunnel or glass panels in skyscrapers.

At the end, there will be a comparison of the different approaches, presentation of the results and suggestions of how they can be used in the design of future projects. The conclusions include:

- Evaluation of the increase of the bending capacity of reinforced concrete sections due to the presence of the steel parts
- Assessment of the ideal section depending on the hanging loads of the design
- Assessment of the ideal distance and section of the shear bolts depending on the used composite section and the hanging load
- Results from the parametrical analysis of the uses of different parts, different shear connections and different effective axial force.

From the results we can highlight the rise of the bending capacity of the concrete section because of the cast – in channels, the relief of the steel reinforcement because of the existence of the channels, the statement that part of the reinforcement can be replaced from these steel parts and the suggestion of setting a lower limit of the effective width of the composite section equal to 1m.

ΕΘΝΙΚΟ ΜΕΤΣΟΒΙΟ ΠΟΛΥΤΕΧΕΝΙΟ
ΣΧΟΛΗ ΠΟΛΙΤΙΚΩΝ ΜΗΧΑΝΙΚΩΝ
ΕΓΑΣΤΗΡΙΟ ΜΕΤΑΛΛΙΚΩΝ ΚΑΤΑΣΚΕΥΩΝ

ΜΕΤΑΠΤΥΧΙΑΚΗ ΕΡΓΑΣΙΑ
ΕΜΚ ΔΕ 2011/04

Μελέτη της συμπεριφοράς πλακών σκυροδέματος με εγκιβωτισμένα μεταλλικά κανάλια

Ζαφειράτος Ε. Γ. (Επιβλέποντες: Βάγιας Ι., Σπυρίδης Π.)

Περίληψη

Τα εγκιβωτισμένα μεταλλικά κανάλια είναι ένας εύκολος και αξιόπιστος τρόπος για την εγκατάσταση των πρόσθετων προσωρινών κατασκευών που απαιτούνται σε διάφορα έργα όπως σήραγγες, γέφυρες, κτίρια και άλλα. Τα συγκεκριμένα μεταλλικά κανάλια συνεργάζονται με το σκυρόδεμα με διατμητική σύνδεση με τη χρήση διατμητικών ήλων, διαμορφώνοντας μια σύμμικτη διατομή. Εκτός από την υποστήριξη των πρόσθετων κατασκευών, τα μεταλλικά στοιχεία αυξάνουν και την καμπτική αντοχή της διατομής.

Σε αυτή την εργασία, γίνεται χρήση της θεωρίας των σύμμικτων διατομών και μελετώνται τα πιθανά οφέλη της χρήσης αυτών των μεταλλικών στοιχείων, εξετάζεται το συνεργαζόμενο πλάτος που μπορεί να επιτευχθεί με βάση την επιλεγόμενη διατμητική σύνδεση, ενώ διερευνώνται και άλλες παράμετροι της συμπεριφοράς της διατομής.

Η έρευνα εξετάζει το πρόβλημα αναλυτικά χρησιμοποιώντας γνώσεις τις διατάξεις του Ευρωκώδικα 4 και υπολογιστικά με χρήση αναλύσεων με πεπερασμένα στοιχεία. Μελετώνται διαφορετικές μεταλλικές διατομές για ύψος διατομής 300μμ και διαφορετικές αποστάσεις διατμητικών ήλων. Τα φορτία που ασκούνται αντιπροσωπεύουν τα πιθανά φορτία που μπορεί να ασκηθούν σε μία συνήθη κατασκευή.

Στο τέλος της εργασίας, γίνεται σύγκριση των διαφορετικών προσεγγίσεων και αναλύσεων και γίνονται προτάσεις για το πως θα μπορούσαν να χρησιμοποιηθούν τα συγκεκριμένα κανάλια στη μελέτη των δομικών έργων. Τα αποτελέσματα περιλαμβάνουν:

- Εκτίμηση της αύξησης της καμπτικής αντοχής της διατομής οπλισμένου σκυροδέματος με την παρουσία των μεταλλικών στοιχείων.
- Άξιολόγηση του κατάλληλης διατομής ανάλογα με τα φορτία που ασκούνται
- Αξιολόγηση της κατάλληλης απόστασης και διατομής των διατμητικών ήλων
- Παρουσίαση αποτελεσμάτων παραμετρικών αναλύσεων που αφορούν τη χρήση διαφορετικών μεταλλικών στοιχείων και διατομών, διαφορετικής διατμητικής σύνδεσης καθώς επίσης εξετάζεται και η επιρροή πιθανής δρώσας αξονικής στη διατομή.

Από τα αποτελέσματα, σημειώνεται η αύξηση που παρατηρείται στην καμπτική αντοχή της σύμμικτης διατομής λόγω της ύπαρξης των καναλιών, παρατηρείται ανακούφιση των τάσεων του χάλυβα οπλισμού, ενώ μέρος αυτού μπορεί να αντικατασταθεί από την αντίστοιχη διατομή καναλιού. Τέλος, με βάση τα αποτελέσματα, προτείνεται να τεθεί ένα κατώτατο όριο του συνεργαζόμενου πλάτους της σύμμικτης διατομής ίσο με 1m.

Ευχαριστίες

Με την ολοκλήρωση των μεταπτυχιακών μου σπουδών, κλείνει ένας ακόμη κύκλος για εμένα και ανοίγουν πολλοί άλλοι. Στη ζωή σημασία έχει η ισορροπία σε όλους τους τομείς αυτής. Η επιτυχία ενός ανθρώπου για μένα κρίνεται από την ευτυχία του στην καθημερινότητά του. Ευχαριστώ την οικογένεια μου για τον τρόπο που με έχει κάνει να διαχειρίζομαι τις διάφορες καταστάσεις που μπορεί να μου παρουσιαστούν όποιες και αν είναι οι συνθήκες. Ευχαριστώ τον πατέρα μου που υπήρξε ο μεγαλύτερος δάσκαλος στη ζωή μου. Τη μητέρα μου που μας έχει διδάξει τι σημαίνει να δίνεις στους άλλους ανθρώπους χωρίς να περιμένεις ανταπόδοση. Τον αδερφό μου και την κοπέλα μου για τον τρόπο που μου δημιουργούν ισορροπίες ο καθένας με το δικό του τρόπο. Ευχαριστώ τους φίλους μου για τη στήριξή τους στις επιλογές μου και τις διάφορες ιδέες που συναλλάσσουμε και εξελίσσουμε ο ένας τον άλλον σε όλους τους τομείς. Ευχαριστώ τους επιβλέποντες μου κ. Βάγια Ιωάννη και κύριο Σπυρίδη Παναγιώτη για την εξαιρετική συνεργασία και την υποστήριξη και την καθοδήγηση που μου προσέφεραν σε διάφορα τεχνικά θέματα και ευχαριστώ επίσης τους καθηγητές μου κατά τη διάρκεια των φοιτητικών μου χρόνων για τον τρόπο με τον οποίο προσπαθούν να μεταβιβάζουν τις γνώσεις τους και να μας κάνουν να αισθανόμαστε και να μελετούμε τη μηχανική και τη φύση αυτής. Εύχομαι ευτυχία σε όλους τους ανθρώπους. Όταν ο χρόνος τελειώνει, να συνεχίζεις να προσπαθείς.

Στη μνήμη του Γεράσιμου Ζαφειράτου

1 Introduction

1.1 Generally

Anchorages and fastenings are generally used in the field of structural engineering. Anchor is an element made of steel or malleable iron either cast into concrete or post – installed into a hardened concrete member and is used to transmit the applied loads to concrete. The words “anchor” and “fastening” are used synonymously.

Connecting building components is as old as building itself. Many ways have been suggested in order to control the job, depending on the case of the structure, the building material, the objects to be supported and many other factors.

Modern fastening technology is getting more and more important for civil engineers. New ideas occur and generally the field is in a state of flux. A huge number of anchors is installed every day all around the world so the behavior and the capability of each application must be fully understood from the user. In general, anchorages transfer applied tension and shear loads to the anchorage material through mechanical interlock, friction, bond or a combination of these mechanisms. Every fastening element is designed for optimal use for a specific application. If the fastening is intended to a situation for which it is not designed, its performance can be negatively affected.

There are many types of fastenings. The most used are presented on chapter 3 of this thesis. The study, provides a general overview on the types of fastenings that are used in the field of civil engineering. Afterwards it focuses on cast in channels, describes their uses and the mechanisms that are activated when they are loaded. Finally, the thesis analyzes their influence on the concrete slab on which they are installed and presents some negative and some positive aspects of their use.

1.2 Thesis structure

The thesis aims to investigate the behavior of cast in channels that are embedded in concrete slabs. This formation has many applications in many cases on the engineering field.

Chapter 1 is an introduction on the problem and gives a brief description of the methods used on the thesis to reach the desired results.

The second chapter is a brief reference to the fastening methods that are used on the civil engineering field, showing the types and the methods of fastening. In addition, the main failure modes are presented.

Chapter 3 makes a more specific approach on cast – in channels. The types of this way of fastening are presented, the advantages of it are highlighted and the special failure modes of cast – in channels are shown.

The next chapter is the theoretical approach of the problem with the theory of composite structures and references to the methods that are given in Eurocode 4 are adapted. The bending resistance of the composite sections, the cracking moment, the plastic zone, the shear connection and other features are calculated.

Chapter number 5, presents the modelling of the problem on the finite element analysis program Abaqus. The parts used on the analyses and the way that they were assembled is spotted. In addition, information is given about the materials used and about the meshing of the parts.

Chapter 6 is analyzing the results of the analyses and compares the different models on all the parametrical analyses that were enforced. The chapter begins with the elastic analyses and afterwards describes the influence of every steel part on the behavior of the composite

section, examines different cast – in channel profile section, analyzes the way that the friction on the interface between the cast – in channel and concrete can be simulated and evaluates the influence of the effective compressive axial force on the section.

The seventh chapter compares the theoretical with the computational analyses, presents the main results of the study and refers to ways on which this investigation could delve deeply.

The last chapter presents the bibliography used on this study on alphabetic order. Books, papers, articles, manuals, regulations and teaching notes are included.

2 Fastening Methods

2.1 Definition of anchoring methods

There are many different methods of fastening that are used on the structures. Here, a variety of them is presented, referring to their main characteristics. Their analysis and their behavior is analyzed in Eurocode 2 Part 4 and in the BSI 1992-4-1. [2], [8]

2.1.1 Cast in place systems

A variety of inserts are used for cast-in place installations. They can be found as inserts for the transportation of precast concrete components, anchor channels, embedded plates with nents, anchor channels, embedded plates with headed studs, bend reinforcing bars equipped with internally threaded unions, as well as custom components for hanging heavy facade panels and for securing mansory. These systems, transfer the external tension loads into the base material by means of mechanical interlock. Their positioning is depended on the reinforcement layout, so they must be placed in parallel. [20]

The advantage of these types is that the place of the applied external load is known and as a result, it can be accommodated smoothly in the design, by forming appropriate reinforcement arrangement. Their disadvantage lies in the extra layouts required and also in the possibility of wrong placement during construction. Lifting inserts are used for the transport of plain and reinforced concrete precast elements. Some types of them are presented on shapes 2.1, 2.2, 2.3, 2.4.

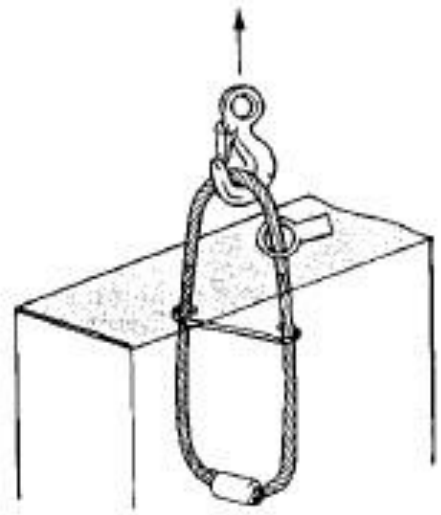

Shape 2.1: Cast – in cable loop for crane hook

Shape 2.2: Steel flatbar with “fishtail”

Shape 2.3: Round-headed transport anchor

Shape 2.4: Lifting tackle with remote release

Shape 2.5 shows the anchor channels. These channels consist of a cold formed or hot rolled steel channel equipped with special anchor fittings. These channels are attached inside of the formwork. After the concrete pouring and the removal of the formwork, a variety of components can be attached with the aid of special T- headed bolts. For this fastening type more details are presented on chapter 4. On shape 2.6 the headed stud anchorages are observed which consist of a steel plate with headed studs butt-welded on. Long headed studs can be produced by welding short studs together. Another cast in place system is presented in shape 2.7. The threaded sleeves consist of a tube with an internal thread which is anchored back into the concrete. They are distinguished into sockets for lifting eyes and sleeve anchor.

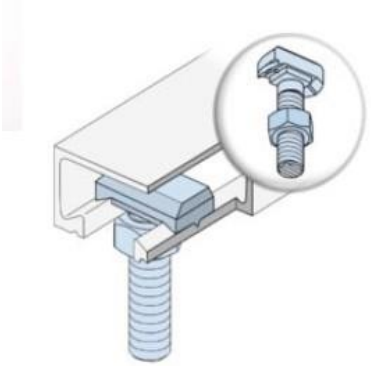

Shape 2.5: Cast – in channels with T – headed bolts installed

Shape 2.6: Steel embedded plate with welded headed studs

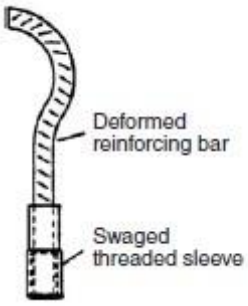

Shape 2.7: Hooked reinforcing bar with swaged threaded sleeve

2.1.2 Drilled – in systems

The advance of the technology of the drilled-in systems has contributed to the widespread use of post-installed anchors. Rotary-impact drills, diamond core drills and rock drills are used depending on the situation. The method of drilling is important, because many anchor systems are sensitive to deviations of the as-drilled hole diameter. National standards can be used to confirm drill bit suitability.

Variation exists also on the installation configuration. Pre-positioned installation, in-place installation and stand-off installation are used. These ways, differ on the drilled hole diameter, the sequence of the placement of the final anchor and on the final position of the anchor. Shape 2.8 shows the installation configurations of these methods. [20], [22]

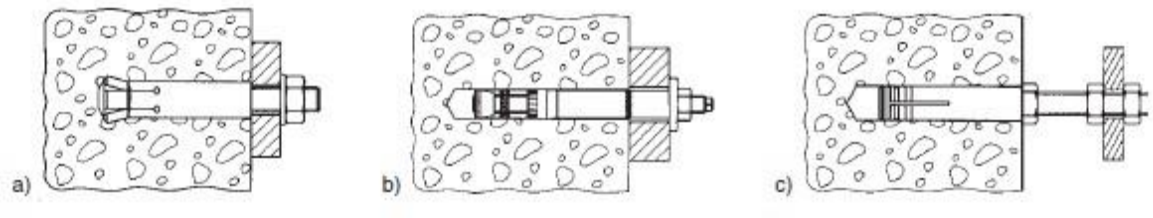

Shape 2.8: Anchor installation configurations with a) Pre-positioned installation b) In-place installation c) Stand-off installation

Drilled-in anchor types include mechanical expansion anchors which are divided into torque-controlled and displacement-controlled anchors. The installation of torque-controlled expansion anchors is achieved by drilling a hole, removing drilling dust and debris and securing it by applying a specified torque to the bolt head or nut with a torque wrench as shown on shape 2.9. Displacement-controlled expansion anchors usually consist of an expansion sleeve and a conical expansion plug, whereby the sleeve is internally threaded to accept a threaded element. They are set via the expansion of the sleeve as controlled by the axial displacement of the expansion plug within the sleeve. Shape 2.10 shows the installation of a common displacement-controlled anchor.

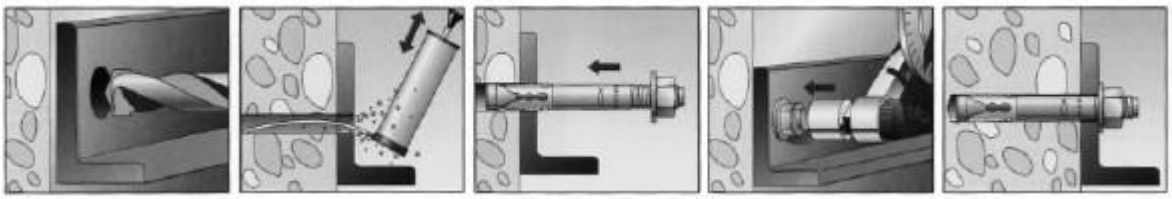

Shape 2.9: Installation of a torque-controlled stud-type expansion anchor

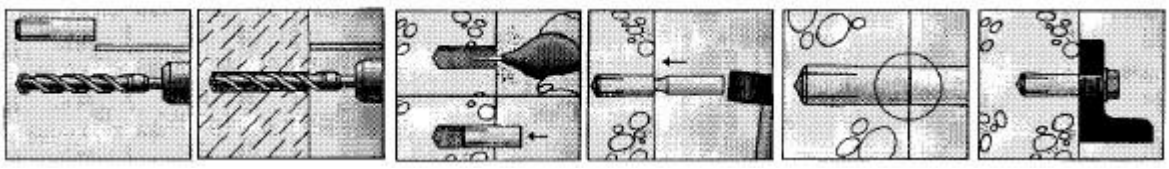

Shape 2.10: Installation of a displacement-controlled anchor

Another type of drilled-in anchors is undercut anchors. These anchors develop a mechanical interlock between anchor and base material. Shape 2.11 shows the installation

of an anchor of this type. Undercut anchors can appear in several forms. Other types of drilled-in anchors are bonded anchors, screw anchors, ceiling hangers and plastic anchors

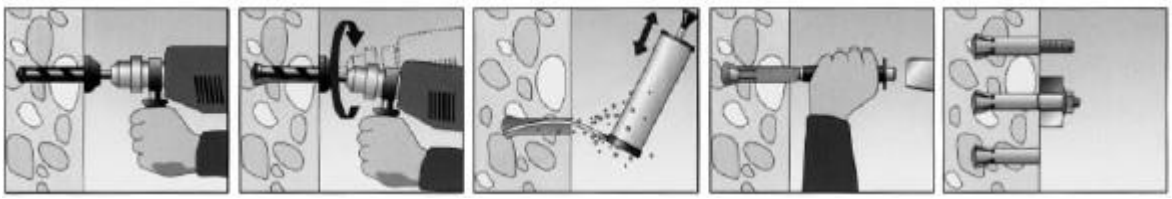

Shape 2.11: Installation of an undercut anchor

2.2 Design codes and loads to be carried

The design of fastenings is a specific task, for which many regulations provide an individual part. The European codes, Eurocodes, provide EN1992-4, Design of fastenings for use in concrete. The code refers to all the failure modes of paragraph 2.3 and analyzes the forces that cause each failure mode and the way of calculating the respective design capacity.

An anchorage system will be forced to carry axial, shear or bending loads as shown on a typical anchorage system in shape 2.12. The formation of the system must be appropriate in order to avoid the occurring of loads for which the system is not designed for. The transmission of these loads is accomplished with 3 mechanisms which are mechanical interlock, friction and bond as shown is shape 2.13. To be able to carry these forces some construction and design requirements must be checked. The following paragraph refers to the calculations required for a safe anchorage design.

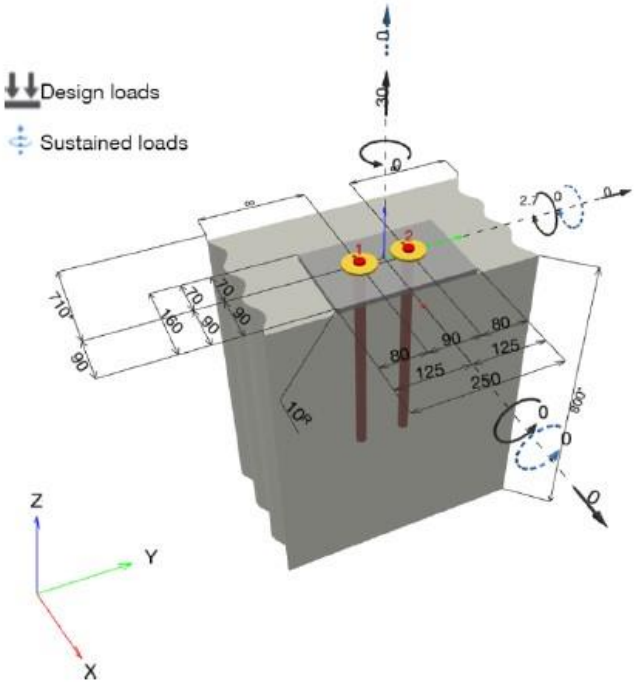

Shape 2.12: Load transmission mechanisms

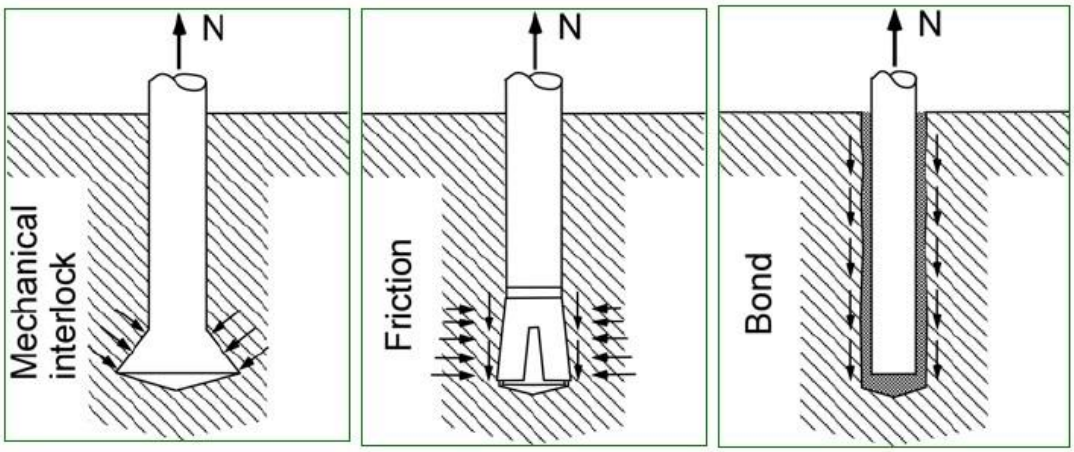

Shape 2.13: Load transmission mechanisms [22]

2.3 Failure modes

An anchorage can fail under many modes. On this paragraph these modes are presented. For the calculation of the resistance of the anchorage on every one of the failure modes, codes and standards exist to face the problem. Failure modes may appear because of the loads mentioned on 2.2. [22], [8]

Tension loads can cause steel rapture failure, concrete splitting failure, concrete breakout, side blow-out failure and pull-out failure. Shapes 2.14 to 2.18 show these types of failure.

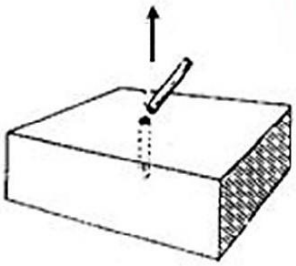

Shape 2.14: Steel rupture failure due to tension loads

Shape 2.15: Concrete splitting failure

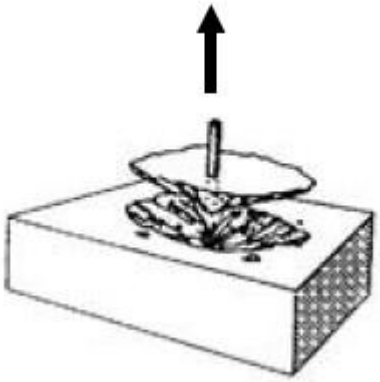

Shape 2.16: Concrete breakout failure

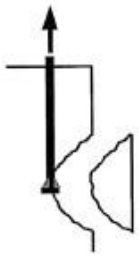

Shape 2.17: Side blowout failure

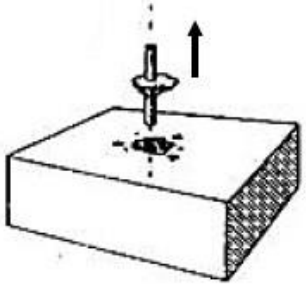

Shape 2.18: Pull-out failure

Failure also appears because of shear loads. Because of these, steel rupture failure, catenary pull-out or flexural failure, concrete spalling opposite to the loading direction – pry out failure and concrete edge failure can appear. Shapes 2.19 to 2.22 show these failure modes. The calculations to avoid all the failure modes presented can be found in all the regulation and in many books and manuals. [8], [2], [22]

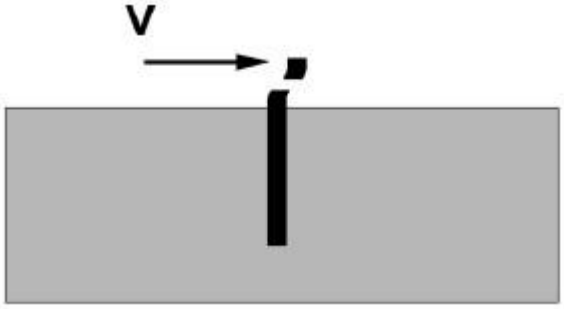

Shape 2.19: Steel rupture failure due to shear loads

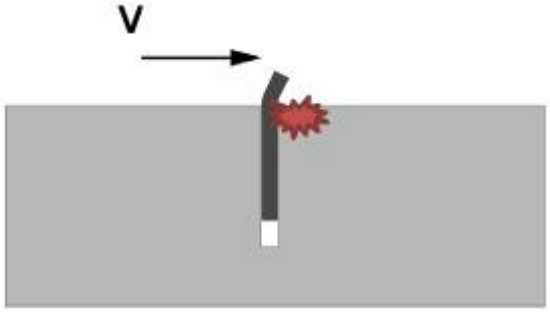

Shape 2.20: Catenary pull-out or flexural failure

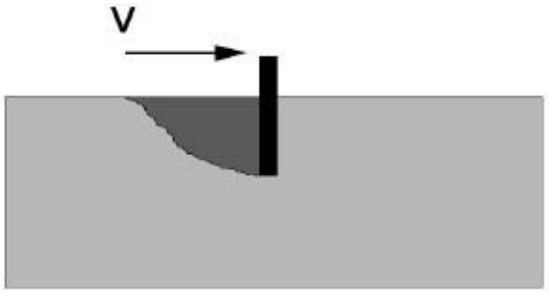

Shape 2.21: Concrete spalling opposite to the loading direction – pry-out failure

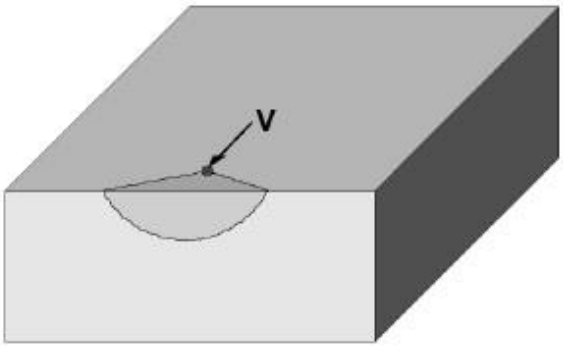

Shape 2.22: Concrete edge failure

2.4 Calculations for the design according to Eurocode 2

In general, the values of the loads must be lower than the resistance on every failure mode. Eurocode 2 – part 4 presents the way to calculate the resistance of the loaded element on every failure mode. [8], [22]

The resistance of *steel failure* is

$$N_{Rk,s} = A_s f_{uk} \tag{2.1}$$

This is calculated for the minimum area of the bolt and for every cross section with different strength.

To calculate the resistance against *concrete cone failure* Eurocode states some calculations.

$$N_{Rk,c} = N^0_{Rk,c} \psi_{s,N} \psi_{re,N} \psi_{ec,N} \psi_{M,N} \tag{2.2}$$

$$N^0_{Rk,c} = k_g \sqrt{f_{ck}} h_{ef}^{1.5} \tag{2.3}$$

Or if there is either an edge or another anchor inside the cone area

$$N_{Rk,c} = N^0_{Rk,c} \frac{A_{c,N}}{A^0_{c,N}} \psi_{s,N} \psi_{re,N} \psi_{ec,N} \psi_{M,N} \quad (2.4)$$

$$A^0_{c,N} = s_{cr,N} s_{cr,N} \text{ with } s_{cr,N} = 3h_{ef} \quad (2.5)$$

The areas $A_{c,N}$ and $A^0_{c,N}$ are presented on shapes 2.23 and 2.24.

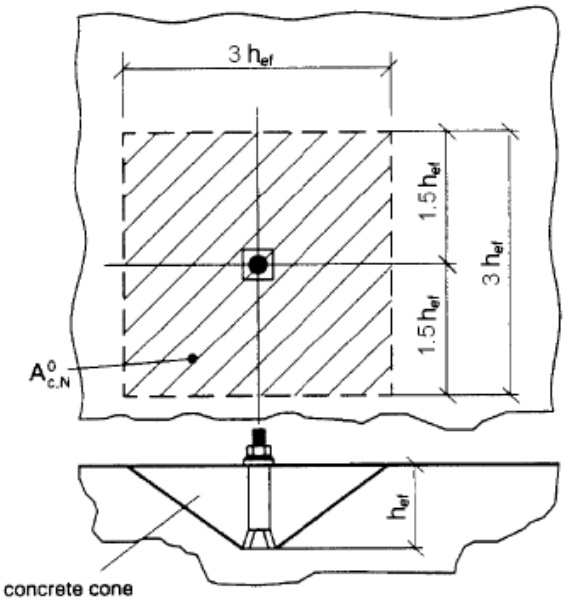

Shape 2.23: Concrete cone for one anchor

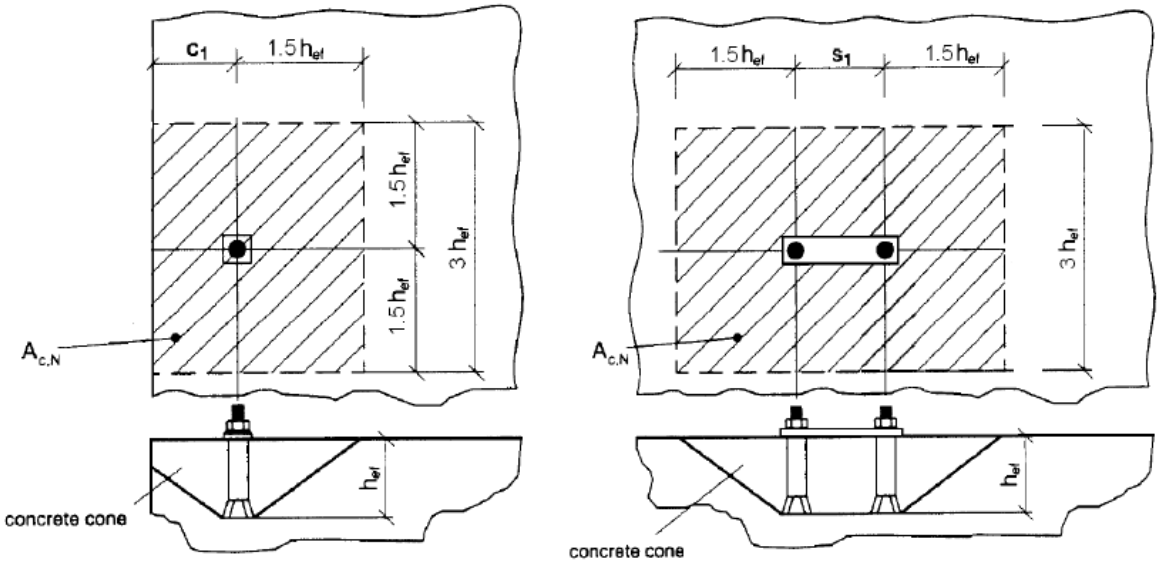

Shape 2.24: Concrete cone for an anchor near an edge or for anchor with nearby anchors

$$\psi_{s,N} = 0.7 + 0.3\frac{c}{c_{cr,N}} \leq 1 \quad (2.6)$$

$$\psi_{re,N} = 0.5 + \frac{h_{ef}}{200} \leq 1 \quad (2.7)$$

$$\psi_{ec,N} = \frac{1}{1 + 2\frac{e_N}{s_{cr,N}}} \leq 1 \quad (2.8)$$

$$\psi_{M,N} = 2 - 0.67\frac{z}{h_{ef}} \quad (2.9)$$

For the case of three or more edge distances less than $c_{cr,N}$:

$$h_{ef} = \max\left(\frac{c_{max}}{c_{cr,N}}h_{ef}; \frac{s_{max}}{s_{cr,N}}h_{ef}\right) \quad (2.10)$$

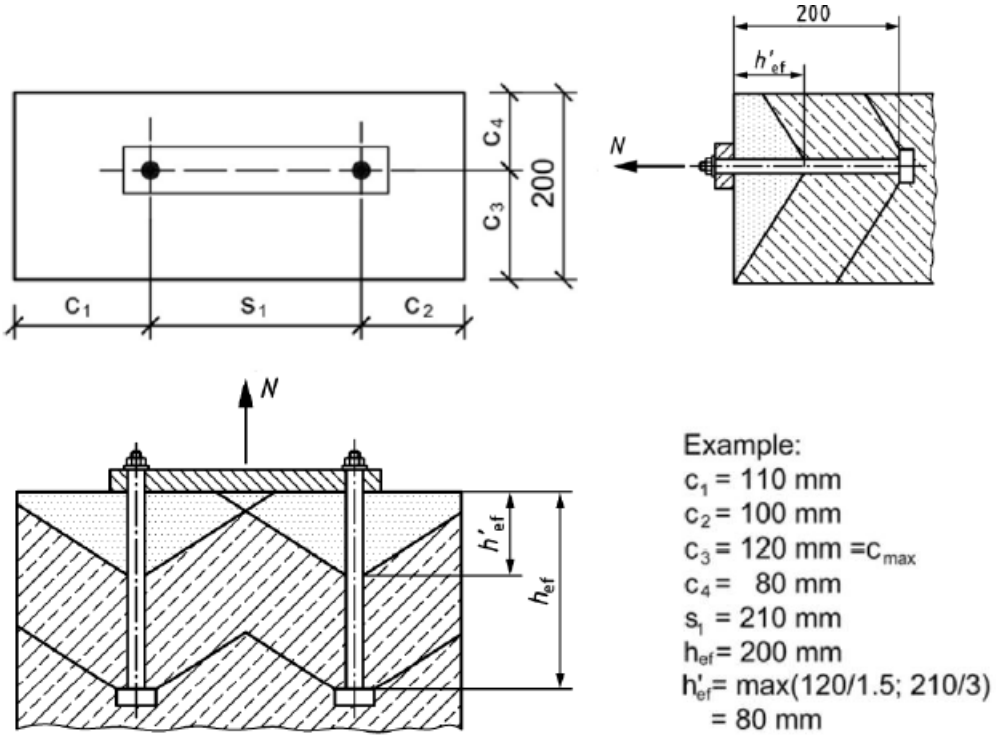

Shape 2.25: Values of c_i, s_i, h_{ef}, h_{ef}' and example of calculations

On some cases the combined pull – out and cone failure may be met. To calculate the resistance against *combined pull – out and concrete failure* the following regulations can be adopted.

$$N_{Rk,p} = N^0_{Rk,0}\frac{A_{p,N}}{A^0_{p,N}}\psi_{g,Np}\psi_{s,Np}\psi_{re,N}\psi_{ec,Np} \quad (2.11)$$

$N^0_{Rk,p} = \tau_{Rk}\pi d h_{ef}$ with τ_{Rk} equal to $\tau_{Rk,cr}$ for cracked and $\tau_{Rk,ucr}$ for non-cracked concrete (2.12)

$$A^0_{p,N} = s_{cr,Np}s_{cr,Np} \quad (2.13)$$

$$s_{cr,Np} = 7.3d\sqrt{\tau_{Rk}} \leq 3h_{ef} \quad (2.14)$$

Where τ_{Rk} is the value $\tau_{Rk,ucr}$ for non-cracked C20/25.

$$\psi_{g,Np} = \psi^0_{g,Np} - \left(\frac{s}{s_{cr,Np}}\right)^{0.5} (\psi^0_{g,Np} - 1) \geq 1 \quad (2.15)$$

$$\psi^0_{g,Np} = \sqrt{n} - (\sqrt{n} - 1)(\frac{\tau_{Rk}}{\tau_{Rk,c}})^{1.5} \geq 1 \quad (2.16)$$

$\tau_{Rk,c} = \frac{k_8}{\pi d}\sqrt{h_{ef} f_{ck}}$ where k_8 is 7.7 for cracked and 1.1 for non – cracked concrete (2.17)

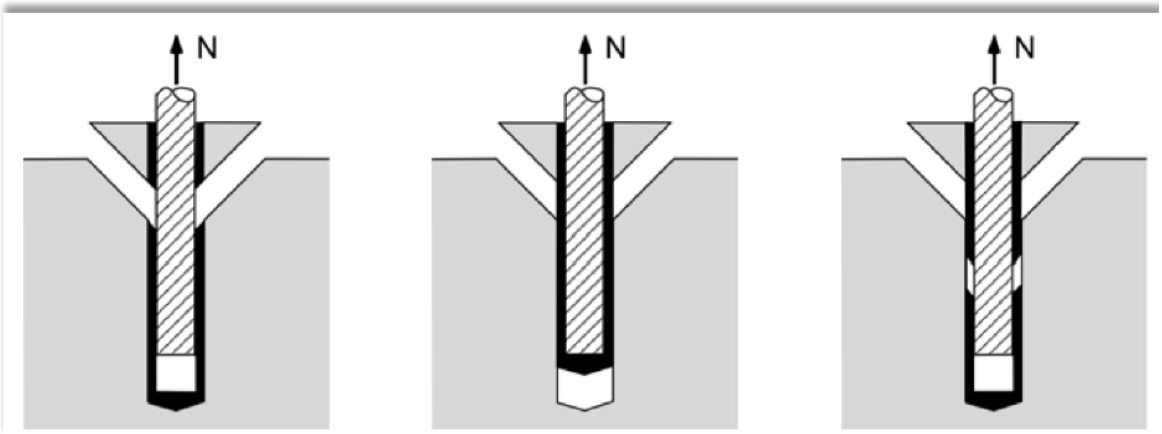

Shape 2.26: Combined pull – out and cone failure

Another failure mode that is presented here is *concrete splitting failure*.

$$N_{Rk,sp} = N^0_{Rk,sp} \frac{A_{c,N}}{A^0_{c,N}} \psi_{s,N} \psi_{h,sp} \psi_{re,N} \psi_{ec,N} \quad (2.18)$$

$N^0_{Rk,sp}$ is given in the relevant European Technical Product Specification

$$\psi_{h,sp} = (\frac{h}{h_{min}})^{\frac{2}{3}} \leq \max\left(1; \left(\frac{h_{ef} + 1.5c_1}{h_{min}}\right)^{\frac{2}{3}}\right) \leq 2 \quad (2.19)$$

with the values of $\psi_{s,N}, \psi_{re,N}, \psi_{ec,N}$ given from 2.6, 2.7, 2.8 respectively.

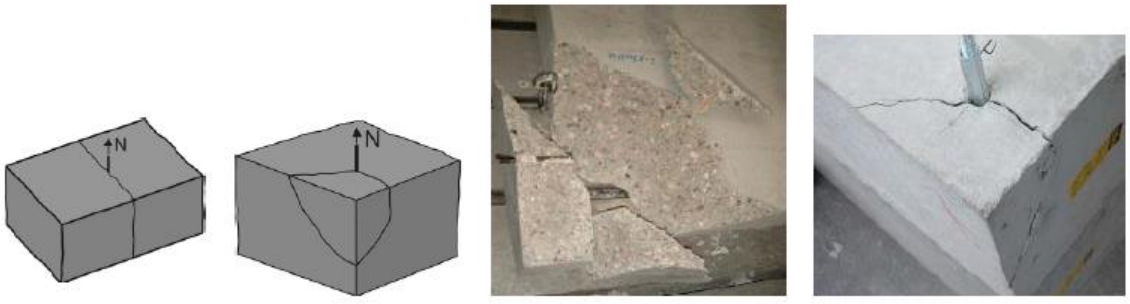

Shape 2.27: Concrete splitting failure

Finally, the calculations for the concrete *blow-out failure* are written down below.

$$N_{Rk,cb} = N^0_{Rk,cb} \frac{A_{c,Nb}}{A^0_{c,Nb}} \psi_{s,Nb} \psi_{g,Nb} \psi_{ec,Nb} \quad (2.20)$$

$N^0_{Rk,cb} = k_4 c_1 \sqrt{A_h} \sqrt{f_{ck}}$ where $k_4 = 8.7$ for cracked concrete and 12.2 for non – cracked concrete (2.21)

$$A^0_{c,Nb} = (4c_1)^2 \quad (2.22)$$

$$\psi_{s,Nb} = 0.7 - 0.3 \frac{c_2}{2c_1} \leq 1 \quad (2.23)$$

$$\psi_{g,Nb} = \sqrt{n} + (1 - \sqrt{n}) \frac{s_2}{4c_1} \geq 1 \quad (2.24)$$

$$\psi_{ec,Nb} = \frac{1}{1 + 2 \frac{e_N}{4c_1}} \quad (2.25)$$

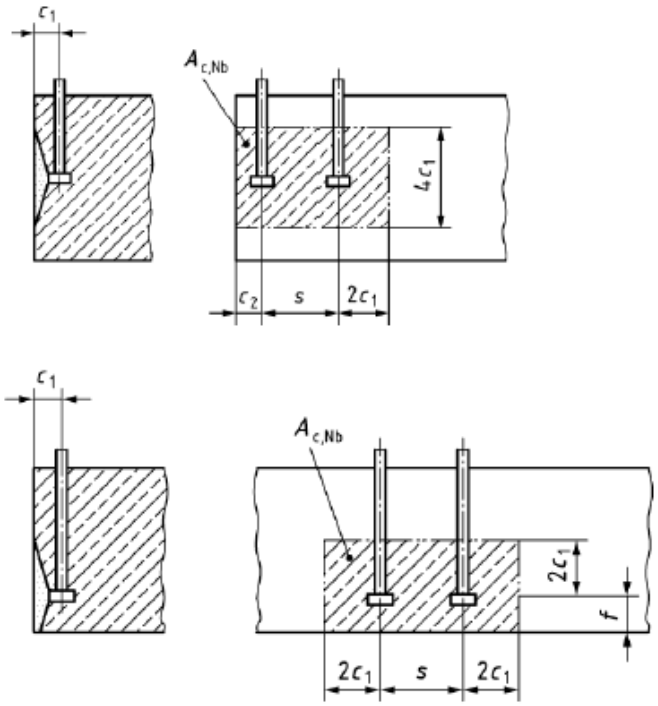

Shape 2.28: Concrete blow-out failure calculations

3 Cast – in channels

3.1 Uses of cast – in channels

Cast-in channels are an efficient and easy way to install adjustable connections to hang heavy loads in many structures. These steel parts collaborate with concrete with the use of shear bolts, forming a composite section.

Some areas of application are bridge and tunnel construction (fastening of pipes or jet fans), construction of sewage treatment plants, chemical industry installations (installations exposed to aggressive substances), ventilated facades and also for structural reinforced concrete elements with higher demands on the concrete cover. Channels of stainless steel can also be used in road tunnels, structures in salt water, indoor swimming pools, areas not routinely deaned, poorly ventilated parking garages and in narrow, major city streets. Some of these applications are presented in shapes 3.1 to 3.3.

In general, cast – in channels can be divided to cold rolled anchor channels, hot rolled cast-in channels and toothed cast – in channels. The manufacturers offer these types of cast – in channels on many profiles to meet the demands of many projects. Also, cast – in channels can be constructed from stainless steel for uses in corrosive environments.

Shape 3.1: Curtail wall application

Shape 3.2: Use on TBM tunnels

Shape 3.3: Application on rafter shoe

3.2 Failure modes

The failure modes that can occur when using a cast – in channel and this is loaded under shear loads are presented on shapes 3.4 to 3.11.

Anchors loaded under shear forces can form a steel failure mechanism when the edge distance and the embedment depth are sufficiently large, whereby conical spalling of the surface concrete precedes steel failure. Steel failures can occur either as steel failure of the screw or local flexure of the channel lip or steel failure of the anchor or failure of the channel – anchor connection.

When anchors are loaded with a shear force near a free edge, failure may be developed in the body of the concrete part, with a form of a semi – conical fracture surface. This failure is called concrete edge failure as shown on shape 3.8. Another possible mechanism occurs if anchors and shear studs that have limited embedment, are loaded with a shear force. Then, they can create a pry – out fracture behind the point of the load application as shown on shape 3.9. Finally, failure modes because of the damaging of the concrete reinforcement or the bond mechanism between the reinforcement and the concrete can also take place as shown on shapes 3.10 and 3.11. [22]

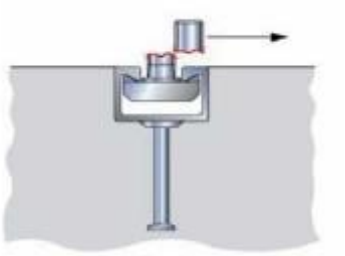

Shape 3.4: Steel failure of the screw

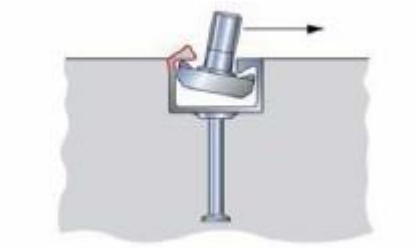

Shape 3.5: Local flexure of the channel lip

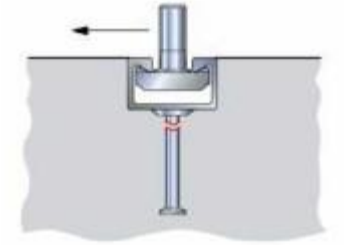

Shape 3.6: Steel failure of the anchor

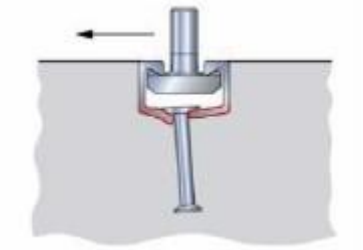

Shape 3.7: Failure of the channel-anchor connection

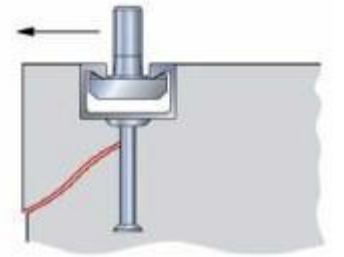

Shape 3.8: Concrete edge failure

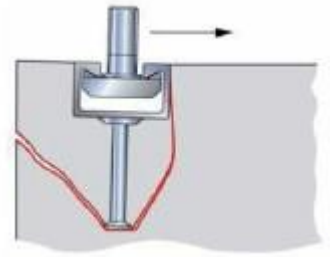

Shape 3.9: Concrete pry-out failure

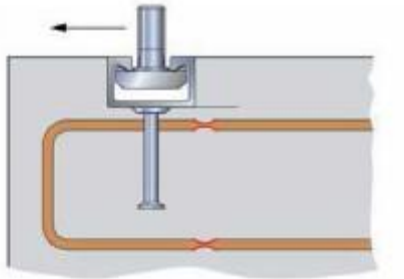

Shape 3.10: Steel failure of the reinforcement

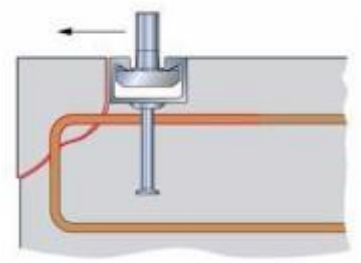

Shape 3.11: Bond failure of the reinforcement

Furthermore, failure can occur because of tensile loads. Shapes 3.12 to 3.20 show the mechanisms that need to be taken into account when designing a cast – in channel. [22]

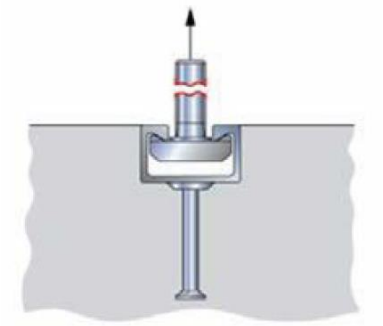

Shape 3.12: Steel failure special screw

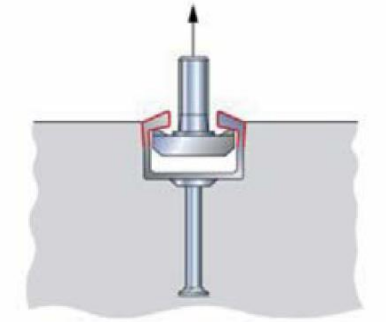

Shape 3.13: Local flexure of the channel lips

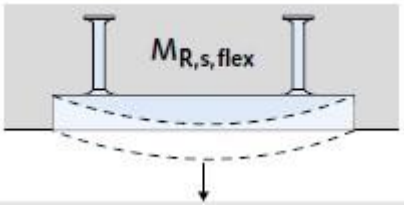

Shape 3.14: Failure due to flexure of the channel

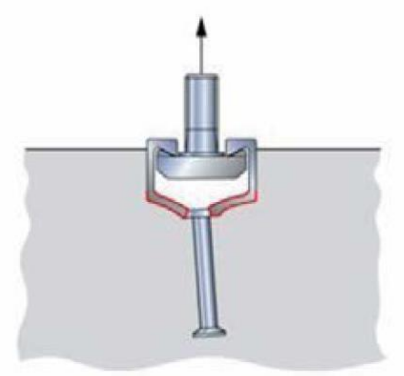

Shape 3.15: Failure of the channel – anchor connection

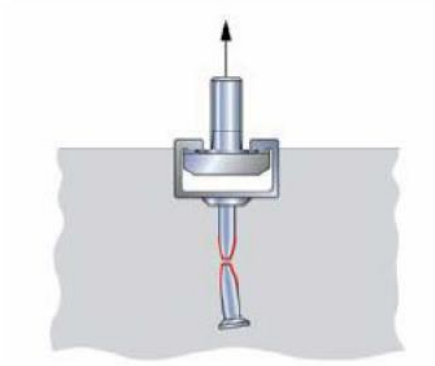

Shape 3.16: Steel failure of anchor

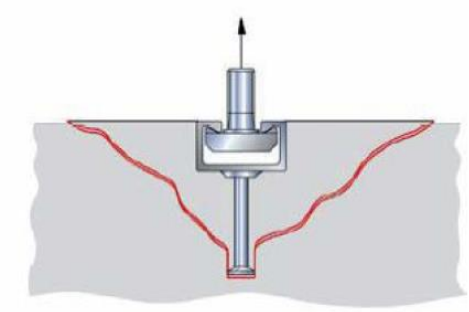

Shape 3.17: Concrete cone failure

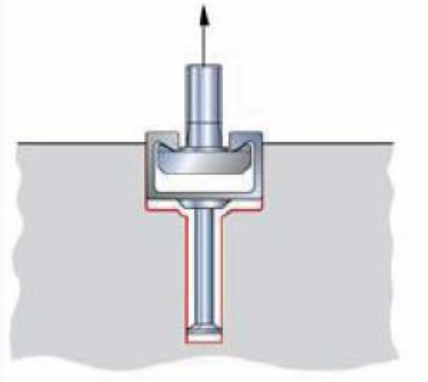

Shape 3.18: Pull - out failure

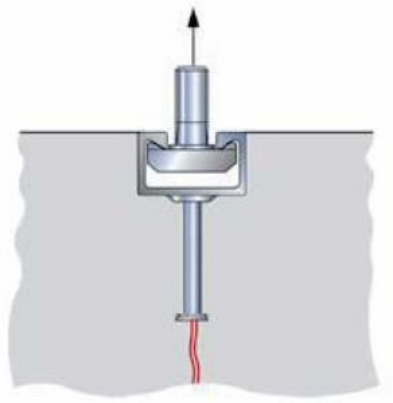

Shape 3.19: Splitting failure

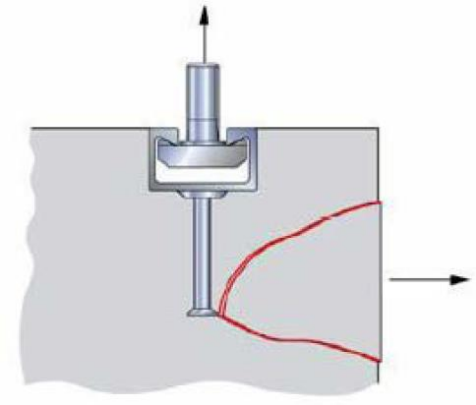

Shape 3.20: Blow - out failure

3.3 Types of cast – in channels and main advantages

Cast – in channels are suitable for various types of construction connections such as facades, precast concrete elements, stadium seating, lift guide – rails, crane runway and other. Besides very good adjustability, cast – in channels save considerable installation time. They commit no damage to the reinforcement, are approved for fire – resistant structural elements, they are suitable for use in concrete pressure and tensile stress zones and also using the appropriate type of cast – in channels can lead to excellent resistant steel members against corrosion or appropriate response under dynamic loads. Also, many economical and temporal results can be achieved with suitable pre-planning and efficient installation layout.

The types provided are the typical profile sections of the cast – in channels, serrated cast – in channels, the power solution cast – in channels and handrail connections cast – in channels. Also, these types can be either cold or hot rolled and they may be galvanized. The appropriate type for every implementation can be found on the technical booklets of the manufacturing companies.

4 Theoretical analysis for full shear connection

Theoretical analysis in accordance to the EN1994 is taking place. On this thesis, the results of the finite element analysis are compared to those that come out from the theoretical analysis. This study investigates the bending behavior of the composite section with cast – in channels embedded. However, it must be mentioned that when designing a section with a cast – in channel embedded, the channel is also carrying the loads of the hanging objects on it. As a result, there are additional stresses caused by these loads, that the designer must take into account when these parts are enforced to participate on the bending behavior of the section. In addition, these extra loads must be considered also in the designing of the shear connection. This thesis examines the bending behavior of these composite sections without taking into account the collaboration of the different types of loads.

4.1 Solution of the problem with the theory of composite structures

Eurocode 4 suggests plastic or elastic analysis, depending on the class of the section and the geometry of the structure. To achieve the comparison of the results, calculations of the plastic bending resistance and the composite behavior of the section were done, using plastic analysis without calculating the class of the cast – in channel profiles. [1], [5]

The materials used on the theoretical analysis are the same used on the finite element analysis. Concrete is regarded as C30/37, B500C for the reinforcement and S355 for the structural steel. The bending resistance is calculated for bending moment that causes tensile stresses on the bottom side of the section and for compression zone inside the concrete part.

4.1.1 Calculation of the bending capacity of the section

The calculations to define the bending behavior of the composite section are presented.

Concrete under compression: $$f_{cd} = 0.85\frac{f_{ck}}{1.5} \quad (4.1)$$

Concrete under compression: $$f_{td} = 0 \quad (4.2)$$

Structural steel: $$f_{yd} = \frac{f_{yk}}{1.0} \quad (4.3)$$

Reinforcement: $$f_{sd} = \frac{f_{sk}}{1.15} \quad (4.4)$$

Compressive force: $$D = b_{eff} z_0 0.85 f_{cd} \quad (4.5)$$

Tensile force of steel section: $$F_a = A_a f_{yd} \quad (4.6)$$

Tensile force of the reinforcement: $$F_s = A_s f_{sd} \quad (4.7)$$

Compression zone: $$z_0 = \frac{A_a f_{yd} + A_s f_{sd} + N}{b_{eff} 0.85 f_{cd}} \quad (4.8)$$

Bending capacity: $$M_{pl,Rd} = 0.8\, z_0\, b_{eff}\, 0.85\, f_{cd}\, (z_e - 0.4 z_0) + F_s(z_s - z_e) + F_a(z_a - z_e) \quad (4.9)$$

where N is the effective axial force and z_e is the center of gravity for the composite section.

The thesis calculates the influence of the cast in channel in the bending capacity of the section. Parametrical analysis is also examined for the effective axial force, for different profiles of cast in channels and also a comparison is proceeded for the bending capacity of the section if either the cast in channel or the reinforcement is removed.

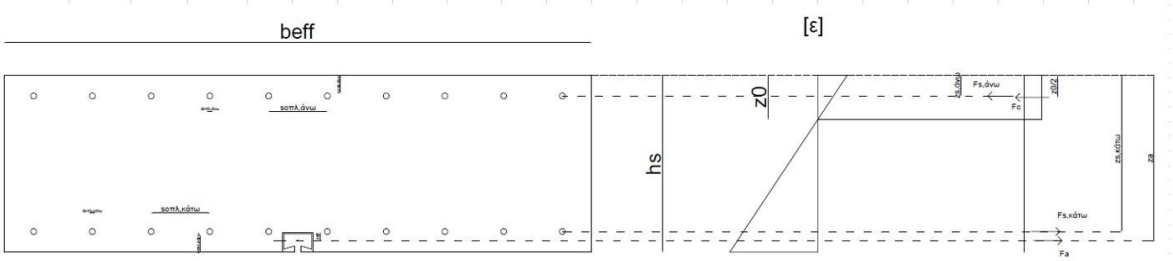

Shape 4.1: Plastic analysis of a composite section

4.1.2 Calculations for the cracking moment of the sections

On this paragraph, the calculations for the cracking moment of the sections are calculated. At the moment of cracking, the strain at the bottom of the section is equal to the cracking strain of concrete.

Young's modulus of concrete: $$E_c = 33000\ MPa \quad (4.10)$$

Young's modulus of structural steel: $$E_a = 210000\ MPa \quad (4.11)$$

Young's modulus of reinforcement: $$E_s = 210000\ MPa \quad (4.12)$$

Coefficient η_c: $$\eta_c = \frac{E_a}{E_c} \quad (4.13)$$

Equivalent steel section: $$A_e = A_a + A_s + \frac{A_c}{\eta_c} \quad (4.14)$$

Elastic gravity center of the equivalent section: $$z_e = \left(A_a * z_a + A_S * z_s + \frac{A_c * z_c}{\eta_c}\right) \Big/ A_e \quad (4.15)$$

Cracking strain of concrete: $$\varepsilon_{c,cr} = \frac{f_{ct}}{E_c} \quad (4.16)$$

Strain on the upper side of the section: $$\varepsilon_{c,o} = \frac{z_e * \varepsilon_{c,cr}}{h_c - z_e} \quad (4.17)$$

Stress on the upper side of the section: $$\sigma_{c,o} = \varepsilon_{c,0} * E_c \quad (4.18)$$

Stress on the center of gravity of the steel section:	$\sigma_a = \varepsilon_a * E_a$	(4.19)
Stress on the reinforcement:	$\sigma_s = \varepsilon_s * E_s$	(4.20)
Cracking bending moment:	$M_{cr} = 0.333 b_{eff} {z_e}^2 \sigma_{c0}(h_c - z_e) + (z_s - z_e)\sigma_s A_s + (z_a - z_e)\sigma_a A_a$	(4.21)

Additionally, the minimum reinforcement to avoid cracking according to EC2-1-1, paragraph 9.2.1.1, is calculated according to equation (4.22).

$$A_{s,min} = 0.26 \frac{f_{ctm}}{f_{yk}} bd \geq 0.0013 bd \tag{4.22}$$

4.2 Shear connection

The composite operation is generally obtained if appropriate adaptation of the shear stresses between concrete and the steel section is achieved. In composite structures this happens with the use of shear connectors. The connectors prevent the slip between the different materials, transfer the shear force and secure the composite behavior.

Shear stresses occur on the vertical and the longitudinal axis. If the connectors transfer all the shear force, there is no slip. This case is called full shear connection. If small displacements are allowed, the connection is called partial. Shape 4.2 shows the difference of the types of shear connections. The calculations for the appropriate connection are presented on the corresponding codes and standards. Eurocode 4 suggests the use of plastic analysis, elastic analysis and elastoplastic analysis. Plastic analysis can be applied if some requirements are met. [1], [5]

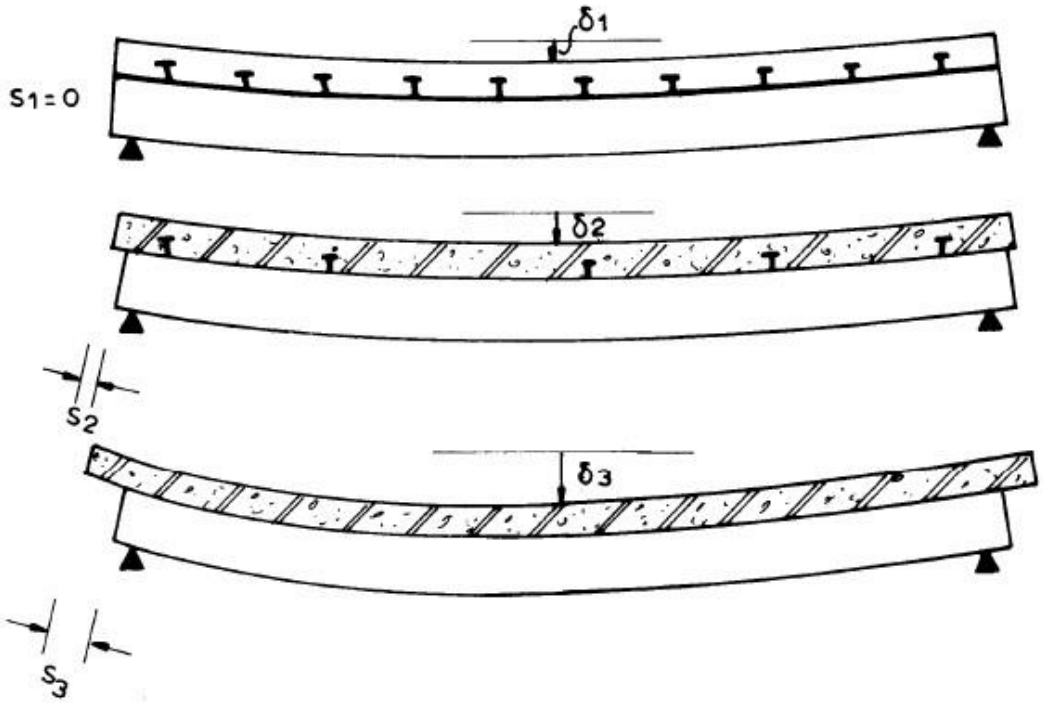

Shape 4.2: Full, partial and zero shear connection

4.2.1 Longitudinal shear force using plastic analysis

According to Eurocode 4, the plastic analysis for the calculation of the longitudinal shear force can be used if the implementation is about structural purposes, with cross – sections of class 1 or 2, with ductile behavior on the shear connectors and calculation about the ultimate limit state.

On the case of using plastic analysis and for the case that this thesis is studying, regarding that the steel section and the concrete reinforcement are under tension and the compressive force needed is provided only from the concrete section, the shear force that must be received from the shear connectors is shown on equation 4.23. However, it is highlighted that when designing composite structures, the engineer must take into account all the factors and use either plastic or elastic analyses depending on the criteria spotted in the regulations.

$$V_l = D = b_{eff} z_0 0.85 f_{cd} = A_a * f_{yd} + A_s * f_{sd} \quad (4.23)$$

4.2.2 Full shear connection

Full shear connection is obtained when the shear connectors are placed to be able to obtain the total amount of the shear force inside a region. The efficient way of setting the shear connectors is suggested on the regulations. The number of the shear connectors needed is calculated on equation 4.24.

$$n_f = \frac{V_l}{P_{Rd}} \quad (4.24)$$

where P_{Rd} is the resistant force of the connector used.

The value of P_{Rd} is the minimum value between the shear resistance of the connectors and the bearing resistance of concrete. P_{Rd} can be calculated from equation 4.25.

$$P_{Rd} = \min \left(\frac{(0.8 f_u \left(\frac{\pi d^2}{4}\right)}{\gamma_v} ; \frac{0.29 \alpha d^2 \sqrt{f_{ck} E_{cm}}}{\gamma_v} \right) \quad (4.25)$$

Where $\gamma_v = 1.25$ is a safety factor and α is defined from the geometrical aspects of the shear bolt. On this thesis, the characteristic values of the stresses of the materials are taken into account so the results are calculated without using the safety factors.

4.2.3 Partial shear connection

Partial shear connection is formed when the effective shear force on the interface is higher than the shear force that the shear connectors can carry. The partial shear connection is allowed under some conditions. On this case, a slip between the concrete and the steel section is taking place. As a percentage of the shear connection is defined the amount η given on equation 4.26.

$$\eta = \frac{n}{n_f} \quad (4.26)$$

where n is the existing amount of shear connectors.

The amount η can be between 0 and 1. The regulations spot that partial shear connection is allowed only in case of positive bending moments and also set limits on the amounts of η

that are allowed to be used. This study aims to calculate the behavior of the examined section under many values of η so these limits are not taken into account.

The bending resistance of the cross section of a beam with partial shear connection is calculated from equation 4.27.

$$M_{Rd} = M_{pl,\alpha,Rd} + \eta\ (M_{Pl,Rd} - M_{pl,\alpha,Rd}) \quad (4.27)$$

4.3 Results

For the calculations, a section of concrete with height 300mm and width of 1000mm is taken into account. The cast-in channels are 3 different profiles named HTA CE 52/34, HTA CE 55/42 and HTA CE 72/48. The reinforcement used is D14/20 with coating of 3cm. The materials used are concrete with quality C30/37, structural steel S355 and reinforcement B500C. The calculations are made for characteristic values and not for design values in order to compare the theoretical analysis with the computational analysis, as characteristic values are also used on the finite element analysis.

4.3.1 Compression zone and bending capacity of the section by changing the participating parts

From the calculations, the results presented on tables 4.1, 4.2 and 4.3 arise for the bending capacity of the sections, when different profiles are used. Shape 4.3 shows the calculations according to EN1994 on an excel sheet.

Table 4.1: Bending capacity of sections using different steel parts for HTA CE 52/34 cast-in channel

Participating Parts	Compression zone z0 (cm)	Bending Capacity Mpl,rd (kNm)
Concrete and Ø14/20	1.60	98.1
Concrete and HTA CE 52/34	0.71	60.7
Concrete, Ø14/20 and HTA CE 52/34	2.51	156.7

Table 4.2: Bending capacity of sections using different steel parts for HTA CE 55/42 cast-in channel

Participating Parts	Compression zone z0 (cm)	Bending Capacity Mpl,rd (kNm)
Concrete and Ø14/20	1.60	98.1
Concrete and HTA CE 55/42	1.22	80.0
Concrete, Ø14/20 and HTA CE 55/42	2.82	175.0

Table 4.3: Bending capacity of sections using different steel parts for HTA CE 72/48 cast-in channel

Participating Parts	Compression zone z0 (cm)	Bending Capacity Mpl,rd (kNm)
Concrete and Ø14/20	1.60	98.1
Concrete and HTA CE 55/42	1.58	102.4
Concrete, Ø14/20 and HTA CE 55/42	3.18	196.2

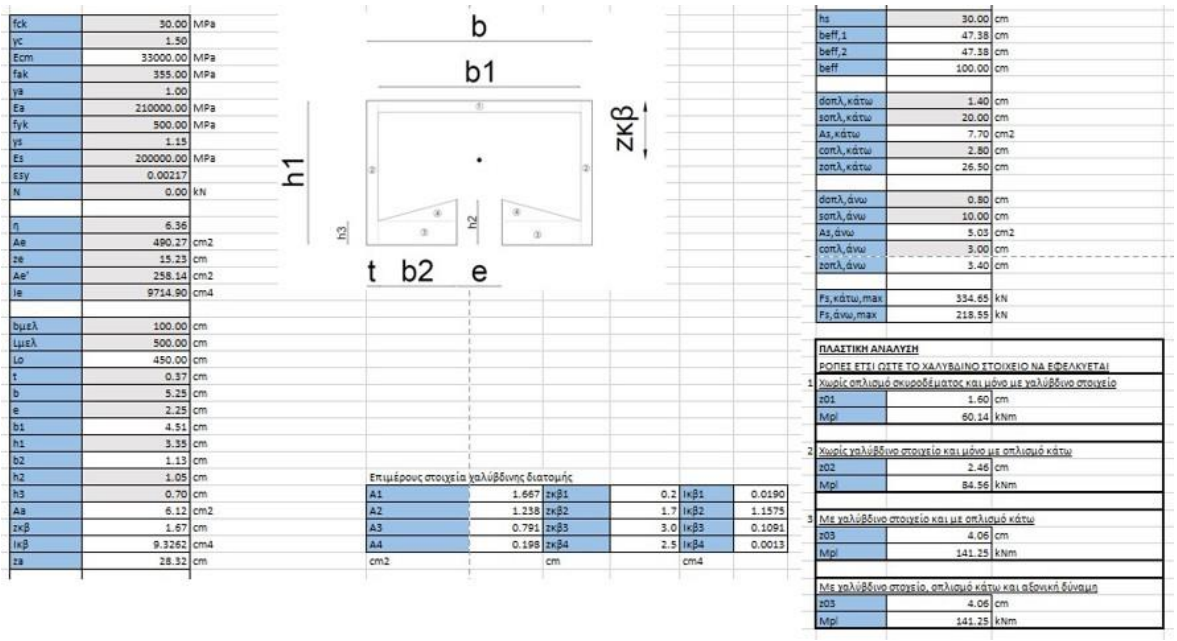

Shape 4.3: Calculations for the plastic bending capacity of the section according to EN1994

4.3.2 Influence of the concrete height

On this paragraph, the height of the concrete section is examined. Using the calculations mentioned before table 4.4 shows the results for different concrete heights.

Table 4.4: Bending capacity of sections with different concrete heights

h_c (cm)	$M_{Rd,nc}$ (kNm)	$M_{pl,HTA52/34}$ (kNm)	$M_{pl,HTA55/42}$ (kNm)	$M_{pl,HTA72/48}$ (kNm)
10	20.62	35.21	38.06	41.73
15	39.86	65.31	71.95	79.93
20	59.10	95.42	105.83	118.13
25	78.34	125.53	139.72	156.33
30	97.58	155.63	173.61	194.53
35	116.83	185.74	207.49	232.73

From these calculations it can be proposed that for reinforcement Φ14/20 and the for the materials used on this analysis, the rise of the bending resistance of the composite section does almost fit the following linear equation, for values of cast – in channel area between 6cm^2 and 11cm^2.

$$M_{Rd} \cong M_{Rd,nc} + (0.35h_c - 1.30)A_{ch} \quad (4.28)$$

where h_c is the height of the concrete section, A_{ch} is the cast – in channel steel area in cm^2 and $M_{Rd,nc}$ is the bending resistance of the reinforced concrete section without cast – in channel in kNm.

4.3.3 Influence of the axial force on the bending behavior

The influence of the axial force on the bending behavior of the section was checked with the theory described on 4.1.1. The axial force was examined for compressive values from 0 kN up to 5200 kN. Shape 4.4 shows the axial force – bending capacity diagram that came out from the theoretical analyses for the three profiles of cast-in channel section. It is assumed that the axial force where the highest bending capacity is achieved is equal to 3800 to 4000 kN and the raise of the bending capacity is very important, as it can reach more than twice the values of the bending capacity of the section with 0 axial force.

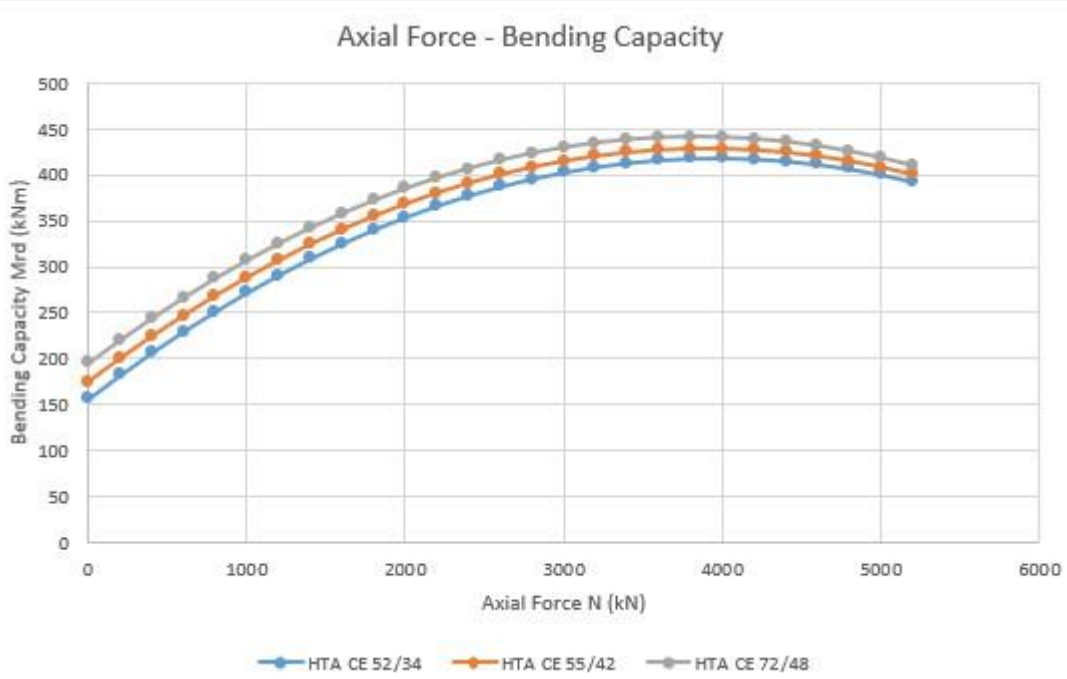

Shape 4.4: Calculations for the plastic bending capacity of the section according to EN1994

4.3.4 Results for the cracking of the section

Solving the problem as mentioned on 4.1.2 of this thesis, the cracking moment of the sections of the analyses are presented on shape 4.5. As it was supposed to be, the steel parts do not influence the cracking moment significantly, because the stiffness of concrete is the main coefficient on the behavior of the section before cracking. On chapter 7, the results from this chapter will be compared to the results of the finite element analysis of chapter 6.

Cross section parts	Mcr (kNm)
C30/37 & Φ14/20	44.64
C30/37 & HTA CE 52/34	45.33
C30/37 & HTA CE 55/42	45.97
C30/37 & HTA CE 72/48	46.7
C30/37 & HTA CE 52/34 & Φ14/20	46.47
C30/37 & HTA CE 55/42 & Φ14/20	47.1
C30/37 & HTA CE 72/48 & Φ14/20	47.82

Shape 4.5: Cracking moment of the sections

Additionally, the minimum reinforcement required to avoid cracking is calculated from equation (4.22). This equation leads to a value of $A_{s,min} = 3.97cm^2/m$ which can be satisfied with Ø14/39 or Ø10/20.

4.3.5 Results for the shear connection

On this paragraph results are presented for the appropriate shear connection of the 3 different profiles that are examined on this thesis. Initially, the shear force is calculated and afterwards the demanded shear bolts with diameter M16 and of quality 8.8 to achieve a full shear connection are estimated. Finally, calculations are provided for the decrease of the bending resistance of the composite section with the HTA CE 52/34 channel and the concrete part.

Table 4.5: Calculation for the shear connection of the composite sections

Participating Parts	Shear force per meter (kN/m)	Distance of the shear bolts (cm)
Concrete and HTA CE 52/34 and Ø14/20	602.1	12.3
Concrete and HTA CE 52/34	217.3	34.0
Concrete and HTA CE 55/42 Ø14/20	677.7	10.9
Concrete and HTA CE 55/42	292.9	25.2
Concrete and HTA CE 72/48 Ø14/20	764.0	9.7
Concrete and HTA CE 72/48	379.1	19.5

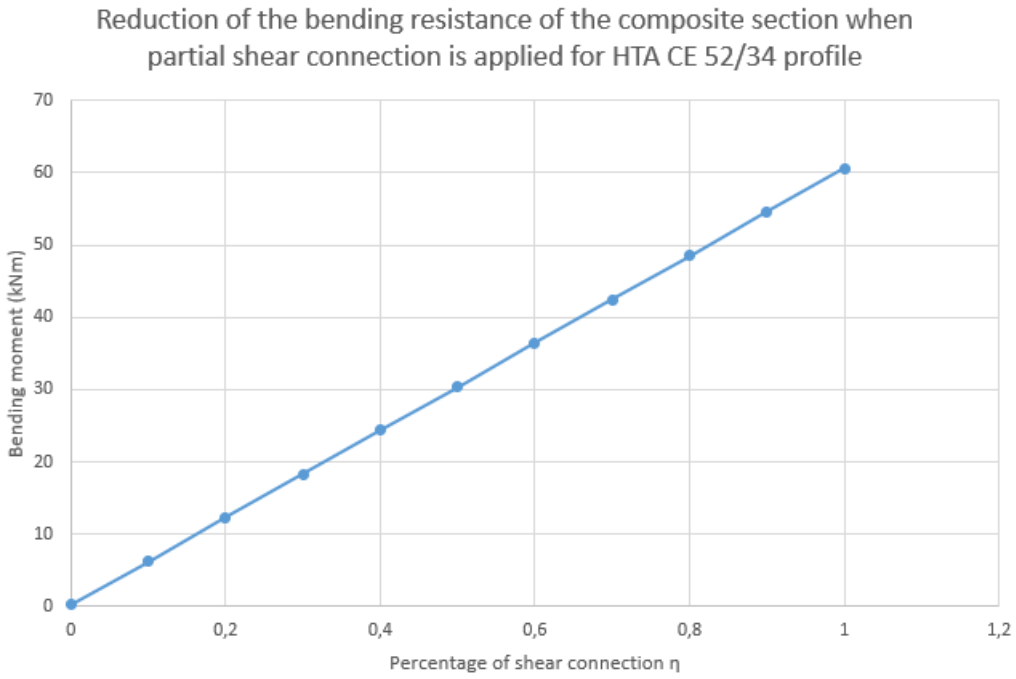

Shape 4.6: Calculations for the reduction of the bending resistance of the section when different percentage of partial shear connection is applied for composite section with concrete and HTA CE 52/34 cast-in channel profile

5 Simulation of the problem

5.1 Parts of the analysis

For the simulation of the problem, the project used the finite element analysis program Abaqus. Different parts used in order to take into account the factors that contribute to the final results. These parts are the concrete section, the cast in channel, the reinforcement and the metal plates for the application of the load and for the boundary conditions. The regarded effective width for the analyses, from which the total width of the model came out is 1000mm. Followingly, the geometry of the different parts is presented.

5.1.1 Cast – in channel

For the main analyses, the cast in channel section used was the HTA CE 52/34 [12], [13]. For the parametrical analyses, two more sections were employed. The profile of the cast in channels is presented on shape 5.1. The geometrical properties for the HTA CE 52/34 are shown on Table 5.1. The length of the part used in the simulations is L=2000mm. This part comes in contact with the concrete section and the metal plates used for the support of the model. Shape 5.2 shows the model of the cast in channel in Abaqus.

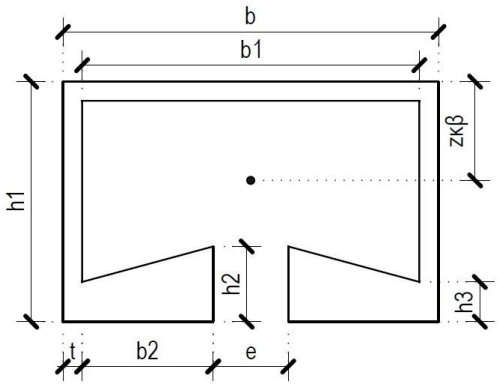

Shape 5.1: Typical cast -in channel section

Table 5.1: HTA CE 52/34 section properties

Property	Symbol	Units	Amount
Height 1	h1	mm	33.5
Height 2	h2	mm	10.5
Height 3	h3	mm	7.0
Thickness	t	mm	3.7
Width	b	mm	52.5
Width 1	b1	mm	45.1
Width 2	b2	mm	11.3
Gap	e	mm	22.5
Gravity center	$z_{\kappa\beta}$	mm	16.7
Area	A	mm^2	612
Inertia	I	mm^4	93262

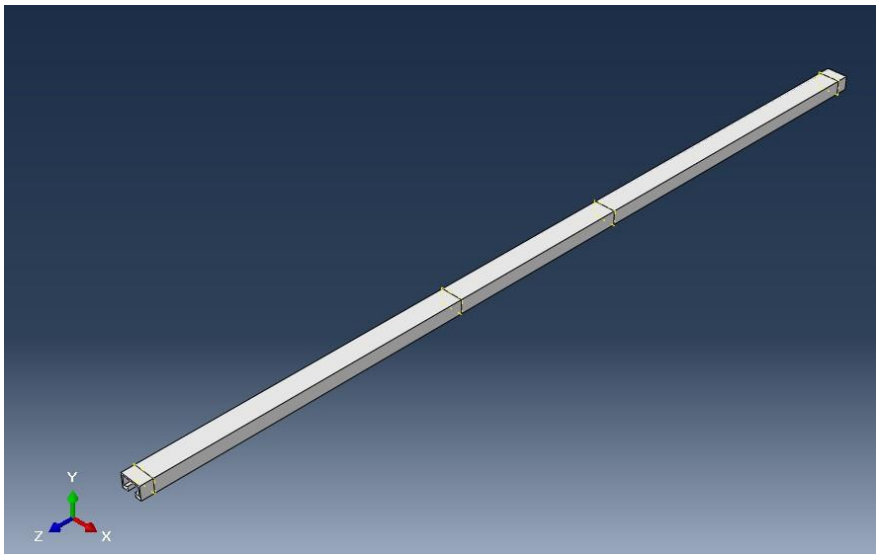

Shape 5.2: Cast-in channel part

5.1.2 Concrete part

The concrete section has a width of 1000mm and a height of 300mm, which is similar to the height of the concrete sections used in tunnels and in other applications. The length of the beam used is L=2000mm. The concrete part has an appropriate setup on its bottom, in which the cast in channel is attached. This part comes in contact with the cast in channel, the reinforcement and with the metal plates. Its simulation is presented on shape 5.3.

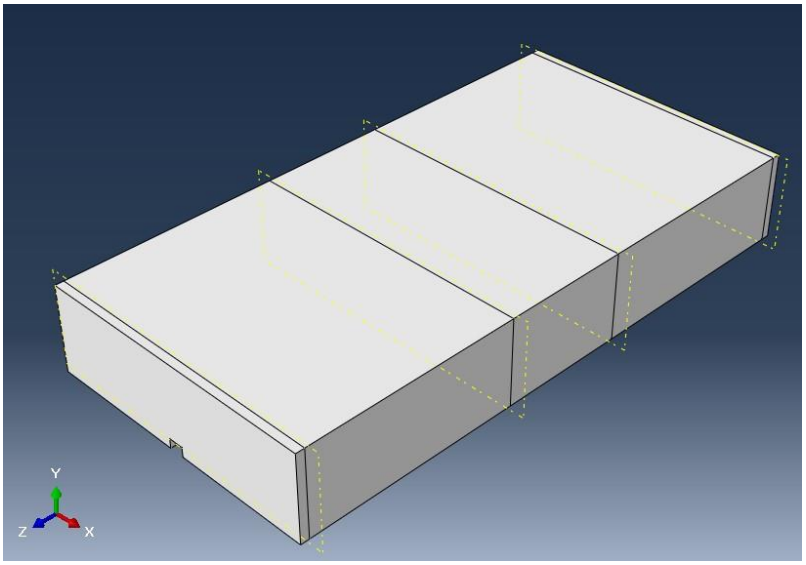

Shape 5.3: Concrete part

5.1.3 Steel reinforcement

To reinforce the concrete section against tensile stresses, steel reinforcement is used. For the main analyses, the reinforcement used was Φ14/20 or 7.97cm^2, which is an amount that is commonly used in tunnels. The bars were placed only at the bottom of the concrete model, with a coating of 30mm. To simulate the desired steel area, a section of 1.54 cm^2 per bar is assigned in every steel part.

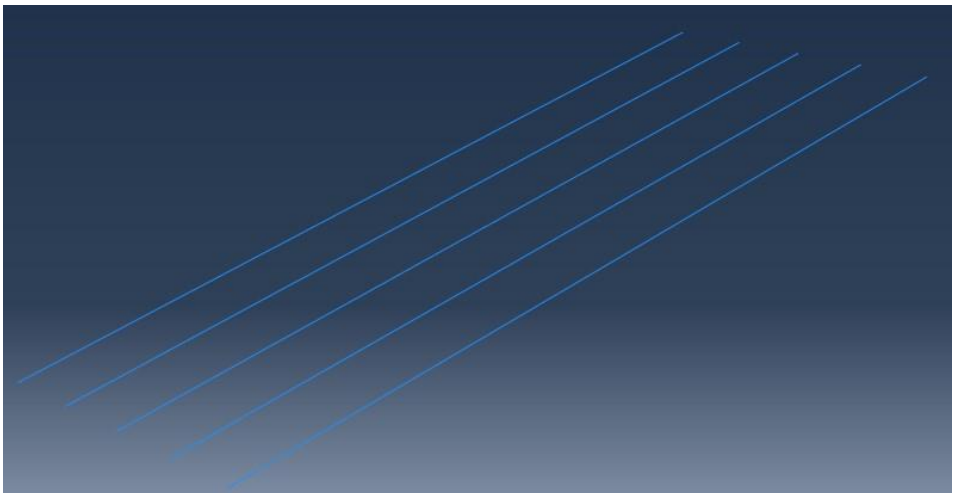

Shape 5.4: Simulation of the reinforcement

5.1.4 Metal plates

The metal plates are used to transfer the assigned load on the concrete beam smoothly, in order to avoid difficulties in the analyses. For the same reason they are used to assign the boundary conditions on them. Their section is 20mm in height and 40mm in width and their length is 1000mm. Four different plates are used to form the whole model.

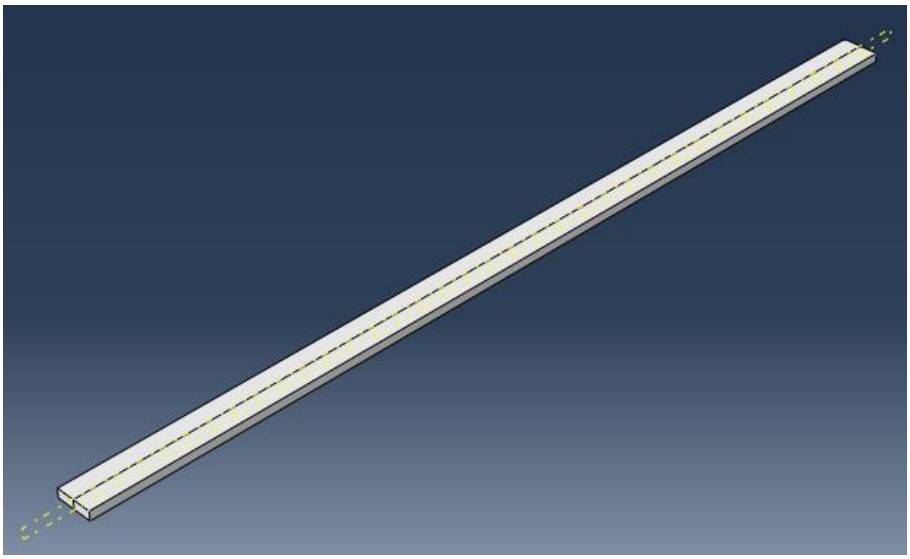

Shape 5.5: Simulation of the metal plates

5.2 Arrangement of the analysis

The model of the analysis is a combination of the parts mentioned as shown on shape 5.6. The concrete part (A) with a total length of 2m, is set on 2 of the metal plates (D). The center of the plates is set on a distance of 30mm on both sides of the model. On these metal plates, boundary conditions are assigned which restrain displacement on both horizontal directions and on the vertical direction. In addition, 2 more plates (D) are set on the top of the concrete part, on which the loads of the analysis are applied. These plates are placed on

a distance of 750mm from the supports. The cast in channel (B) is set in the alcove of the concrete part (A) at its bottom on its full length. On shape 5.7, the cast in channel is highlighted.

The loading of the analyses is assigned on the two metal plates at the top of the model. The load is assigned as pressure load on a maximum value of p (kN/mm^2) which is equal to P(kN) = p*1000*40 = 40000p (kN) / plate. This load is set in order to achieve a maximum bending moment of P(kN)*0.75m = 0.75P (kNm). The load is assigned linearly while time proceeds. The calculations are performed using static-type analyses with the Newton's method. The duration of the analysis is 1sec and the maximum increment of the analyses is 0.005sec. For the execution of the main analyses and for the parametrical analyses, the same model is analyzed, using different parameters. Also, some models do not simulate all of the parts. In every analysis, the different assets of it are mentioned. [6], [7]

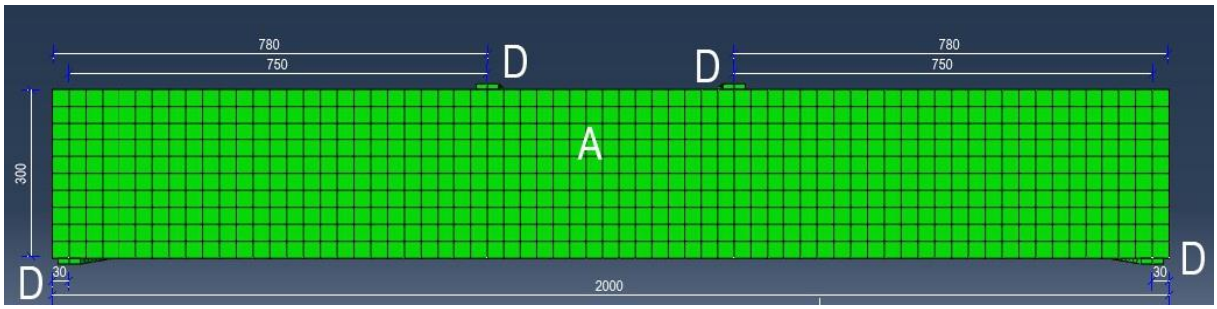

Shape 5.6: Position of the metal plates on the concrete part

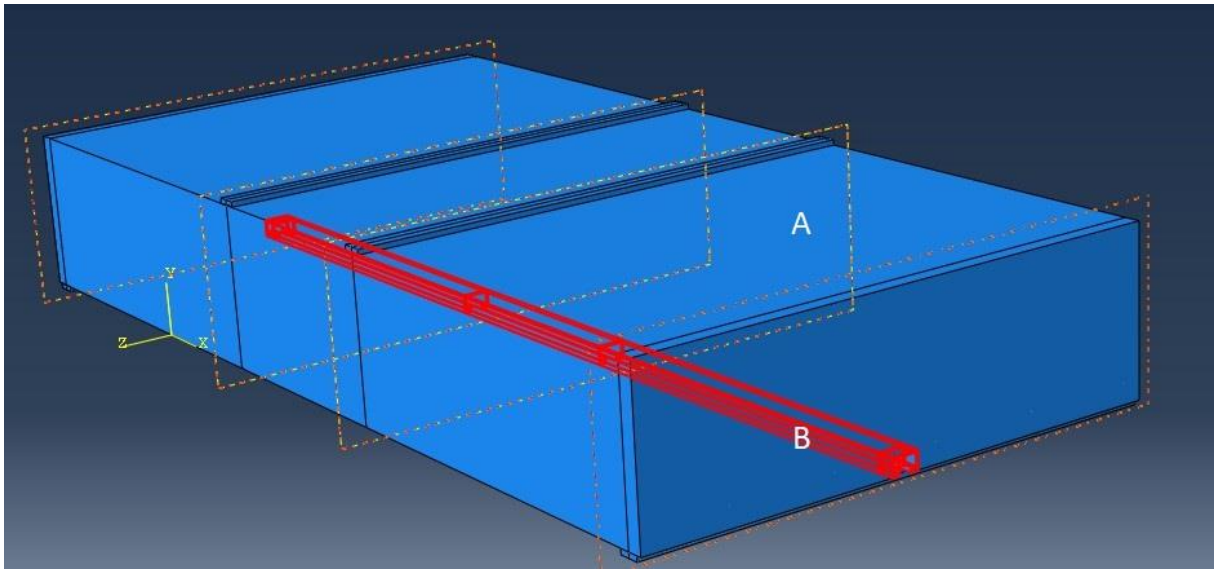

Shape 5.7: Concrete part and cast-in channel

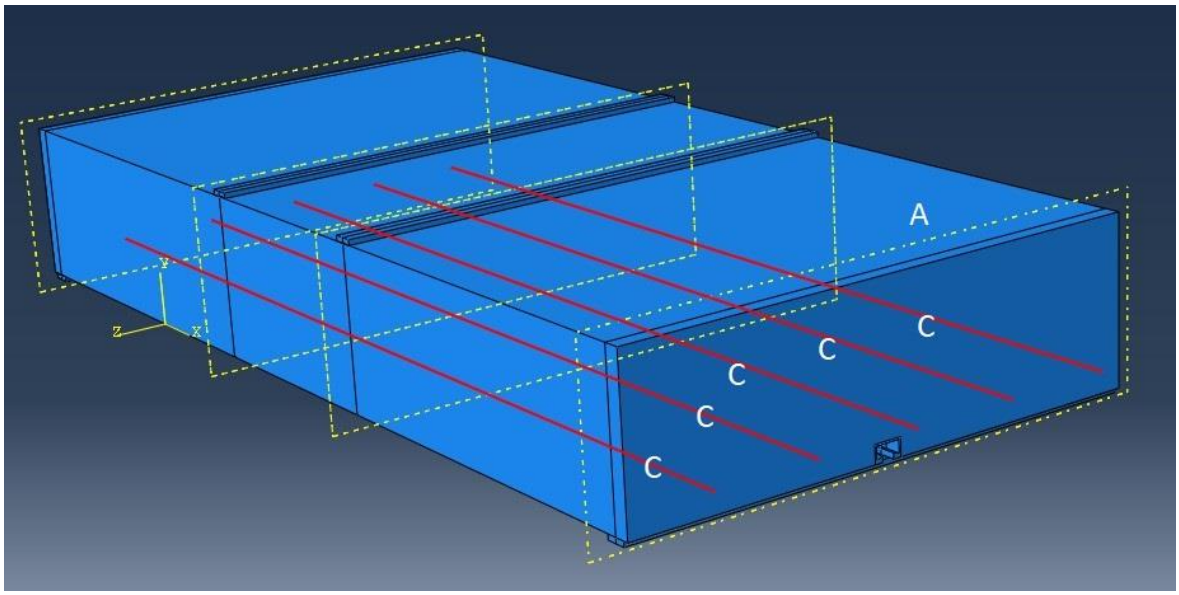

Shape 5.8: Arrangement of the analysis with the reinforcement highlighted

5.3 Materials

On this paragraph, the materials used on the parts of the model are described. Abaqus provides some special functions in order to assign some special features on the materials, so these functions will also be mentioned.

5.3.1 Concrete

Concrete is simulated with the concrete damaged plasticity function. The analyses use concrete C30/37 according to EN1992-1-1. The main strength parameters are presented on Table 5.2.

Table 5.2: Concrete properties

Amount	Value
f_{ck} (MPa)	30
$f_{ck,cube}$ (MPa)	37
f_{cm} (MPa)	38
f_{ctm} (MPa)	2.9
E_{cm} (GPa)	33
ε_{c2}	0.002
ν	0.2

To simulate the concrete damaged plasticity model, the compressive and the tensile behavior and the plasticity parameters must be defined. The behavior of concrete in compression is expressed from equations 5.1 and 5.2 depending on the value of the compressive strain of concrete. The same equation is also applied for design values but on

the analyses, the characteristic values are used. Shape 5.9 shows the stress – strain diagram of concrete. [10], [16], [18]

To define the tensile behavior of concrete and the propagation of cracking, Abaqus provides 3 different ways. The post-failure stress – cracking strain relation, the yield stress-displacement relation and the GFI fracture energy criterion. [6], [7] On this thesis the GFI fracture energy criterion is used. With this approach, the concrete's brittle behavior can be specified directly as a material property. The fracture energy G_f is depended on the mean compressive stress of the material. GFI fracture energy results from expression 5.3 as mentioned in [9] and the cracking displacement at which complete loss of strength takes place is given on equation 5.4. This model assumes a linear loss of strength after cracking as shown on shape 5.10 with $G_1 = G_f$ and $\sigma_{10} = \sigma_{t0}$. [6], [7] Finally, the plasticity parameters used on this thesis arise from the paper of Szczecina and Winnicki (2015) and are shown on table 5.3.

$$\sigma_c = f_{ck}\left(1 - \left(1 - \frac{\varepsilon_c}{\varepsilon_{c2}}\right)^n\right) for\ 0 \le \varepsilon_c \le \varepsilon_{c2} \tag{5.1}$$

$$\sigma_c = f_{ck}\ for\ \varepsilon_{c2} \le \varepsilon_c \le \varepsilon_{cu} \tag{5.2}$$

$G_f = 73 {f_{cm}}^{0.18}$ in N/m with f_{cm} in MPa and for C30/37 G_f = 140.5 N/m (5.3)

$u_{t0} = \frac{2G_f}{\sigma_{t0}}$ where $\sigma_{to} = f_{ctm}$ =2.9 MPa for concrete C30/37 (5.4)

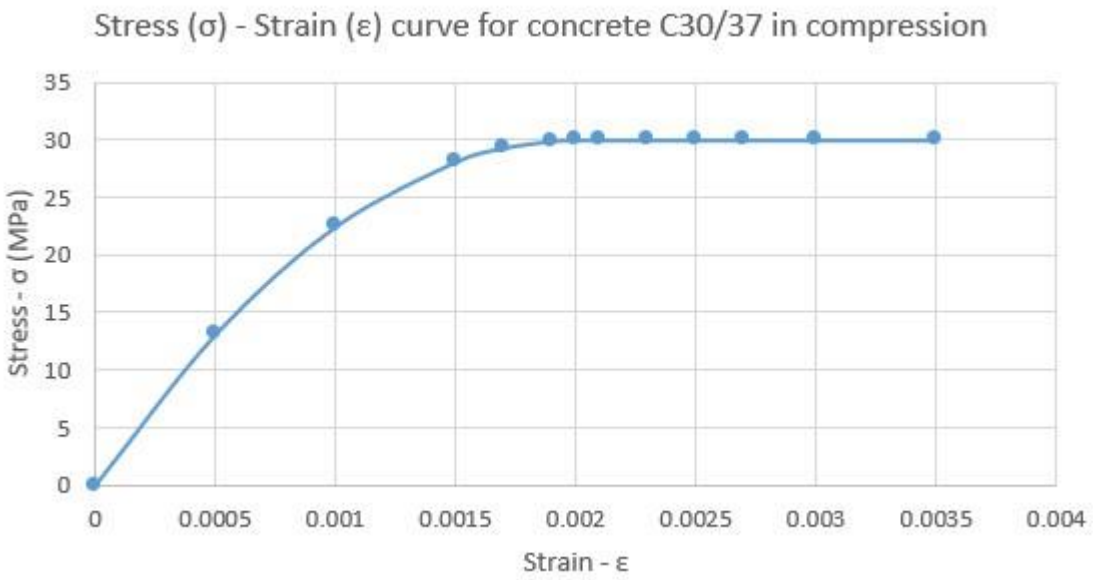

Shape 5.9: Stress – strain diagram for concrete under compression

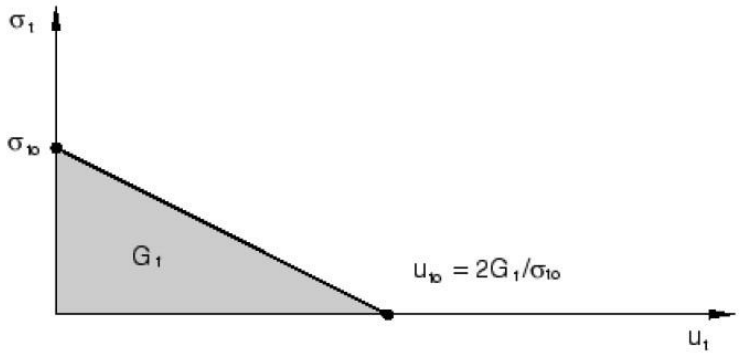

Shape 5.10: GFI fracture energy criterion

Table 5.3: Plasticity parameters [23]

Amount	Symbol	Value
Dilation angle	δ	5
Eccentricity	e	0.1
f_{b0}/f_{c0}	f_{b0}/f_{c0}	1.16
K	K	0.667
Viscocity	μ	0.0001

5.3.2 Reinforcing steel

The material used for the simulation of the steel reinforcement of concrete is steel B500C as mentioned in EN1992-1-1, using the characteristic values and without ductility. The diagram of EN1992-1-1 is presented on shape 5.11. The modulus of elasticity used is E=200 GPa and the Poisson's ratio is ν=0.3. For the simulation of the elastoplastic behavior of steel and to achieve the reallocation of stresses on the steel body part, the plastic behavior was defined. The propagation of plastic strain begins when the yield stress is reached. The plastic strain keeps on, until the regarded failure value of 7.5 % is reached. This plastic behavior is presented on the shape 5.12.

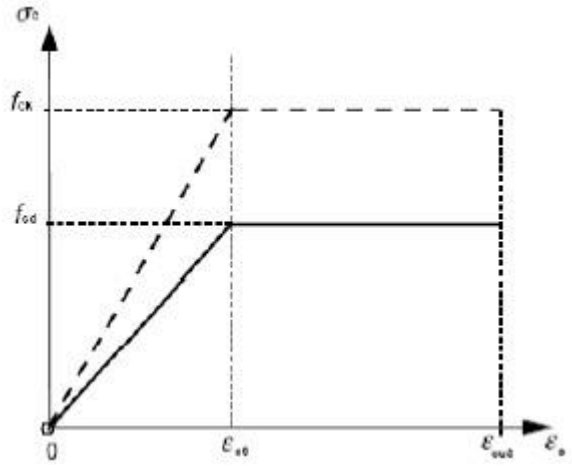

Shape 5.11: Stress-strain diagram from EN1992-1-1 for reinforcing steel

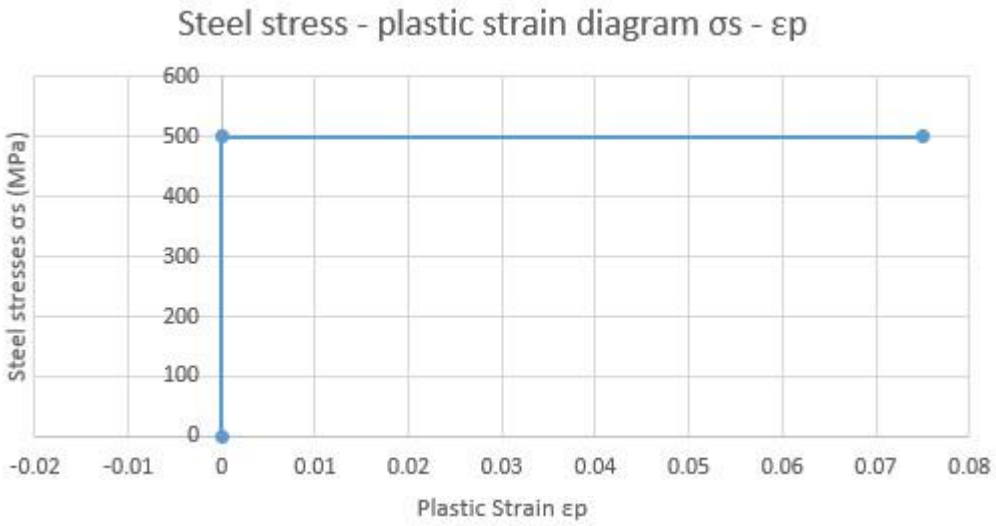

Shape 5.12: Stress-plastic strain diagram for the analyses for the reinforcing steel

5.3.3 Structural steel

The analyses used structural steel S355 according to EN1993-1-1. The modeling of structure steel is similar to the modelimg of the reinforcing steel described before. The value of the modulus of elasticity is E = 210 GPa and the Poisson's ratio is ν = 0.3. No ductility is simulated.

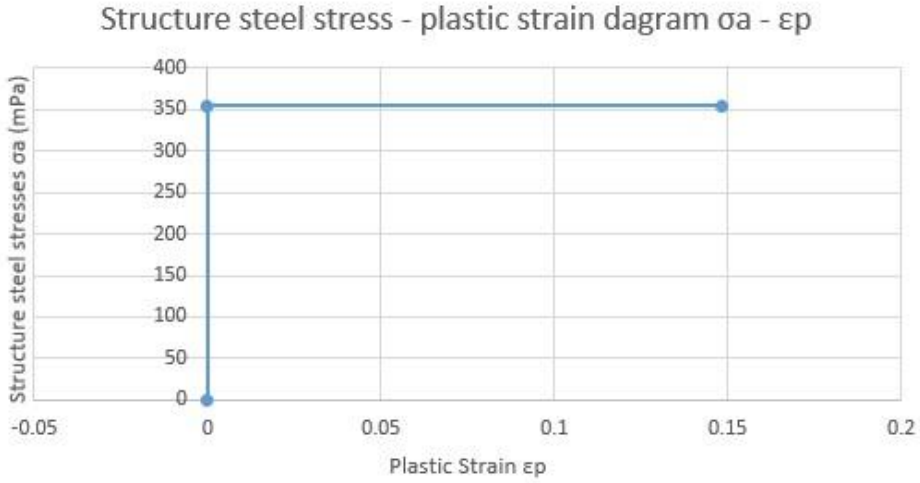

Shape 5.13: Stress-plastic strain diagram for the analyses for the structural steel

5.3.4 Materials for the plates

For the simulation of the plates, an elastic material is used, with modulus of elasticity E = 210 GPa and with Poisson's ratio ν = 0.3.

5.4 Meshing

The calculations are performed using finite element analyses. The meshing of every part is described below.

5.4.1 Concrete part

The concrete part is modeled using 3D-stress elements of linear order with 8 nodes and with reduced integration, from the Abaqus finite element library (C3D8R). Every element is cubic with an edge of approximately 30mm in general. Specifically, near the cast in channel, the mesh is becoming denser, to achieve a better simulation of the interaction between the parts. 40736 elements are used. [6], [7]

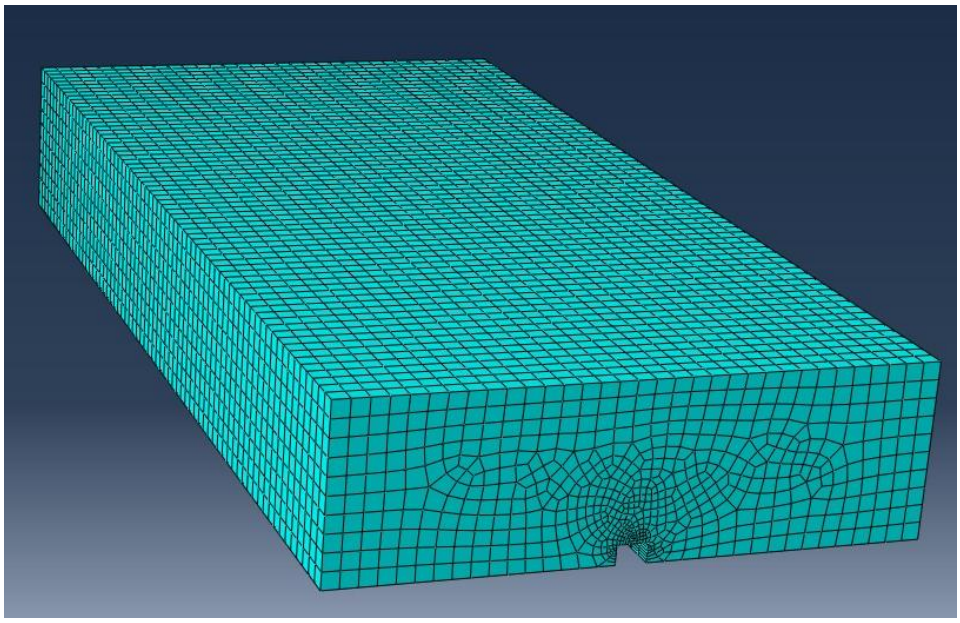

Shape 5.14: Meshing of the concrete part

5.4.2 Cast-in channel part

The cast in channel part is modeled using the same type of elements. The dimensions of the elements are 30mm on their length and 5mm on the section that is bended, to achieve a better simulation of the behavior of the channel. The elements needed to simulate the part are 2546. [6], [7]

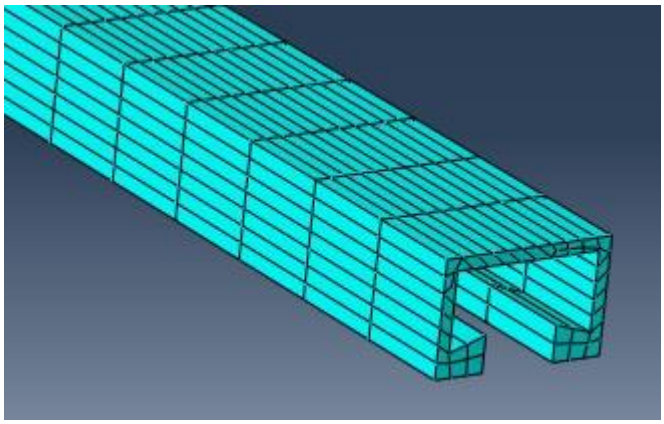

Shape 5.15: Meshing of the cast-in channel part

5.4.3 Steel reinforcement

To simulate the reinforcement, the analyses use 3D truss elements of quadratic order with 3 nodes (T3D3). These elements react to external loads by developing axial stresses. Another type of simulation that could be used is also the 3D stress elements, but this would make the calculations harder. [6], [7]

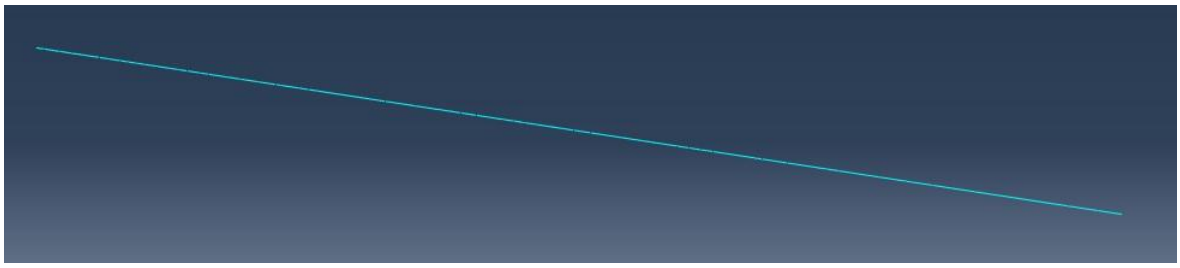

Shape 5.16: Meshing of the concrete reinforcement

5.4.4 Metal plates

The plates are meshed using also C3D8R elements. 66 elements are forced to simulate every plate. [6], [7]

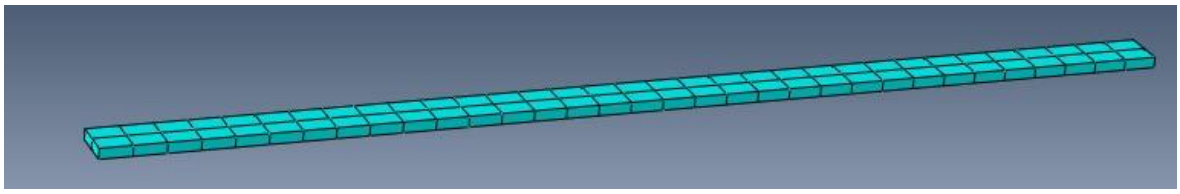

Shape 5.17: Meshing of the metal plates

5.5 Interaction between parts

The interaction between the different parts is simulated by setting the appropriate conditions. The concrete part interacts with all the parts of the model. Between the concrete part and the plates, a hard contact for the transmission of the vertical loads is applied. Additionally, a friction coefficient of 0.3 is applied between the parts. This interaction is also applied between the cast in channel and the plates.

To simulate the interaction between the concrete part and the cast in channel, two different interaction models are assigned, depended on the type of the desired shear connection. These interactions are assigned to simulate the shear bolts, that are not simulated as different parts, because their simulation would make the model more complicated. If the desired shear connection is a full shear connection, a tie constraint is applied on the interface between the cast in channel and the concrete part. In the parametrical analyses of the friction coefficient, on which the partial shear connection is simulated, a hard contact and a friction coefficient between 0 and 1 is applied at the top surface of the cast in channel. The collaboration of the concrete part and the reinforcement is achieved using the embedded type constraint. This constraint is suitable for the modeling of the rebar reinforcement. [6], [7]

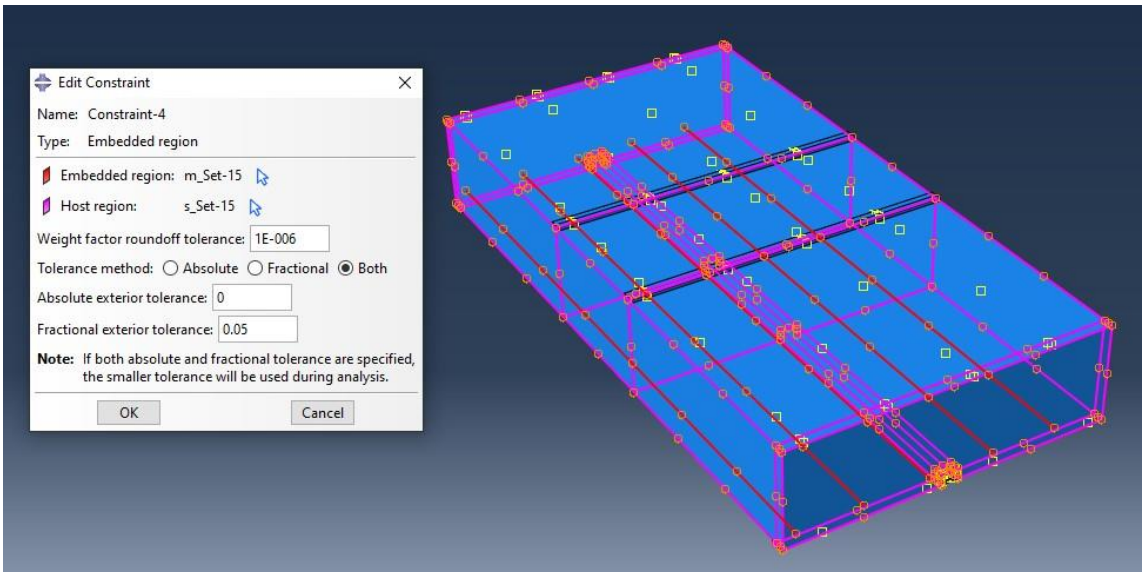

Shape 5.18: Embedded constraint between rebar and concrete

Finally, the simulation of the initial axial force in order to simulate the behavior of the model under compression is achieved by using the tool predefined fields that is provided from Abaqus. Using this tool, the user can assign initial stresses on the desired directions. On the analyses, an initial stress on the longitudinal direction is assigned on the concrete part.

6 Finite Element Analyses

On this chapter the parametrical analyses of the model will be presented. Stresses, displacements and the obtaining extension of the compressive zone of the sections will be examined. The behavior of the section is a function of the steel parts used and of the characteristics of the materials. The analyses aim to compare the different formations of the section and give prominence to the advantages and the disadvantages of every case.

A note that must be stated about the plastic analyses is that because of the computational load from the calculations, the majority of the models cannot lead to deformations where the steel parts reach their maximum plastic strains. Additionally, in some cases the models reach deformations which would not be achieved on a real – life experiment because the calculations can balance on points where no stability exists. This phenomenon is owed to the non – linearity of the material proposed with the CDP model and the plastic behavior of the steel parts used on the analyses. Further explanations about this behavior can be found on the non - linear analyses theory stated in many books and articles. Because of this, in many cases of the finite element analyses there is necessity of finding a step – time, or a displacement or generally a reference variable, where the comparisons will be referenced to.

6.1 Elastic analyses

The elastic analyses aim to detect possible errors in the formation of the model and to give a first thought of the behavior of the sections. Analyses proceeded starting from the concrete section and followingly the steel parts were added. Some results of the calculations are presented. Shape 6.1 shows the stresses on the concrete section for a bending moment of 135 kNm. The maximum compressive strength is -9.3 MPa and the maximum tensile stress is 8.6 MPa. This tensile stress is greater than the tensile resistance of concrete so on a plastic analysis, this stress would not occur. Shape 6.2 shows the allocation of stresses in the middle section.

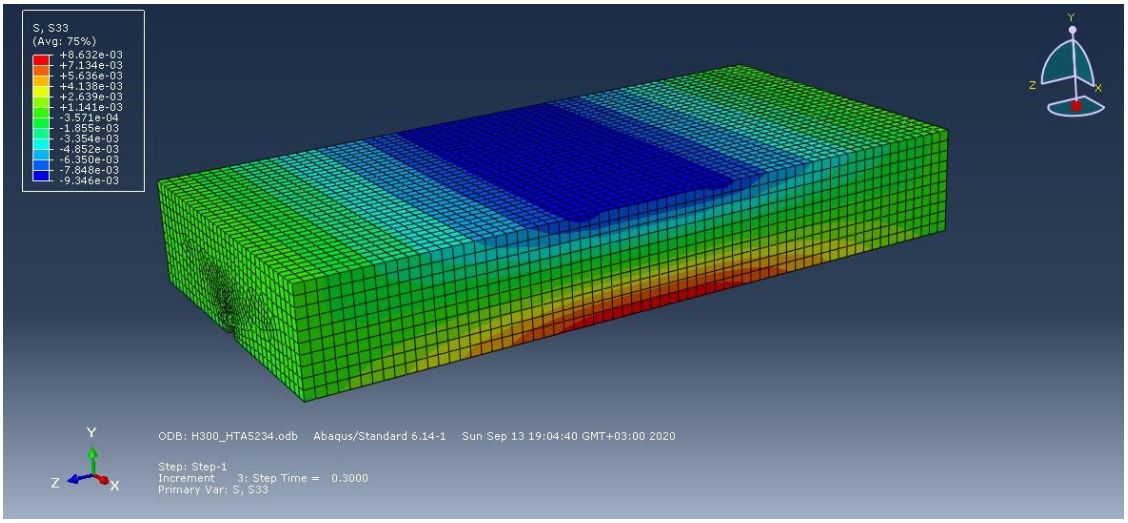

Shape 6.1: Normal stresses on the longitudinal axis of the section for bending moment M=135kNm

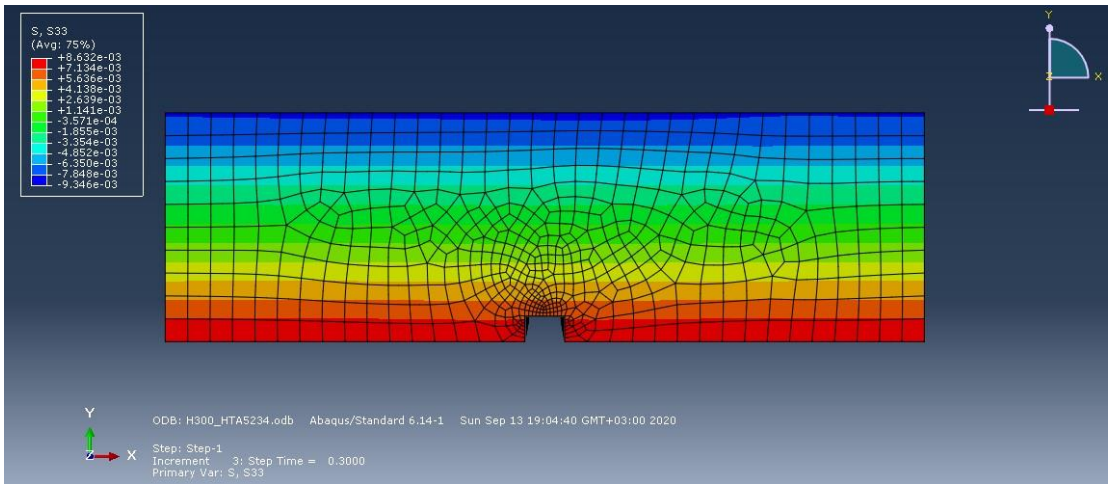

Shape 6.2: Normal stresses on the middle section of the concrete body for bending moment M=135kNm

Followingly, the normal stresses are presented on the HTA-CE 52/34 part and on the rebar with a section of 7.97cm2 (5Ø14). The maximum tensile stress on the HTA CE 52/34 part is 55.1 MPa and on the rebar it is 42.6 MPa as shown on shapes 6.3 and 6.4. Afterwards, picture 7-5 presents the vertical displacement for bending moment equal to 135kNm and picture 7-6 presents the bending moment to vertical displacement diagram for the different models.

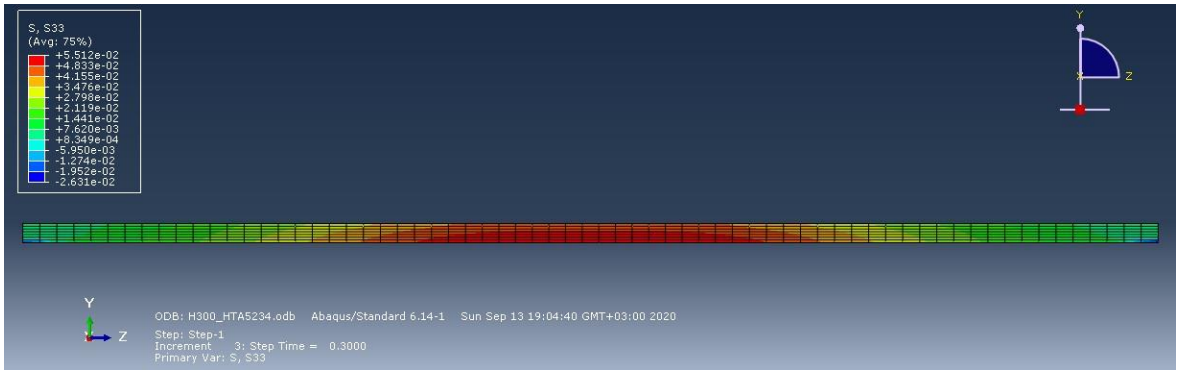

Shape 6.3: Normal stresses on the HTA CE 52/34 part for bending moment M=135kNm

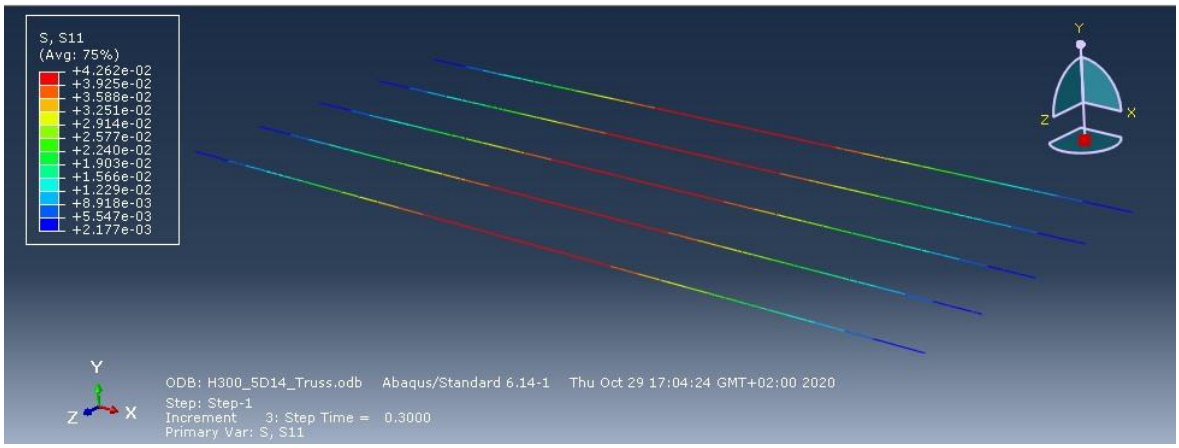

Shape 6.4: Normal stresses on the rebar for bending moment M=135kNm

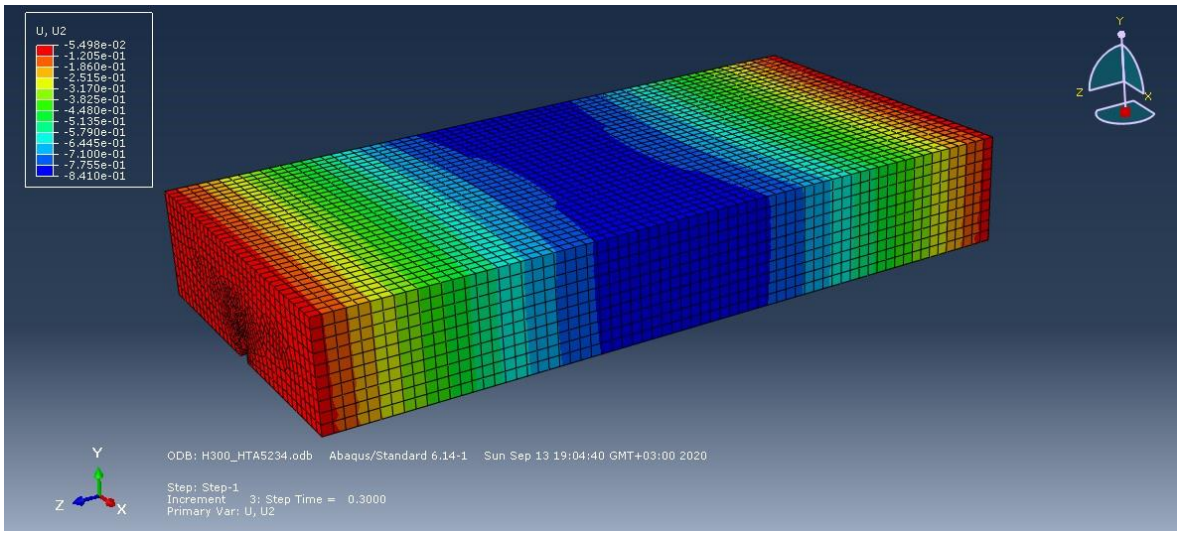

Shape 6.5: Vertical displacements for bending moment M=135kNm

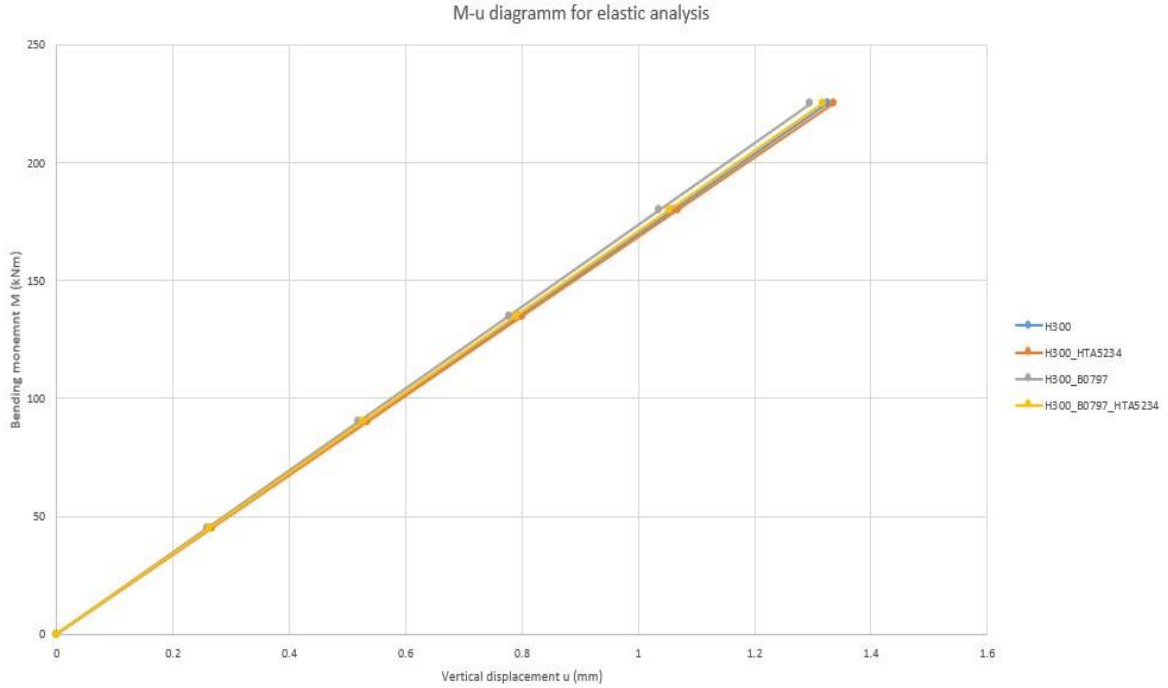

Shape 6.6: Bending moment – vertical displacement diagram for elastic analyses

As it was predicted there are not remarkable differences in the procession of the vertical displacements while raising the load. The stiffness of the section is approximately K=170000 kNm/m and for a bending moment of 135 kNm the vertical displacement is around u=0.8mm. This happens because the oversized body of the concrete part, compared with the volume of the steel parts, determines the propagation of the phenomenon. However, this behavior is not developed as the concrete is cracking when its tensile resistance is surpassed. Cracking affects the stiffness of the section and the results differ significantly from the results of the elastic analysis. The following paragraphs give more details about the plastic analyses of the section and it is worth to compare the charging of the section for the same loads.

6.2 Plastic analyses – Examination of the steel parts used on the section

In order to assess the behavior of the different parts proposed for the analyses, different models were formed. It is interesting to observe the following results:

- Bending moment – vertical displacement diagram
- Stiffness reduction when load rises
- Cracking moment according to the calculations, when plastic zone starts forming
- Compressive zone when the theoretical bending capacity is achieved
- Stresses on the concrete part when cracking begins
- Stresses on the steel parts while cracking propagates
- Strains on the parts of the analyses

The following models are examined:

- Model 01 – Concrete part reinforced with As = 7.97 cm^2
- Model 02 – Concrete part reinforced with As = 1.58 cm^2 and HTA CE 52/34
- Model 03 – Concrete part with HTA CE 52/34
- Model 04 – Concrete part reinforced with As = 7.97 cm^2 and with HTA CE 52/34

Shape 6.7 presents the bending moment – vertical displacement diagram. On this diagram it is obvious that the initial stiffness of the section is the same, because the concrete part is the main variable that influences this quantity. Also, with a first sight, we can observe that the cracking moment of the section is around 50kNm and after that, a reduction on the stiffness is taking place. This happens because the tensile stresses create the cracks that lead to this phenomenon. After that point, the section keeps carrying the additional loads, as long as the steel parts can provide their section to bear the occurring tensile stresses and the compressive strain of concrete is lower than the strain where concrete fails. The more the load is increased, the more the diagram tends to be horizontal and this finally happens, when the steel parts reach their maximum capacity. The reduction on the stiffness of the section is presented on shape 6.8.

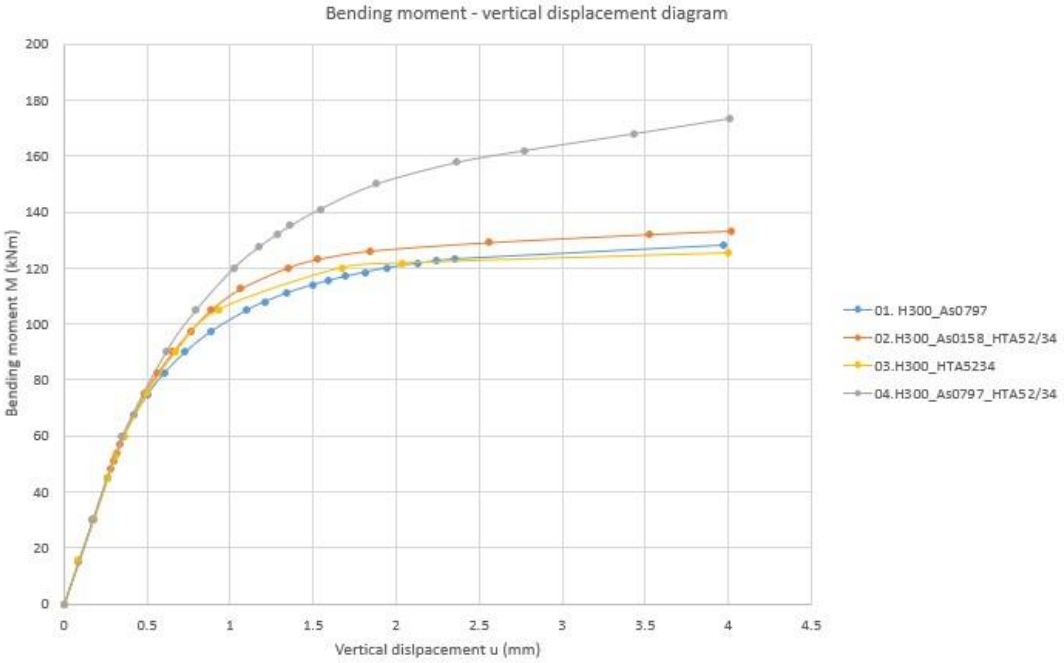

Shape 6.7: Bending moment – vertical displacement diagram for plastic analyses comparing the influence of the different parts used

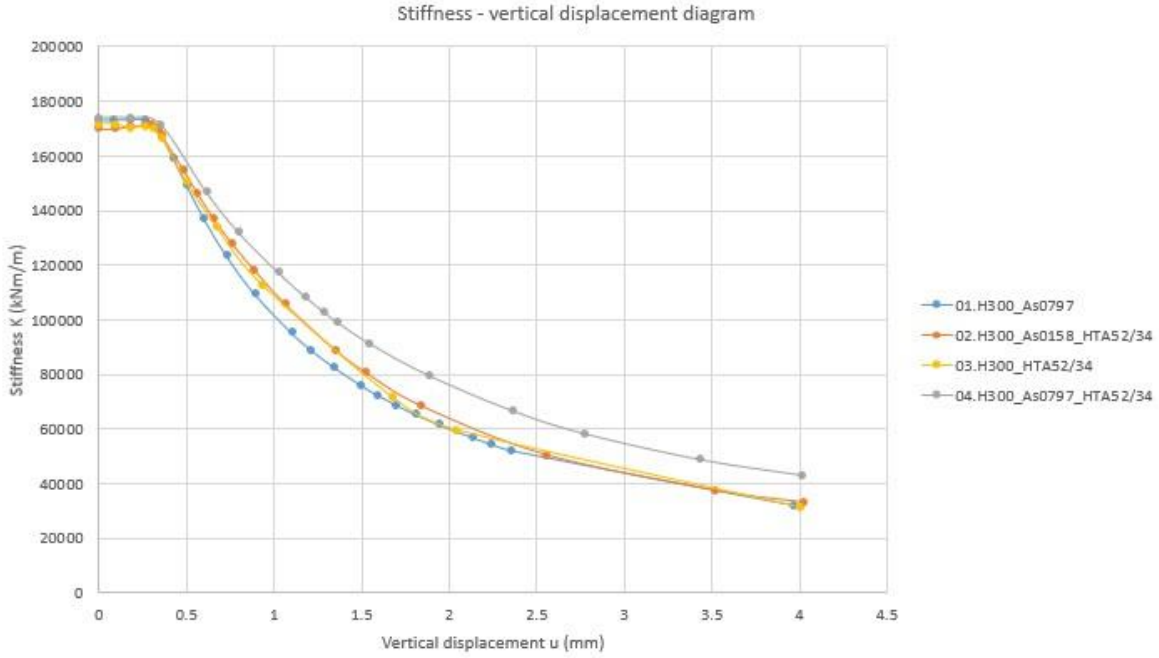

Shape 6.8: Stiffness – vertical displacement diagram for plastic analyses comparing the influence of the different parts used

Followingly, the study is analyzing the diagrams presented, by taking a closer look on the occurring stresses and strains of the parts of the models.

6.2.1 Model 01 - Concrete part reinforced with As = 7.70 cm^2

On this model p = 0.005 kN/mm^2 which means that the maximum value of P = 200kN and the maximum bending moment could be 150kNm. The cracking moment of the model is the moment when plastic zone starts forming. In model 01, this happens on step time 0.32,

when the bending moment is 48kNm and the vertical displacement is 0.28mm as shown on shape 6.9. On this time, the tensile stress on the concrete part is 2.9MPa as we can observe on shape 6.10 and this is the tensile capacity of the material used on the analyses.

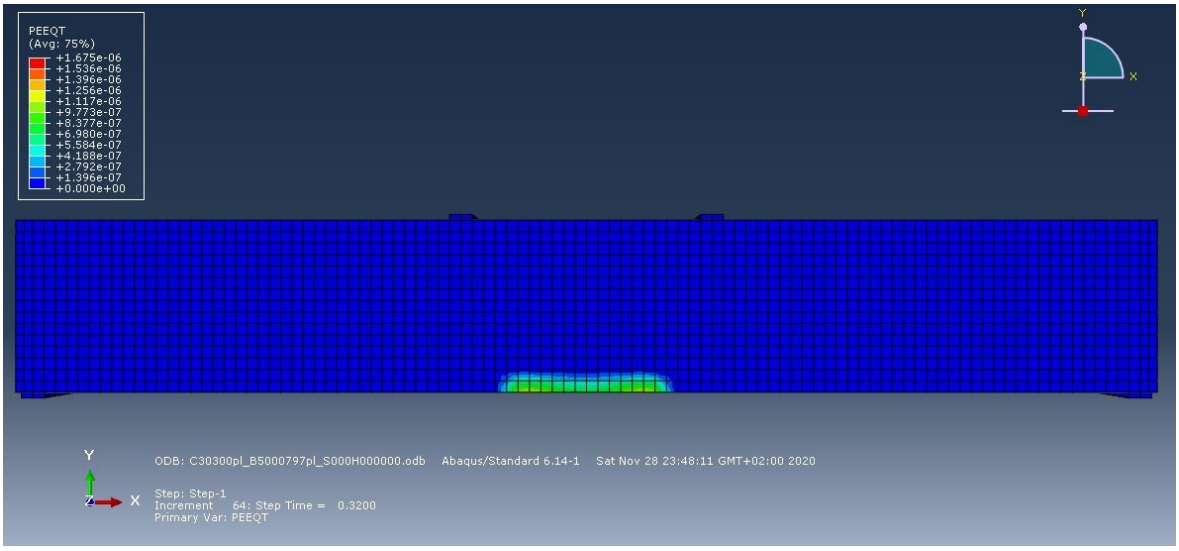

Shape 6.9: Plastic zone on step time 0.32

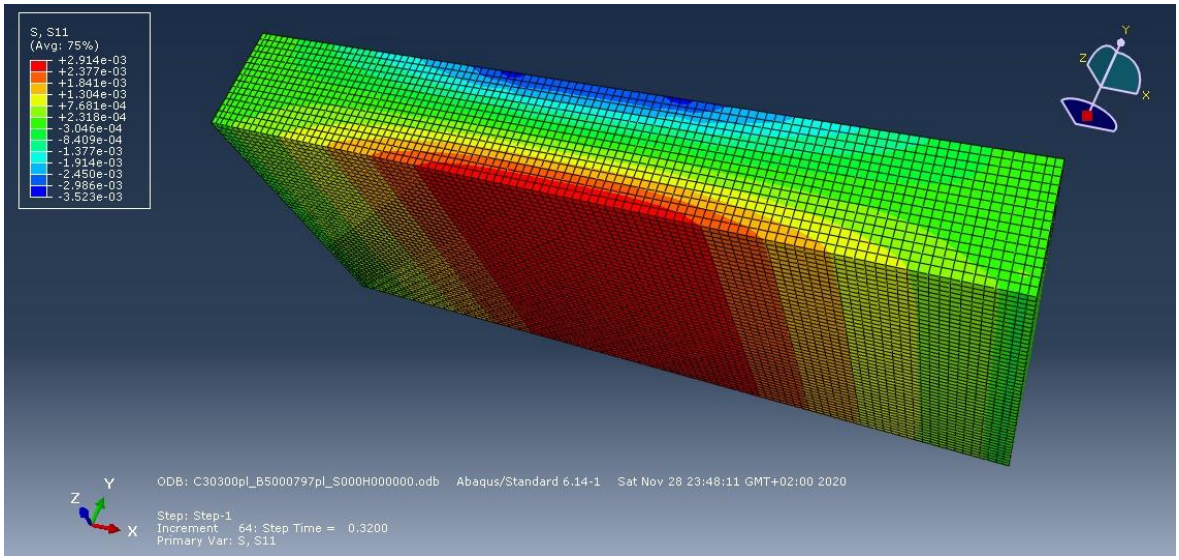

Shape 6.10: Normal stresses on the concrete part when cracking starts propagating

As the load raises, more elements of concrete reach the tensile capacity and crack. At the end of the analysis, the elements that have formed inelastic strain are shown on shape 6.11. From this result we can state that the compression zone of the section is about 8cm. This result corresponds to the time when the vertical displacement of the section is 4mm. On this time step the bending moment is 128kNm. Another observation to be mentioned is that after cracking starts, the steel parts are forced to carry the extra tensile stresses. On shape 6.12 the tensile stresses on the rebar are presented. It is worth mentioning that after the cracking moment, the rhythm of the increase of the tensile stress on the rebar is more intense.

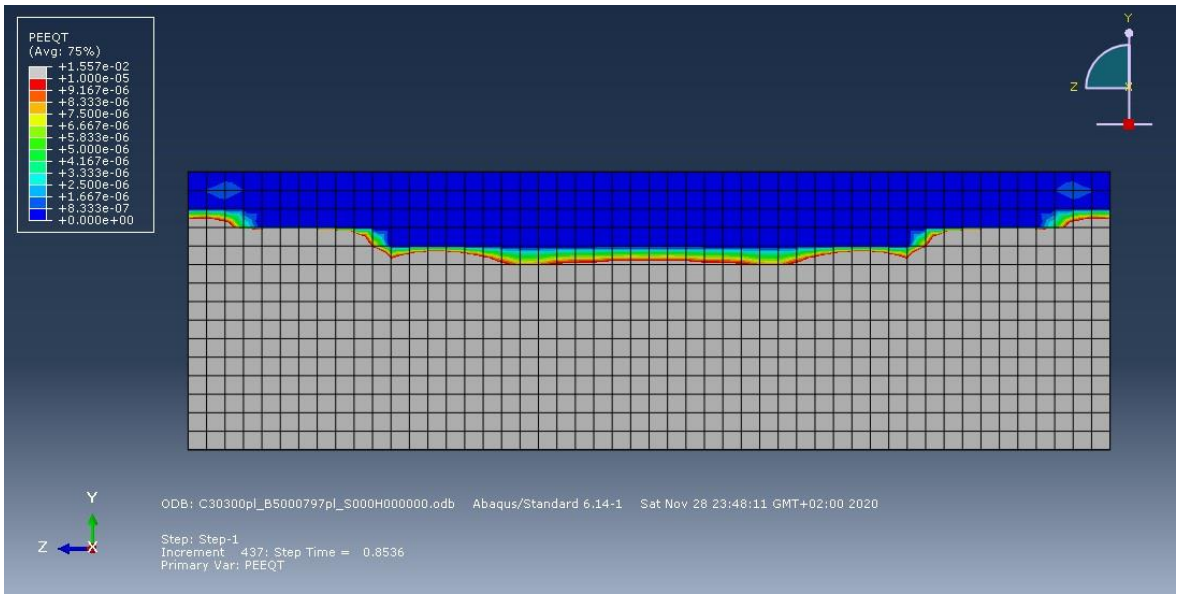

Shape 6.11: Inelastic strains on the concrete part

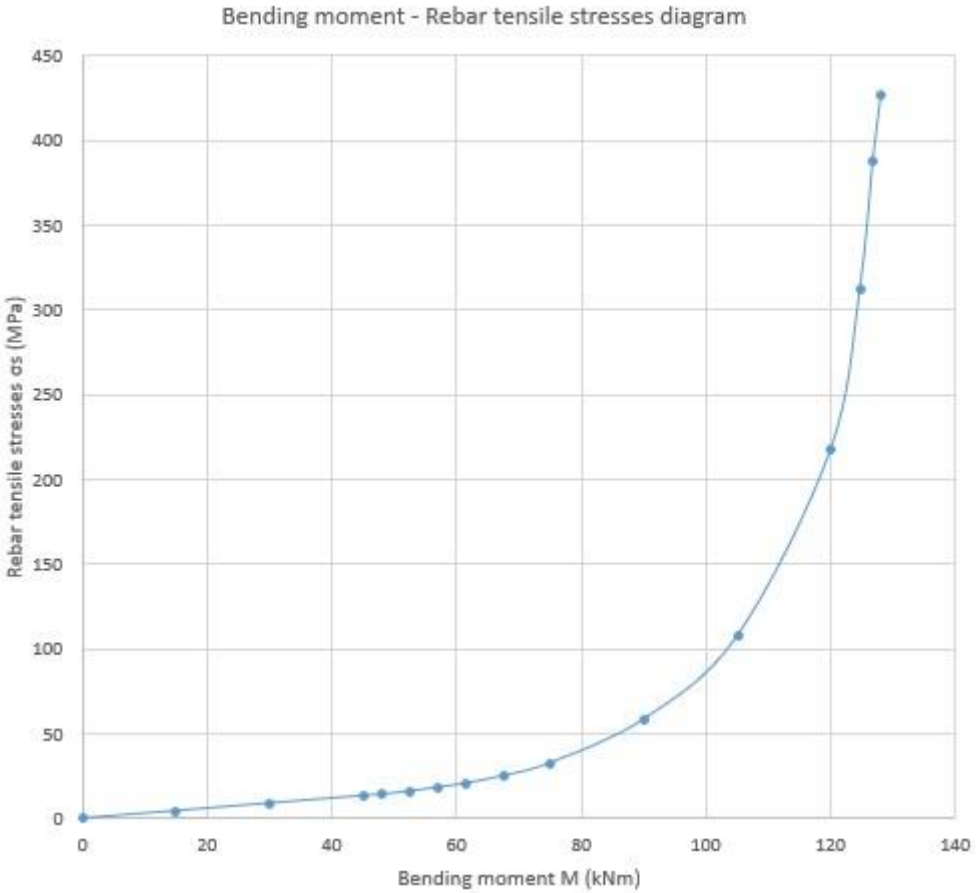

Shape 6.12: Tensile stresses on the rebar

A closer look on the behavior of concrete is useful. Shape 6.13 presents the development of compressive stresses on the concrete part on the upper side of the middle section. It is observed that the concrete part has not reached its maximum potential on carrying compressive stresses.

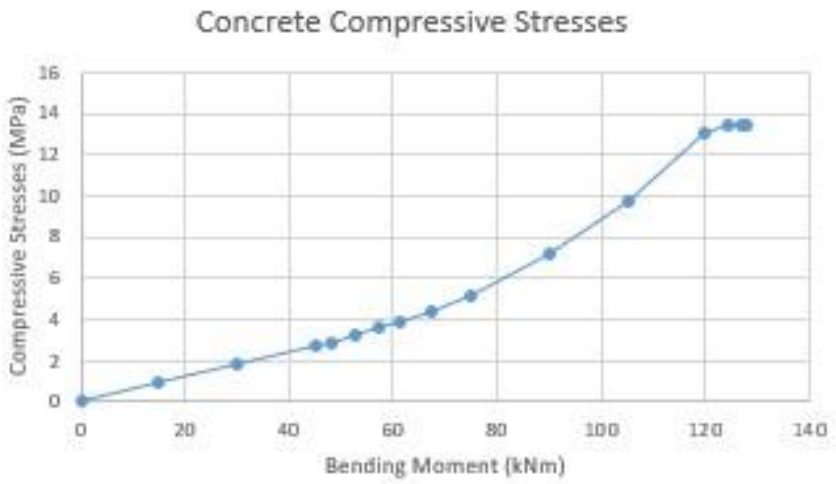

Shape 6.13: Concrete compressive stresses

The behavior observed on this analysis denotes that this section could possibly balance on higher loads. However, convergence problems did not allow for further raising of the load. However, useful results arise about the behavior of a reinforced concrete section without a cast – in channel embedded, so these results can be used to compare this model with the other models of the analyses.

On the following paragraphs, the influence of the use of the different parts of steel on the stresses of the rebar and the cast-in channel is evaluated.

6.2.2 Model 02 - Concrete part reinforced with As = 1.58cm^2 and HTA CE 52/34

This model is simulated, aiming to find out the influence of the replacement of 6.12 cm^2 of reinforcement with 6.12 cm^2 of steel section. On this case, p = 0.005 kN/mm^2. Cracking begins on step time 0.315, where the bending moment is 47.25kNm, so this is the cracking moment of this section. As mentioned in model 01, after cracking begins to propagate more concrete elements enter the plastic zone. After that time, the steel parts are enforced to carry the additional loads. Shape 6.14 shows the tensile stresses of the steel parts. It is observed that the steel parts gain additional stresses after the moment that concrete cracks. It seems that the cast-in channel is the first to receive the additional stresses, however as the analysis propagates, the reinforcing steel takes on tensile stresses and reaches its yield stresses.

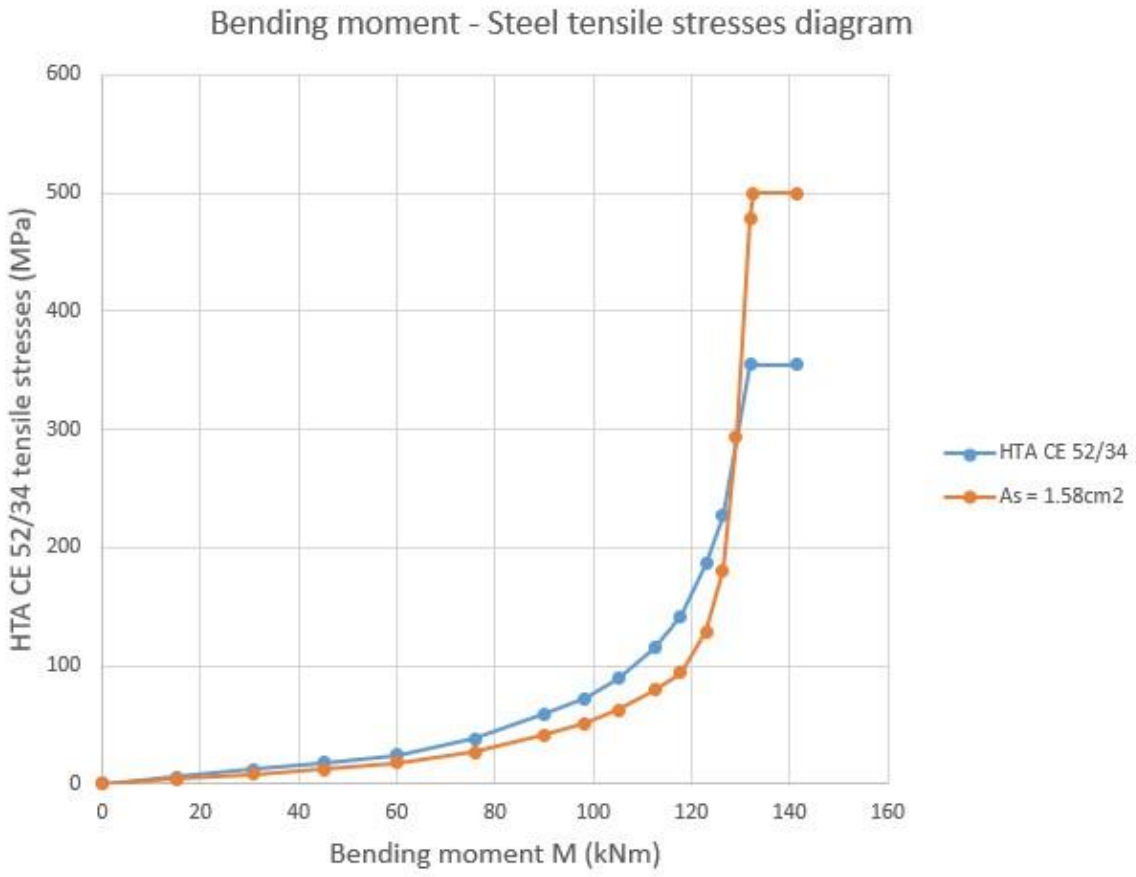

Shape 6.14: Tensile stresses on the steel parts

Another characteristic worth to be mentioned is the compression zone at the time when vertical displacement is 4mm. Shape 6.15 shows that at the middle section the compression zone is approximately 7 cm. Taking a closer look at this picture, it is observed that as we leave the middle of the section where the cast in channel is, a smaller compression zone in formed. This seems to happen because the influence of the cast – in channel is weakened and concrete forms plastic zone aiming to equal the force of the reinforcing steel that is located near the side of the section and only a little percentage of the force that comes from the cast – in channel. This observation is a first indication to reach a result of a suggested effective width for the cast – in channels.

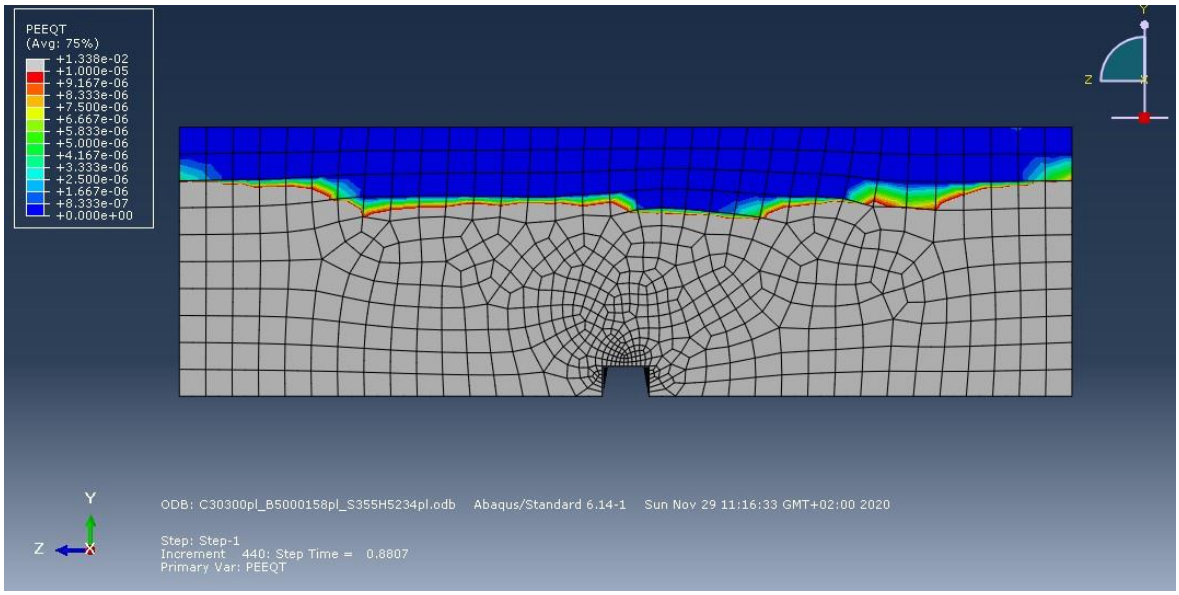

Shape 6.15: Inelastic strains at the time step that corresponds to 4mm vertical displacement – model 02

6.2.3 Model 03 - Concrete part with HTA CE 52/34

This model is simulated, aiming to find out the behavior of a section of concrete, reinforced with a cast-in channel with profile HTA CE 52/34. On this case, p = 0.005 kN/mm^2. The cracking of the concrete section starts on time step 0.3104 where the bending moment is 46.56kNm. The plastic zone formed at the time that corresponds to 4mm vertical displacement of model 03 is presented on shape 6.16. The same observation as model 02 about the form of the plastic zone can be observed also on this case. Taking a closer look at more steps of the analysis, it seems that the cast – in channel influences the whole width of the section and only in the final steps, the formation of the plastic zone becomes more intense at the sides of the section.

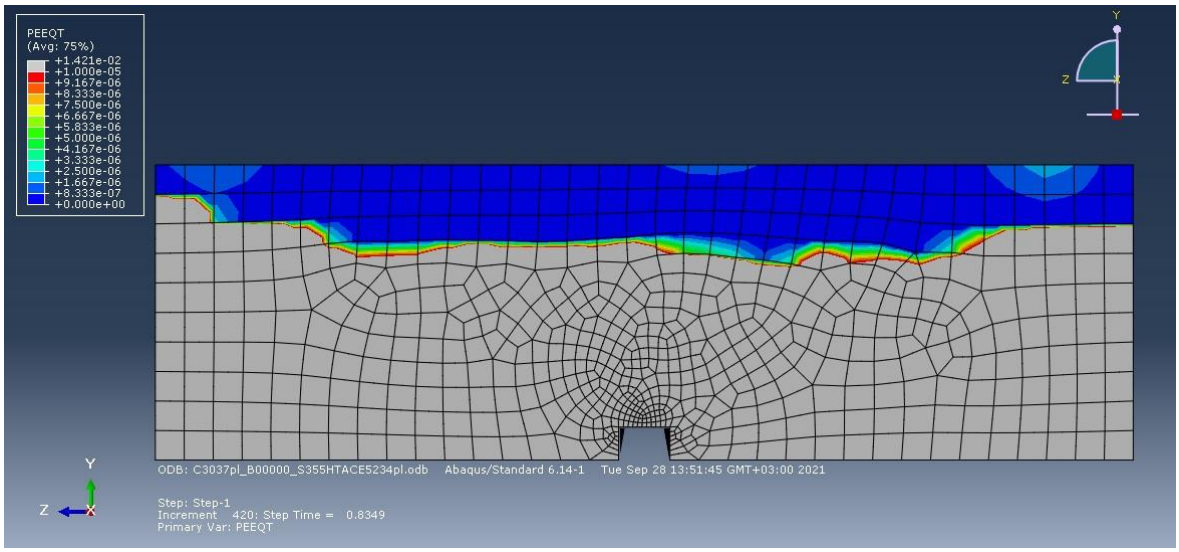

Shape 6.16: Inelastic strains at the time step that corresponds to 4mm vertical displacement – model 03

6.2.4 Model 04 - Concrete part reinforced with As = 7.70 cm^2 and with HTA CE 52/34

This model is simulated, aiming to find out the behavior of a section of concrete, reinforced with a cast-in channel with profile HTA CE 52/34 and with 7.70cm^2 of steel reinforcement. On this case, p = 0.01 kN/mm^2. Shape 6.17 shows the compression zone when the vertical displacement is 4mm. The extend of the compression zone is approximately 9.5cm on this case.

Shape 6.18 shows the normal stresses on the concrete part on the step time mentioned. It is observed that the bottom side of the model is almost under tension at its total range. On the middle sections the tensile stresses conquer a higher height of the section. It can be observed that the maximum compressive stress on the concrete part is 28 MPa at this stage. A notice that can be stated because of these shapes is the symmetry of the formation of the compression zone. This notice makes us state that the influence of the cast – in channel reliefs the total width of the section in all its range. As a result, we can suggest that a lower limit of the effective width of the composite section is the width used on the analyses which is equal to 1m.

Followingly, shapes 6.19 and 6.20 show the Von Mises stresses and the elastic strains of the cast-in channel, on the step time that we have referred to. On that stage, stresses have reached the maximum capacity on some elements and inelastic strains start forming.

Shape 6.21 shows the tensile stresses of the steel parts. From this diagram it is observed that at the initial stage of the analysis, the HTA CE 52/34 carries more tensile stresses than the reinforcement. When the cast – in channel reaches its yield stress, the stresses of the reinforcement rise with a higher rhythm. From this observation, it is concluded that the cast-in channel reliefs the stresses of the rebar. Additionally, a look on the propagation of the compressive stresses on the concrete part is needed. Shape 6.22 shows the compressive stresses on the middle section of the concrete part. The value of 30 MPa is reached when the bending moment of the section is about 130 kNm. Finally, shape 6.23 presents the compressive normal stress versus inelastic strain on the concrete section. It is observed that inelastic strains start when the value of 13.125 MPa is reached. After that, the inelastic strains rise according to the compressive behavior diagram defined. However, it would be more effective if on a further investigation, a downwards sector on the yield stress – inelastic strain diagram of the material of the model was defined.

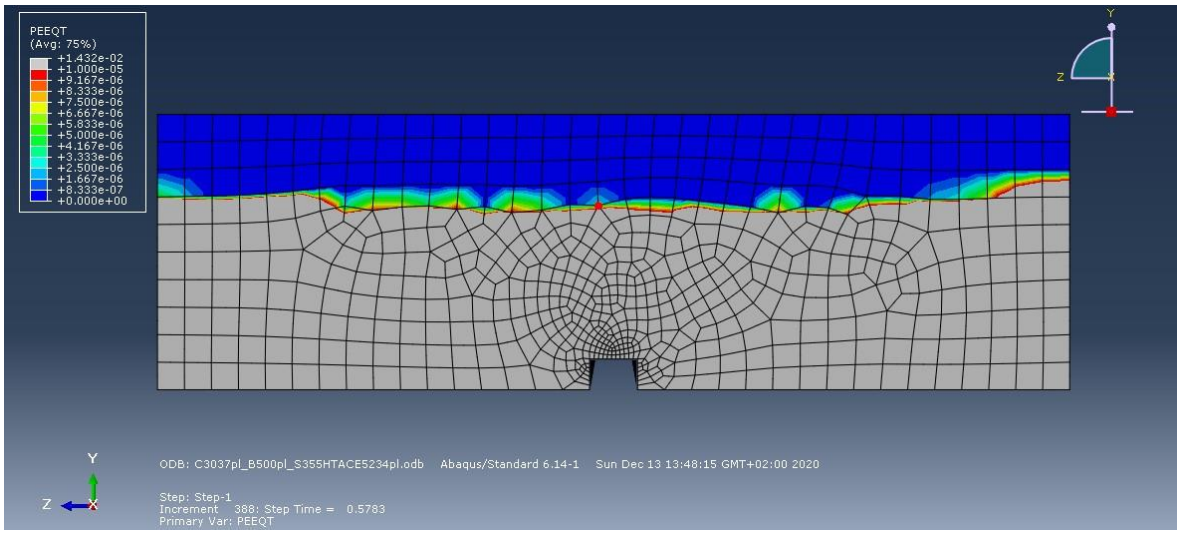

Shape 6.17: Inelastic strains at the time step that corresponds to 4mm vertical displacement – model 04

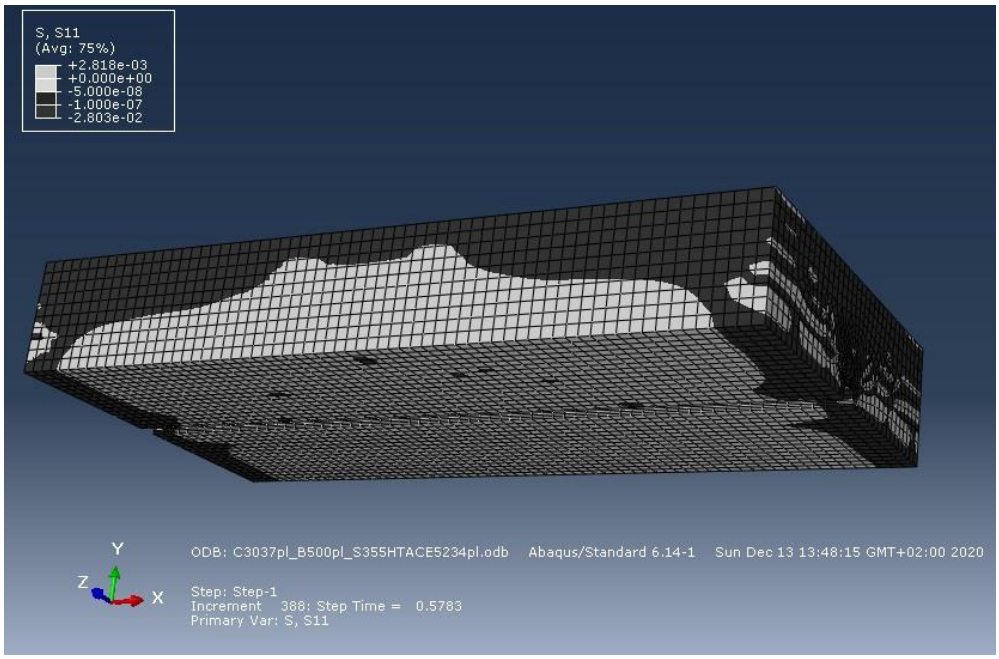

Shape 6.18: Tensile and compressive stresses on the concrete part at the time step that corresponds to 4mm vertical displacement – model 04

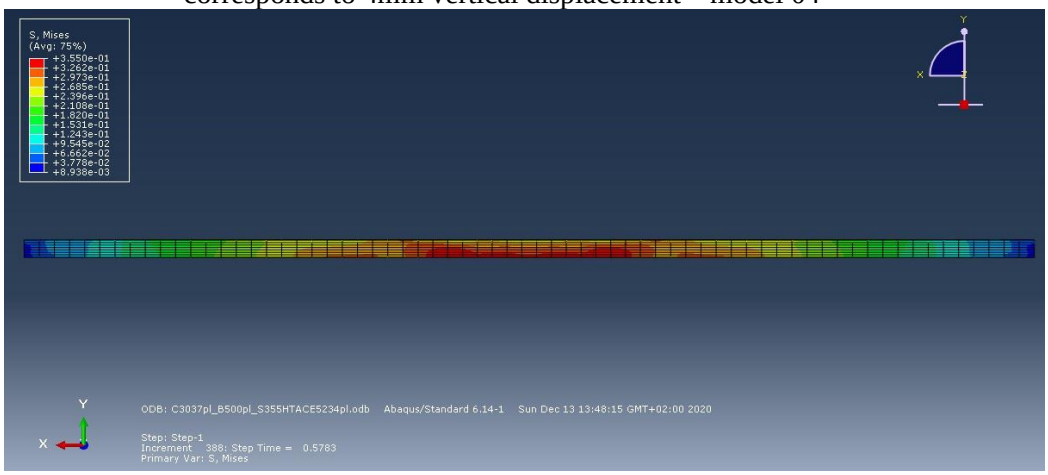

Shape 6.19: Von Mises stresses on the cast – in channel part at the time step that corresponds to 4mm vertical displacement – model 04

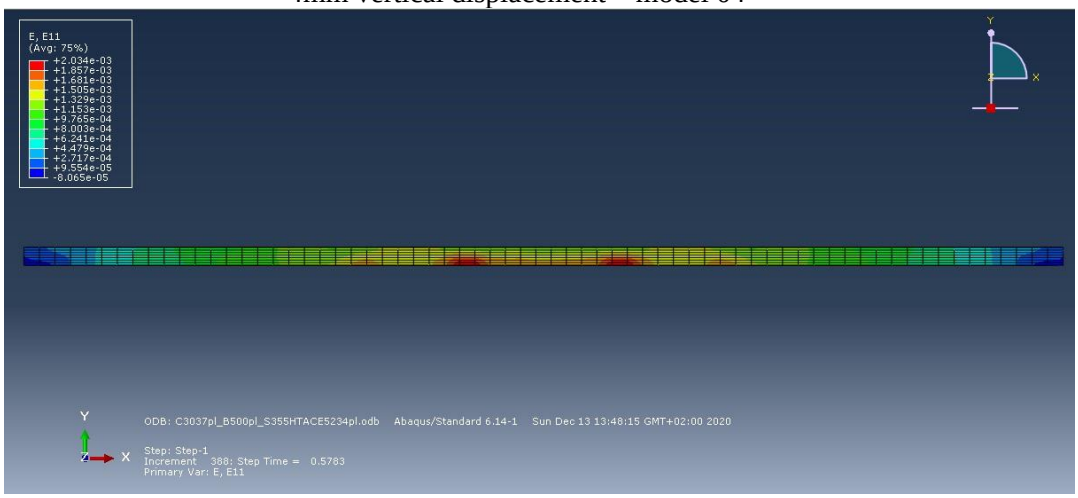

Shape 6.20: Elastic strains on the cast – in channel part at the time step that corresponds to 4mm vertical displacement – model 04

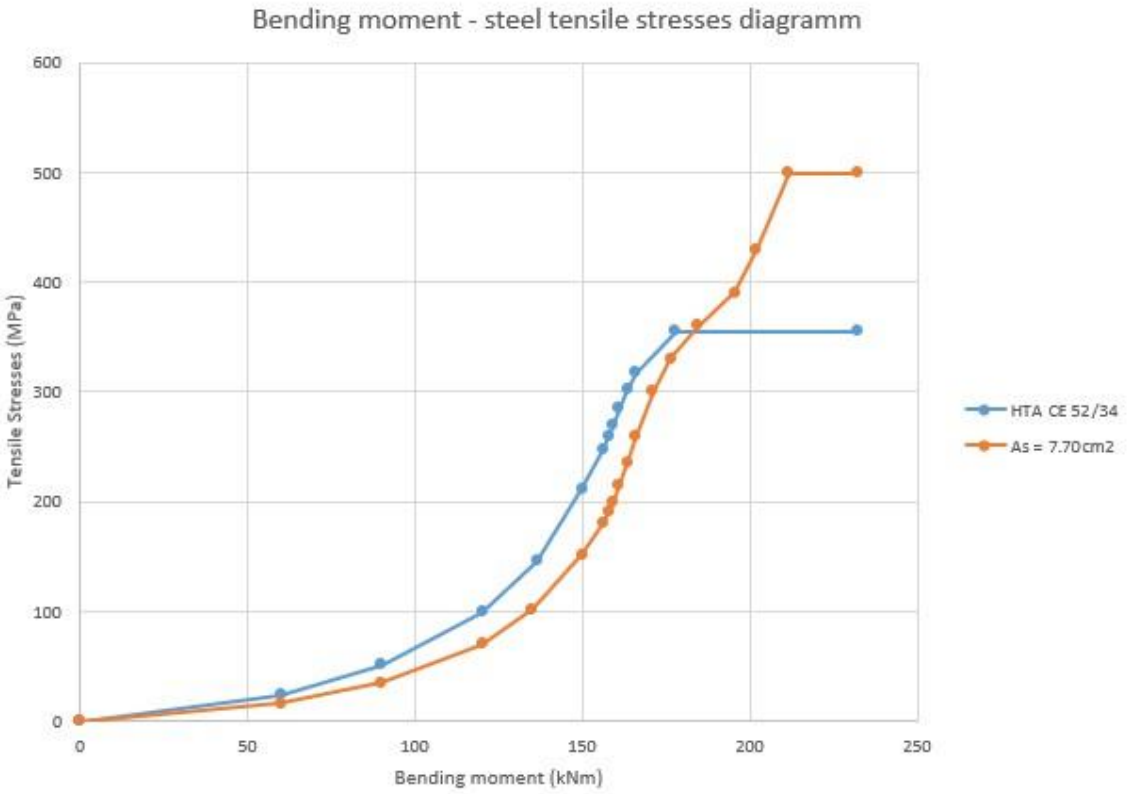

Shape 6.21: Tensile stresses on the steel parts on model 04

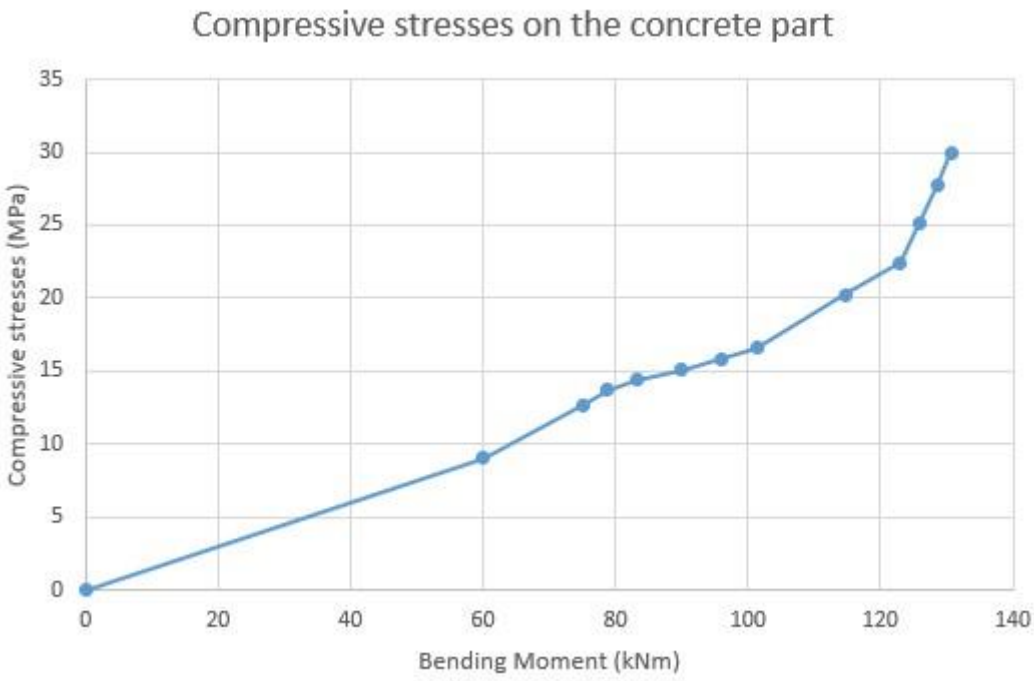

Shape 6.22: Compressive stresses on the concrete part up to 30MPa

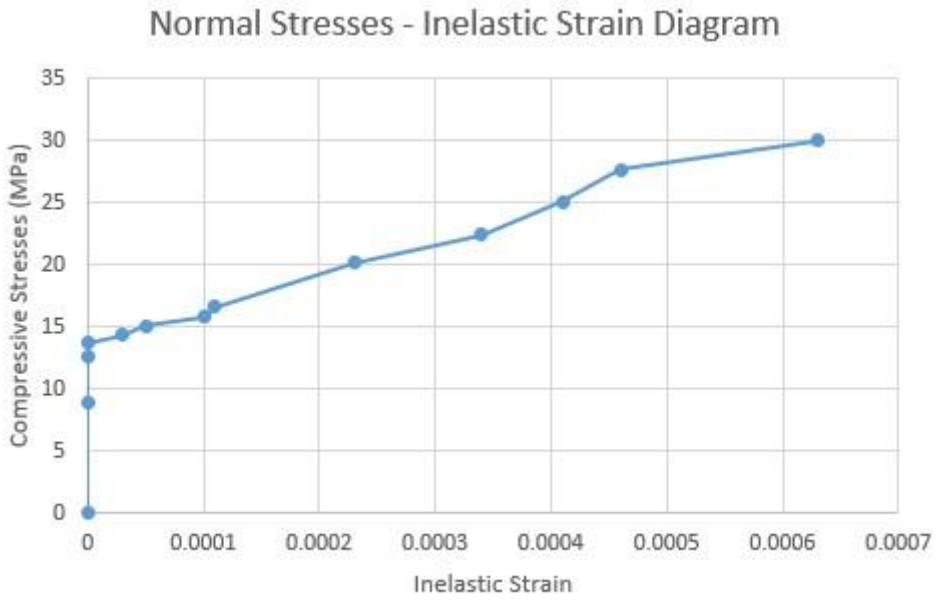

Shape 6.23: Normal stresses – inelastic strain diagram on concrete part

Shapes 6.24 and 6.25 show the comparison of the tensile stresses of the steel parts between the four different models. The first diagram shows the tensile stresses of the HTA CE 52/34 cast – in channel and the second shows the tensile stresses of the reinforcement. From the results mentioned until this point, it is concluded that the existence of the cast – in channel, enhances the bending behavior of the section. The section gets stiffer as the load rises, the reinforcement is alleviated because of the cast – in channel and generally the section can reach higher bending moments when the cast – in channel exists. One of the reasons for the last result is the no need for coating on the cast – in channel, making it locate on the outer side of the section and thus raising the lever – arm between the tensile and the compressive forces of the section.

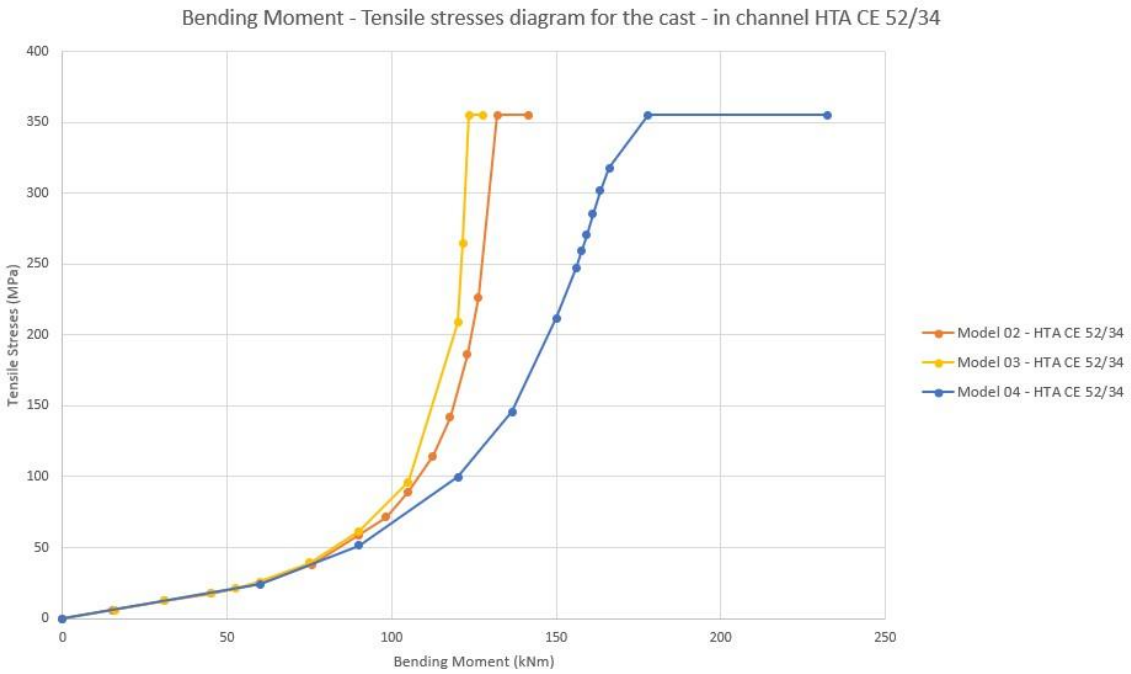

Shape 6.24: Comparison of the tensile stresses on the HTA CE 52/34 cast – in channel for the different models

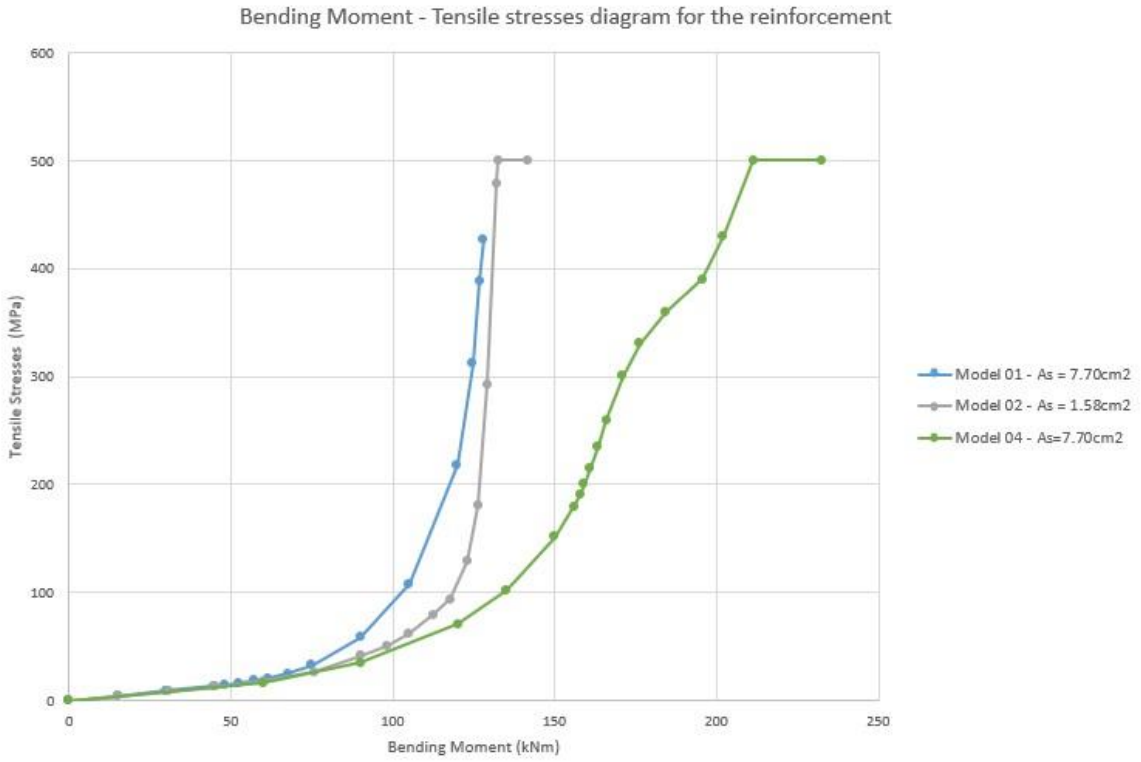

Shape 6.25: Comparison of the tensile stresses on the reinforcement for the different models

6.3 Plastic analyses – Examination of the cast – in channel section

On this paragraph, the following models are compared with model 04.

- Model 05 – Concrete part reinforced with As = 7.97 cm^2 and with HTA CE 55/42
- Model 06 – Concrete part reinforced with As = 7.97 cm^2 and with HTA CE 72/48

6.3.1 Model 05 - Concrete part reinforced with As = 7.70 cm^2 and with HTA CE 55/42

On this model, the area of the cast – in channel is 8.25cm^2. The maximum assigned load is, p = 0.02 kN/mm^2. As it was predicted cracking starts on step time 0.08, when M = Mcr = 48kNm which is approximately the same cracking moment as the models mentioned on paragraph 6.2. Shape 6.26 shows the compression zone formed in the middle section of the beam when the vertical displacement is 4mm at step time 0.3054. The extent of it is about 10cm and the bending moment is M=183kNm. The presence of tensile and compressive stresses on the model can be observed on shape 6.27. The maximum compressive stress is 26MPa on this stage of the analysis.

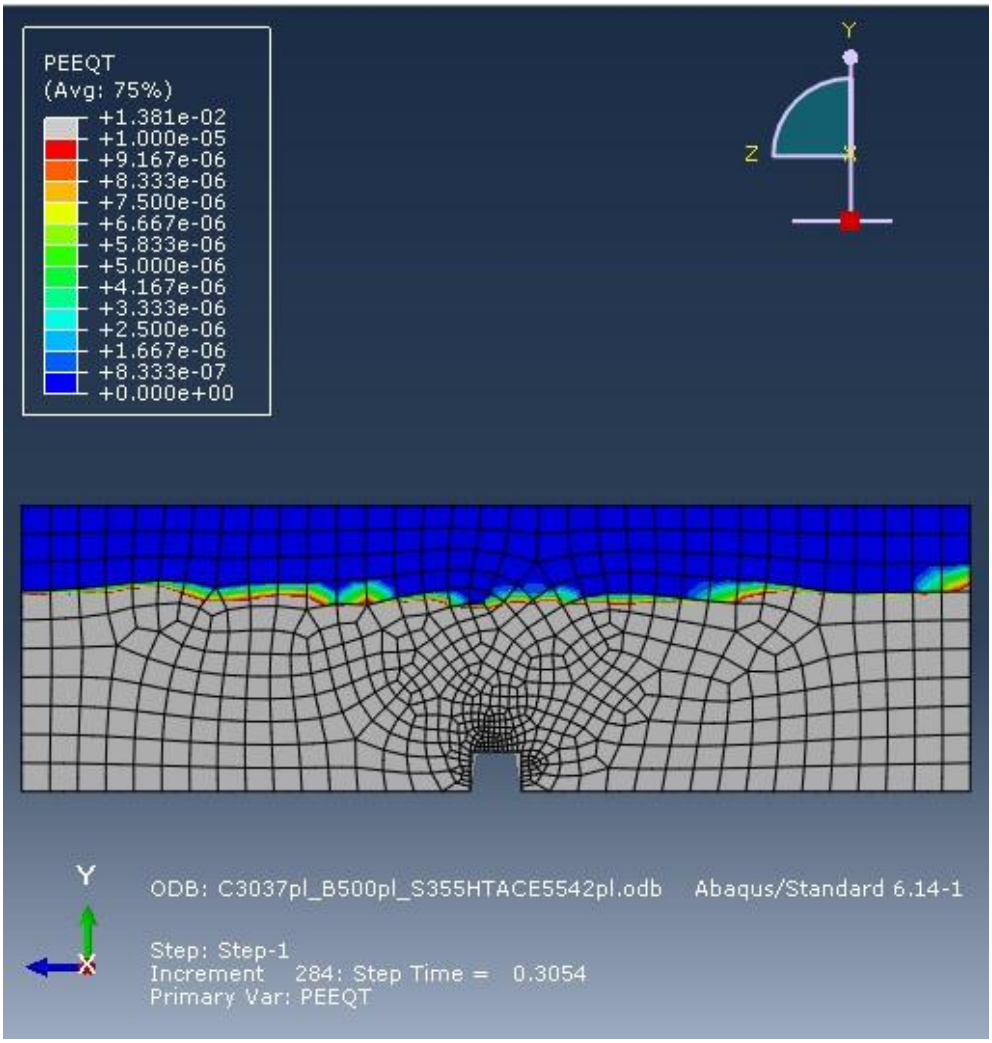

Shape 6.26: Cracked region at the time step that corresponds to 4mm vertical displacement – model 05

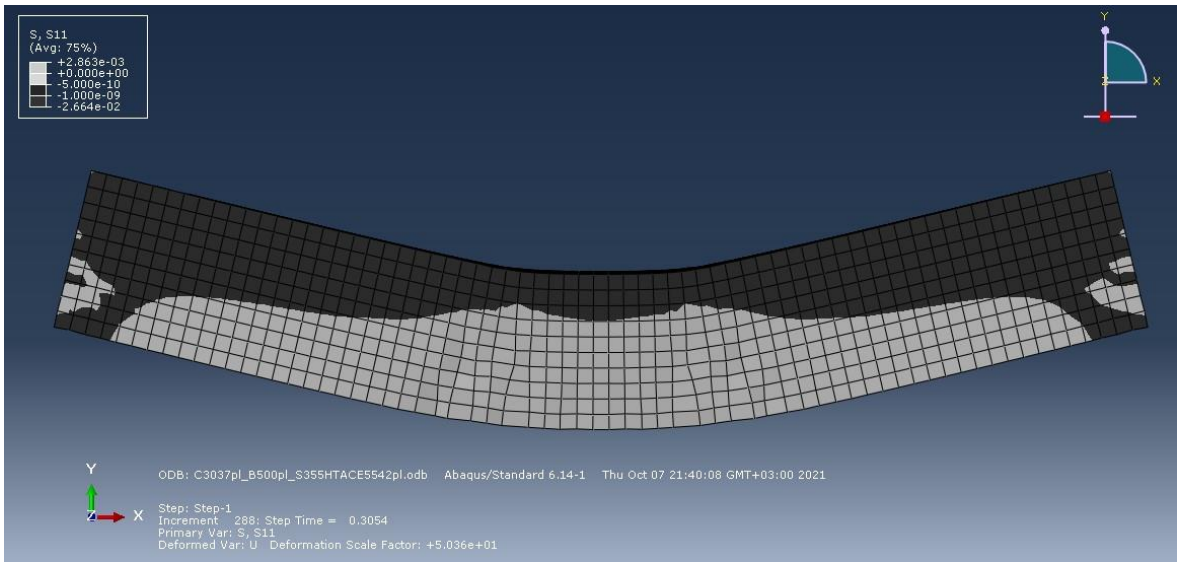

Shape 6.27: Stresses on the concrete part that correspond to 4mm vertical displacement – model 05

This model succeeded in reaching convergence on high levels of strains and therefore it is used to obtain some results about the situation that conquers when strains near failure occur. Shapes 6.28 and 6.29 present the plastic strains and the corresponding Von Mises stresses of the cast – in channel on its deformed shape when the plastic strain reaches the value 0.14831 which is the limit of the inelastic strain that has been defined for steel S355. It can be observed that the inelastic strains conquer the whole body of the section on the middle of the model and that a wide range of the cast in channel carries its maximum capacity. For this reason, these parts must be designed appropriately, in order to be adequately ductile to carry these stresses, when uses for increasing the bending capacity of the section. On this time step, the bending moment approximately M = 363 kNm.

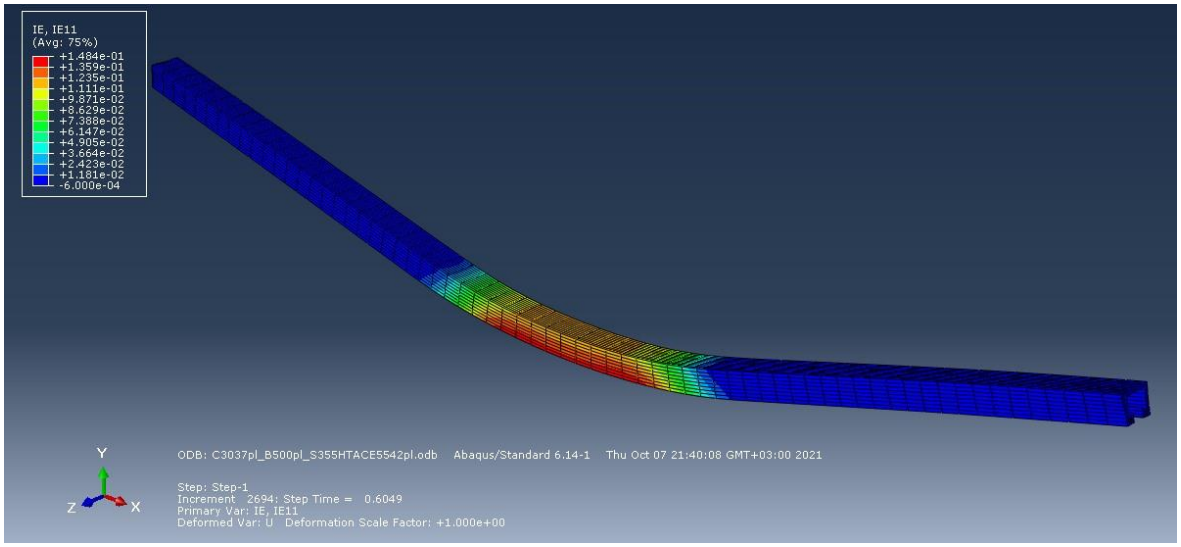

Shape 6.28: Inelastic strains on the cast – in channel when plastic strain reaches the maximum plastic strain of S355 – model 05

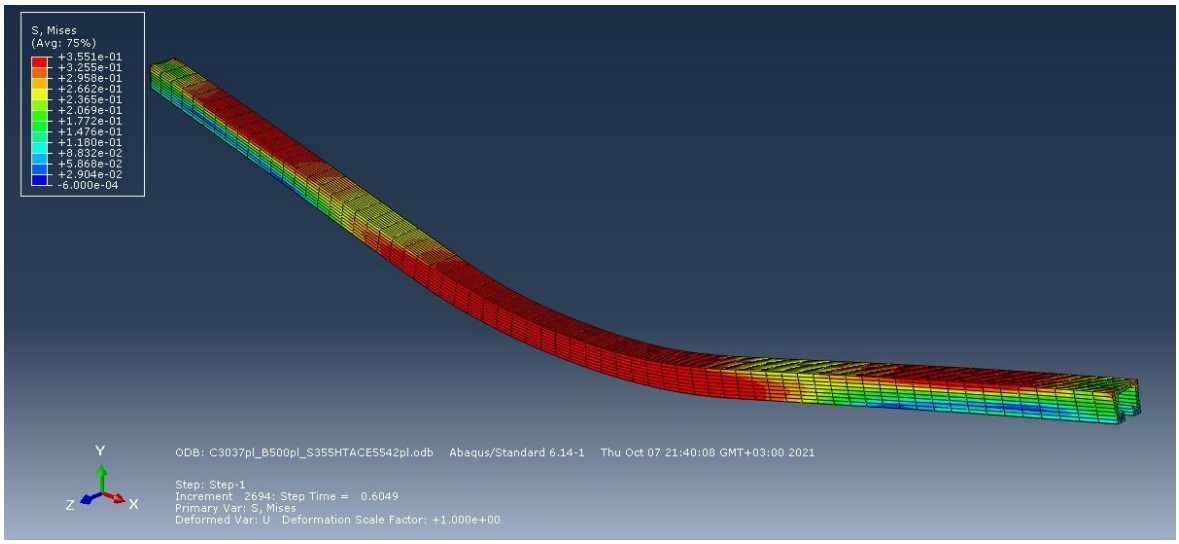

Shape 6.29: Von Mises stresses on the cast – in channel when plastic strain reaches the maximum plastic strain of S355 – model 05

6.3.2 Model 06 - Concrete part reinforced with As = 7.70 cm^2 and with HTA CE 72/48

On this model, the area of the cast – in channel is 10.68cm^2. The maximum assigned load is, p = 0.02 kN/mm^2. The cracking moment of the section is similar to this mentioned on the previous models at about 48 kNm. Shape 6.30 shows the cracked region at the step time when the vertical displacement is 4mm. On this shape, the compressive zone is approximately 10cm.

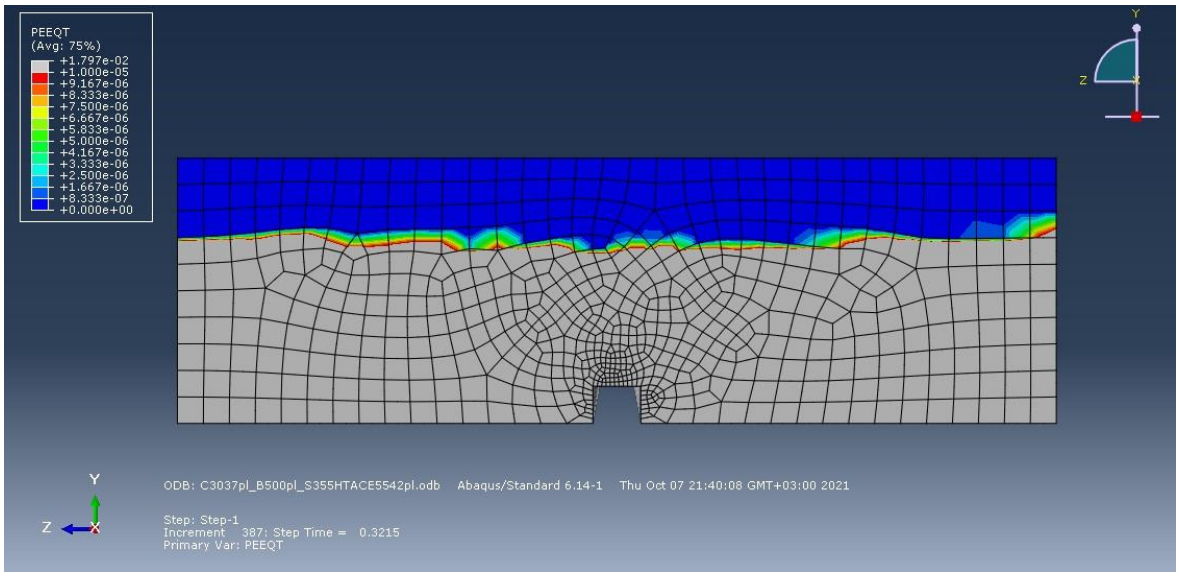

Shape 6.30: Bending moment – vertical displacement diagram for different cast – in channel profile sections

To evaluate the effects of the cast – in channel used on the behavior of the whole section, the results of models 04, 05 and 06 are compared. These results are also compared with them of model 01. Shape 6.31 shows the bending moment – vertical displacement diagram for the

different cast – in channel sections. We can observe that higher cast – in channel area leads to better behavior of the section. The initial stiffness is constant, as the concrete section is the main part that influences this parameter. However, it can be observed that stiffness is reduced on a lower rate when bigger steel sections are used and for the same bending moment, the vertical displacement is smaller for the section which contains a cast – in channel with higher steel section.

Shape 6.32 compares the evolution of the tensile stresses on the middle rebar of the model, comparing 4 different models with no or different cast – in channel section. It is clear that the higher steel section of the cast – in channel results to relief on the stresses of the steel reinforcement. More specific, it is observed that when the bending moment is 210kNm, the rebar on the model with the HTA 52/34 cast – in channel reaches the maximum tensile stress that can carry which is 500 MPa. On that time, the rebar on the model with the HTA 55/42 carries 275MPa while the model with the HTA 72/48 has just surpassed 200 MPa. Finally, from this shape, the fact is that the presence of a cast – in channel reliefs the tendance of the rebar of the section.

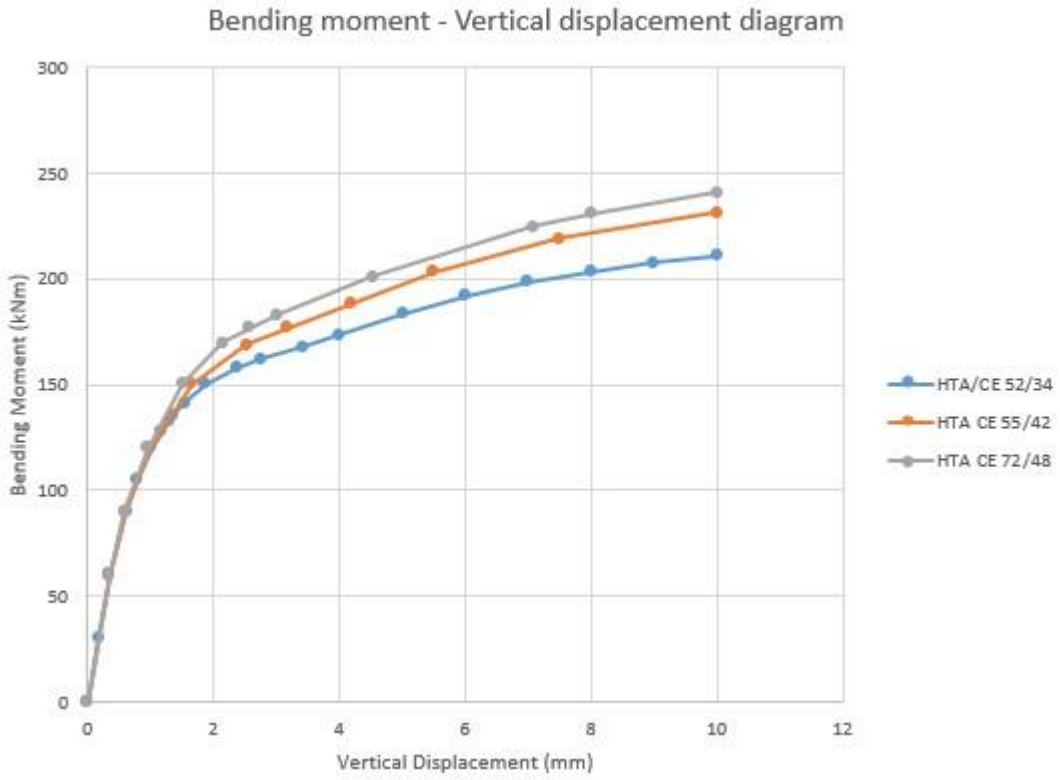

Shape 6.31: Bending moment – vertical displacement diagram for different cast – in channel profile sections

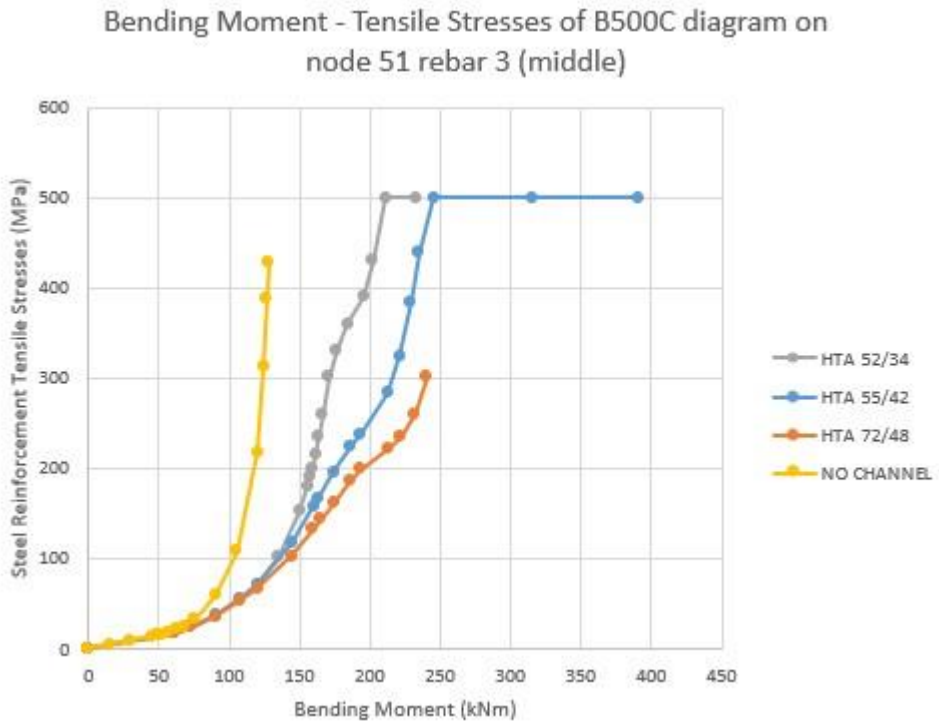

Shape 6.32: Bending moment – Tensile Stresses of B500C on the middle section on the middle rebar of the model

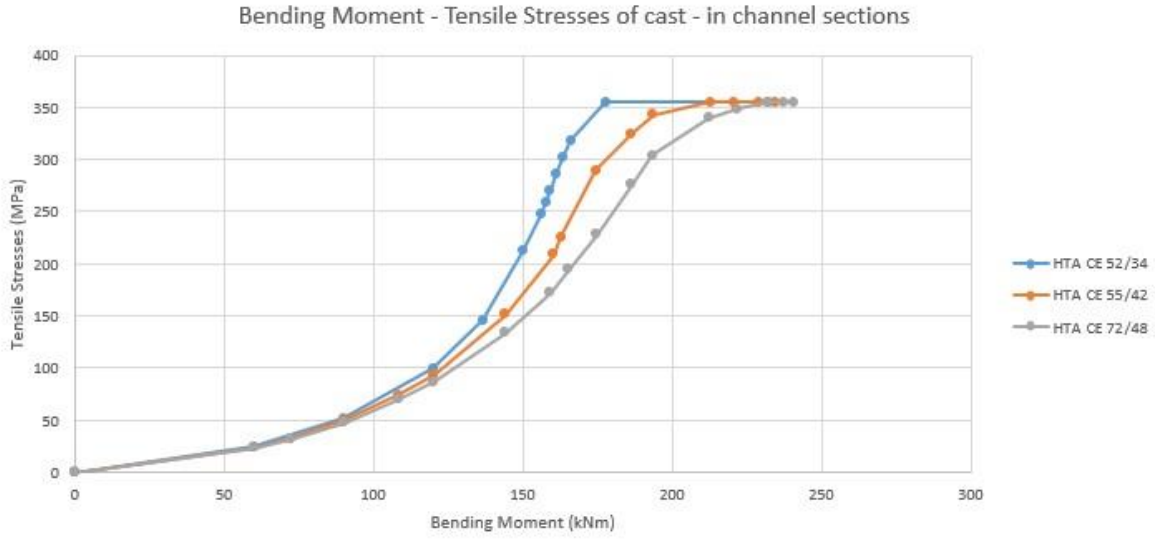

Shape 6.33: Bending moment – Tensile stresses of B500C on the middle section on the middle rebar of the model

Shape 6.33 shows a comparison of the tensile stresses of the cast – in channels as the bending moment rises. The larger the cast – in channel section is, the larger is the bending moment where the channel reaches its yield stress. The remark mentioned on 6.2.4 about the changes on the behavior of the tensile stresses of the rebar is still on when the other cast – in channel profiles are used.

6.4 Plastic analyses – Examination of the shear connection between concrete and the cast – in channel

On this paragraph, the following models are compared with model 04.

- Model 07 – Concrete part reinforced with HTA CE 52/34 and friction coefficient μ = 0.1
- Model 08 – Concrete part reinforced with HTA CE 52/34 and friction coefficient μ = 0.3
- Model 09 – Concrete part reinforced with HTA CE 52/34 and friction coefficient μ = 0.5

This parametrical analysis aims to evaluate the effects of the assigned tangential behavior on the interface between the concrete part and the cast – in channel. For this purpose, the HTA CE 52/34 cast – in channel is used. No concrete reinforcement is provided on any of these analyses.

Shape 6.34 is formed to understand the modelling of the tangential behavior and the tie constraint. On this shape, we can observe the horizontal differential displacement between the two parts used on the analyses. The model with the tie constraint does not allow any displacement between the parts. On the other hand, the models with the tie constraint allow these displacements. Specifically, we can observe that a higher friction coefficient leads to a better behavior on the interface, as higher bending moment is needed to reach the same differential horizontal displacement when a higher friction coefficient is used. On civil engineering, higher friction coefficient is obtained with higher amount of shear connectors. Their calculation is provided on the appropriate regulations for composite structures.

A more accurate calculation would be achieved if the connectors could be simulated on the analysis. However, this simulation would make the models heavier and computationally not affordable, so for the purposes of this thesis this simulation is estimated as not necessary.

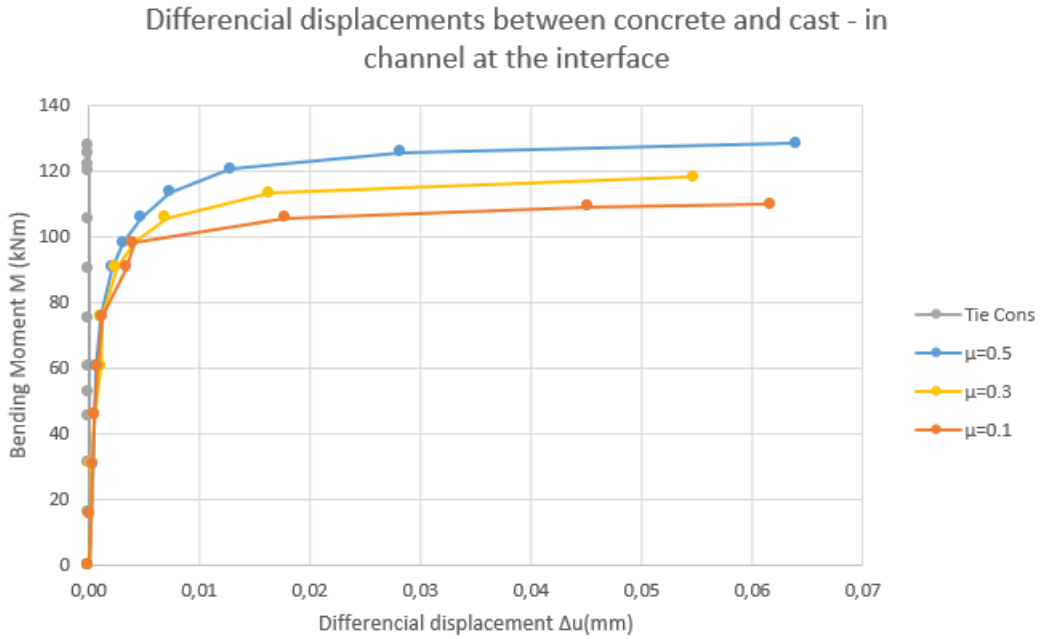

Shape 6.34: Differential displacements between concrete part and cast – in channel

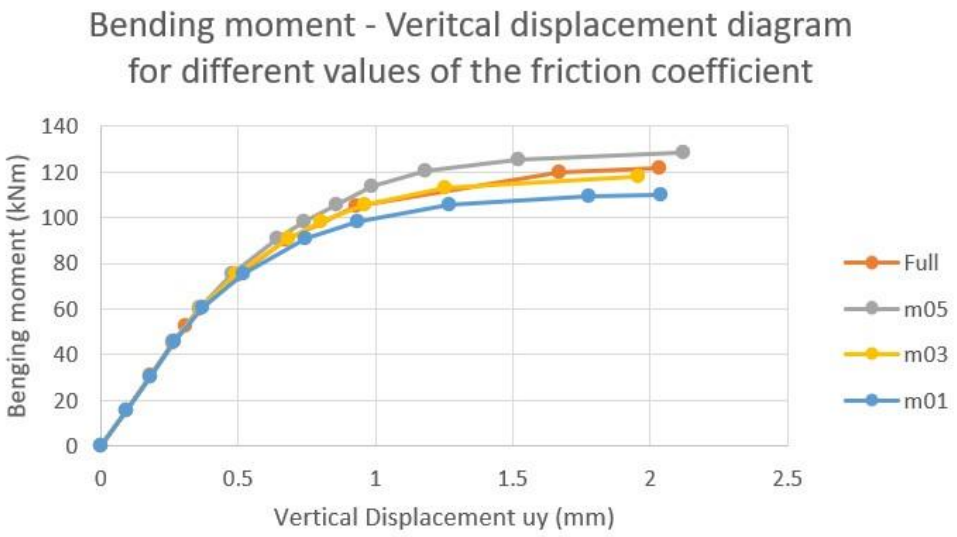

Shape 6.35: Bending moment – Vertical displacement for different values of μ

.

Shape 6.35 presents the bending behavior of the model when different values of friction coefficient is used on the interface of the cast – in channel and concrete. It is observed that when the friction coefficient raises, the bending behavior becomes better. Also, we can notice that the tie constraint is less effective than a friction coefficient of value 0.5. This behavior suggests that further investigation must be released about the way of simulation of the shear connection without modelling the shear bolts. However, we can state that the full tie constraint reaches a reliable first estimation of the behavior of the section.

6.5 Plastic analyses – Examination of effective axial force on the section

On this paragraph, the following models are compared with model 04. The assigned load of the models is p = 0.01kN/mm^2 which corresponds to a maximum bending moment of 300kNm.

- Model 10 – Concrete part reinforced with As = 7.97 cm^2 and with HTA CE 52/34 and axial force of N=1000 kN
- Model 11 – Concrete part reinforced with As = 7.97 cm^2 and with HTA CE 52/34 and axial force of N=2000 kN
- Model 12 – Concrete part reinforced with As = 7.97 cm^2 and with HTA CE 52/34 and axial force of N=3000 kN
- Model 13 – Concrete part reinforced with As = 7.97 cm^2 and with HTA CE 52/34 and axial force of N=4000 kN
- Model 14 - Concrete part reinforced with As = 7.97 cm^2 and with HTA CE 52/34 and axial force of N=5000 kN

This parametrical analysis is launched in order to observe the influence of a compressive axial force on the behavior of the section. Initial stresses are inserted on the concrete part simulating an effective axial force. This assignment is visible on shape 6.36 for effective axial force equal to 3000kN, where the compressive stresses on the whole concrete part are 10MPa. Shape 6.37 shows the bending moment – vertical displacement diagram of the section for compressive axial forces from 0 kN to 5000 kN.

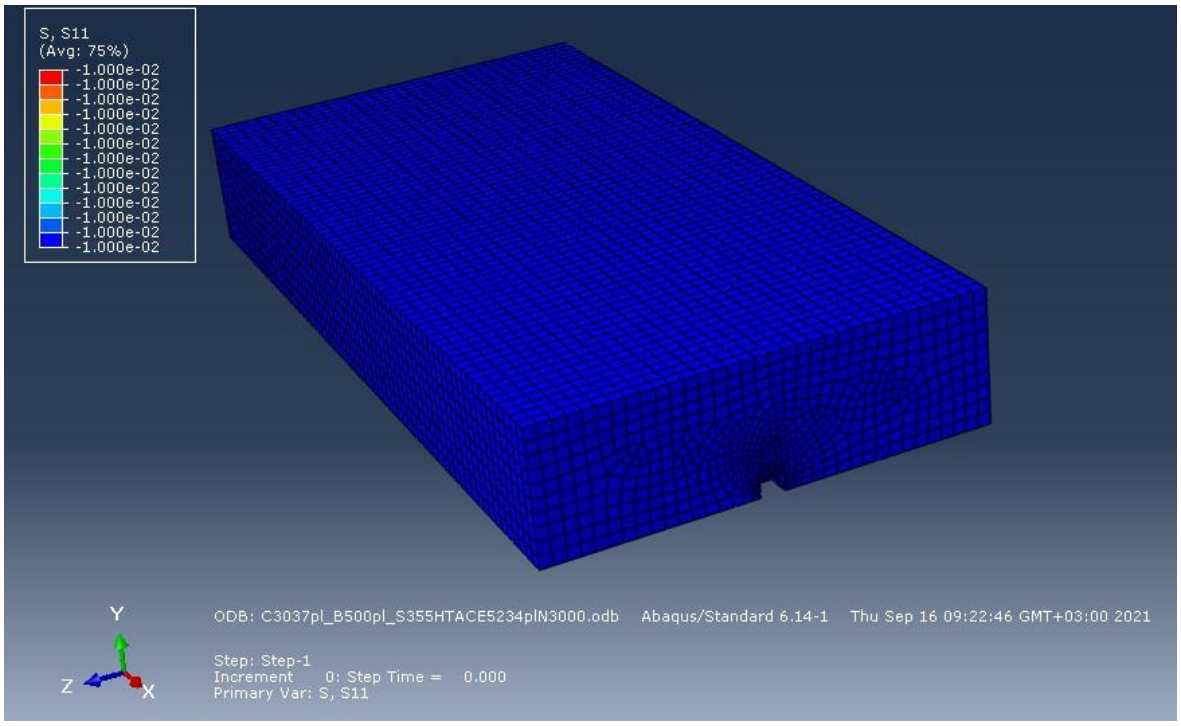

Shape 6.36: Normal stresses on the longitudinal axil at the starting step of the analysis with compressive axial force equal to 3000kN

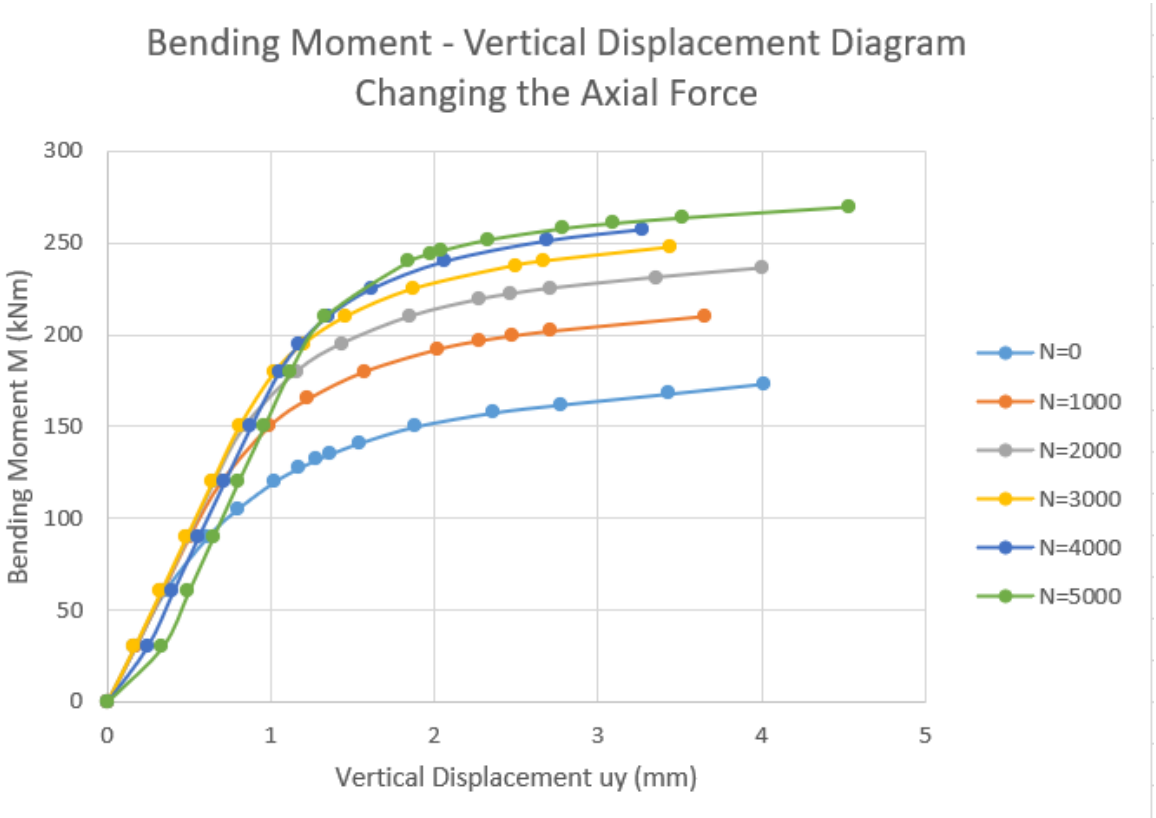

Shape 6.37: Bending moment – Vertical displacement diagram for different compressive axial forces

From this diagram we can observe that raising the compressive force of the section boosts the behavior of the section. The positive effects of the compressive axial force are more intense on lower compressive forces. A 25% rise of bending moment is needed to reach the

same vertical displacement, for the model of N=1000kN compared to the model with N=0kN. The same percentage for the moment with axial force equal to 5000kN is approximately 60%. Shape 6.38 shows the percentage of the boost of the bending behavior of the section depending on the assigned axial force. However, there is no difference on the starting stiffness of the model, as this parameter obeys to the behavior of the concrete part as mentioned before.

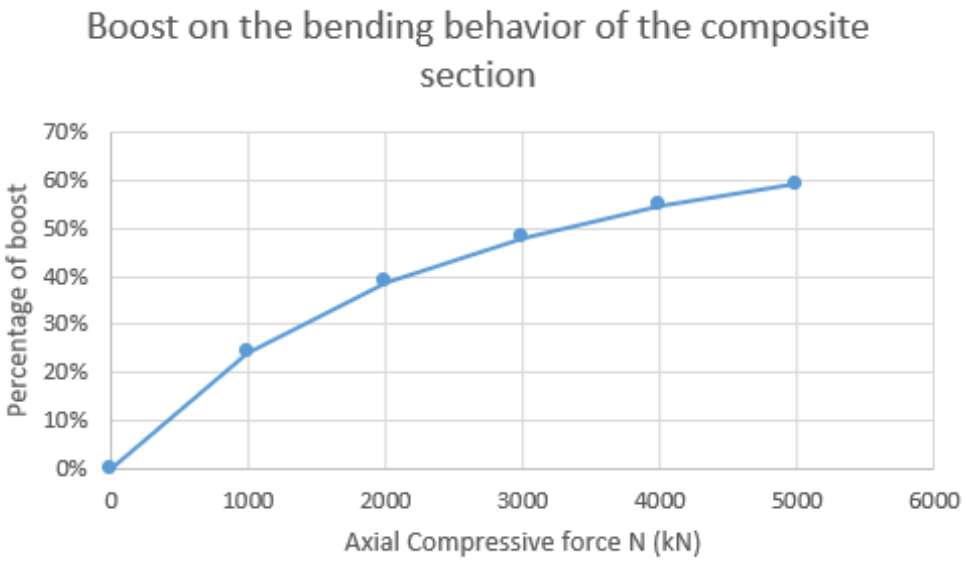

Shape 6.38: Boost on the bending behavior of the section

From these analyses, we can also observe a rise on the cracking bending moment of the section. Shape 6.39 shows the beginning of cracking on the model with effective compressive axial force equal to 3000 kN which happens at time step 0.5150. As a result, the cracking moment of the section is equal to 154.5 kNm. This fact agrees with shape 6.37 where a significant loss on the stiffness of the section occurs at that point. Table 6.1 shows the cracking moments of the models for different compressive axial forces.

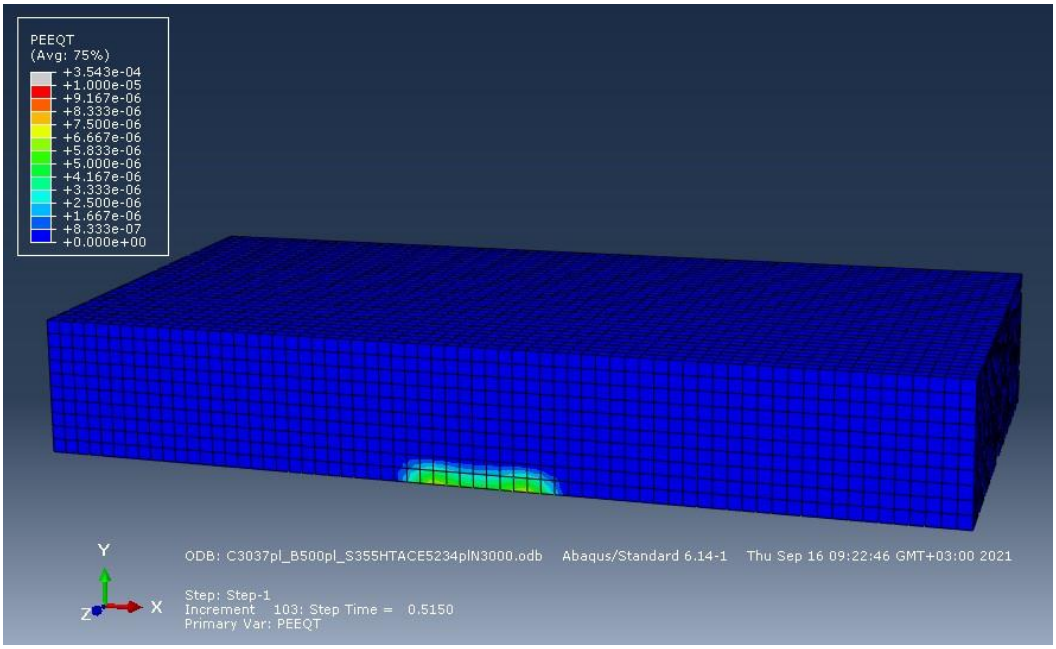

Shape 6.39: Cracking starts forming on the analysis with compressive axial force equal to 3000kN

Table 6.1: Cracking moment depending on the effective compressive axial force of the section

N_{ed} (kN)	M_{cr} (kNm)
0	48
1000	97.6
2000	132
3000	154.5
4000	169.5
5000	189

Finally, a chart is presented on shape 6.40 about the stresses that the steel reinforcement has to carry for model 12 where the effective compressive axial force is 3000 kN.. These stresses are compared with them of model 04 where the axial force is 0kN. It is observed that the carrying stresses of the steel reinforcement have reduced for the same bending moment at every stage of the analysis. The influence on the stresses of the cast – in channel is equivalent.

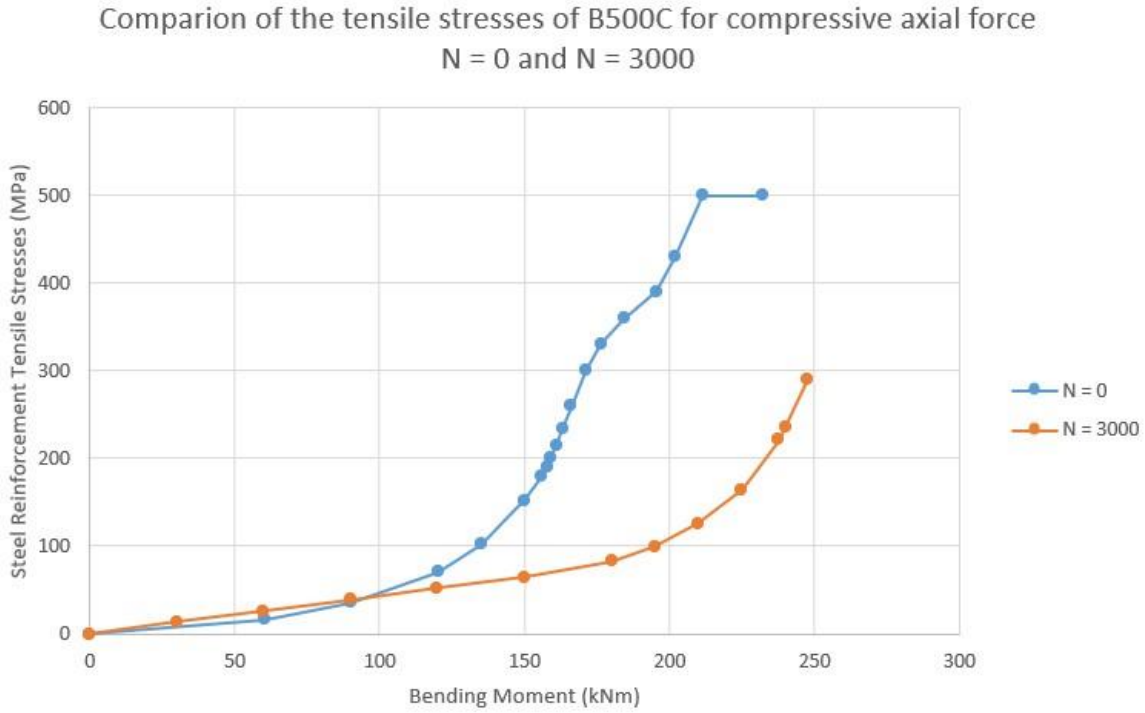

Shape 6.40: Comparison of the tensile stresses of B500C for compressive axial force equal to 0 kN and 3000kN

7 Conclusions

Cast – in channels have a widespread use. This thesis examined their influence on the bending behavior when they are used on concrete sections and form a composite section. On this chapter, the main results of the analyses are presented. Followingly, the results of the computational analyses are compared to these of the theoretical analyses. Finally, the main results and suggestions for further investigation are presented.

7.1 Overview of results

From the analyses presented the following results can be stated:

- Cast in channels increase the bending capacity of the section where they are set. If the distance between the parts is adequate, then they can increase the total bending capacity of the structural member.
- A value for the effective width of the cast – in channels needs to be evaluated. From the analyses a lower limit of 1m can be proposed. However, there are many details that need to be taken into account like the length of the beam, the spacing of the shear bolts, the section used and others.
- The raise of the bending capacity depends on the section used and on the boundary conditions on the interface between concrete and the cast – in channel. The bending capacity can increase up to 2 times, if appropriate section is used.
- Replacing a part of the steel reinforcement with cast – in channel section does not reduce the bending capacity of the section. In fact, a rise on the bending capacity is observed from shape 6.7.
- The existence of the cast - in channel reliefs the tensile stresses of the steel reinforcement. Ostensive, shape 6.21 shows that when the cast – in channel reaches its maximum capacity, the raise on the stresses of the steel reinforcement is faster than before and the diagram forms a step.
- The cast – in channel does not influence the initial stiffness of the section because this characteristic is governed from the concrete part. As cracking propagates, the stiffness of the section is reduced.
- Both the cast – in channel and the steel reinforcement are enforced to carry extra loads when cracking begins. As cracking propagates the carrying stresses are increased on a greater intense.
- Shear connection is important for the collaboration of the parts. The computational analysis of this needs further investigation.
- The presence of a compressive axial force is beneficial for the section as reliefs the tensile stresses of the steel parts and it offers pretension to the concrete part. This status can be encountered in some cases of structural engineering and a characteristic situation is the tunnel construction.
- The presence of a compressive axial force increases the cracking moment of the section.
- A composite section can fail either because of the bending capacity or because of the shear connection’s capacity or a combination of these mechanisms. The designer must take into account all the possible combinations when designing this type of section.

- When designing the cast – in channels, the designer needs to take into account the extra stresses that these channels carry because of the hanging loads of the structure.

7.2 Comparison between theoretical and computational analyses

The comparison between theoretical and computational analyses aims to investigate the application of the equations used on the regulations for the composite structures, when cast – in channels are used.
From the comparison of the two kinds of analysis we can claim that:

- The theoretical analysis is more conservative about the formed plastic zone and the bending capacity of the section.
- The theoretical analysis produces the same values of cracking moment with the computational analysis.
- The theoretical analysis is more trustworthy about the study of the shear connection at this point, as it is based on experiments and in the general experience. The computational analysis of the shear connection needs to be further investigated.
- The theoretical analysis suggests that when applying a compressive axial force on the section, the rise on the bending behavior of the section is higher in percentage and value than the computational analysis. The theoretical analysis states that the maximum bending capacity is achieved on a value, after which the bending capacity is reduced. This behavior is not met on the computational analysis.

The computational analysis can produce results with more details for the total behavior of the section as the load raises. These analyses are needed for research purposes or for projects with special needs. For accustomed problems, the theoretical analyses can give us reliable results. In general, these results are unfavorable, so with this strategy we have an extra safety factor.

7.3 Conclusions and further investigation

This study exported some interesting results. From the analyses, it is suggested that the cast – in channel can boost the bending behavior of the section and replace a part of the steel reinforcement used. For the conventional concrete used on civil engineering structures, the minimum reinforcement needed to avoid cracking needs to be used. The rest required steel section to reach the adequate bending capacity of the design could possibly be reached with the adjustment of cast – in channels in appropriate distances. In case of using fibber reinforced concrete, the steel reinforcement could be replaced totally. However, it is noted that further investigation should also take place about the percentage of the capacity of the cast – in channel that can be taken into account to improve the bending capacity of the section, as part of its capacity is used to carry the hanging loads of the structure. The same problem exists on the capacity of the shear bolts, as part of their resistance is used to face the operational loads for which these channels are set for.

However, more investigation could be executed in order to find more information about the collaboration of cast – in channels with concrete and their influence on the bending behavior of the composite section. A future study, could analyze the behavior of a section with different concrete heights and different concrete widths. In addition, the examination

of different values for the parameters of the concrete damaged plasticity model would be interesting. Furthermore, different simulation of the tensile behavior of the concrete section could be simulated. For this goal, either the yield stress – cracking strain model or the yield stress – displacement model could be used. Additionally, further modeling can be defined on the behavior of concrete under compression after the yield stress is achieved, where a downwards sector could be taken into account. The same simulation could be used for the tensile stresses of the steel parts. Moreover, further investigation should be carried on the behavior of the cast – in channels and the places where these parts are mainly stressed for different ways of loading. This analysis needs a more detailed model with further discretization on the cast – in channel part. Another aspect that should be tested is the modelling of the shear connection of the cast – in channel and the concrete by simulating the shear connectors. Moreover, the simulation of concrete can be with fibber reinforced concrete and not with a steel reinforced concrete. Also, the model should be examined under dynamic loads that occur in many structures where these channels are used. Finally, an experimental investigation should be executed to find out the behavior of these composite sections and to find out if the finite element analyses reach reliable results that can be applicable on the civil engineering field.

8 References

1. Βάγιας Ιωάννης, «Σύμμικτες κατασκευές από χάλυβα και οπλισμένο σκυρόδεμα», Εκδόσεις Κλειδάριθμος, 3η έκδοση
2. BSI British Standards Part 4-1, «Design of fastenings for use in concrete»
3. Casanova A., Jason L., Davenne L. (2012) "Bond slip model for the simulation of reinforced concrete structures", Engineering Structures Journal 39 (2012), 66-78
4. Cicekli U., Voyiajidis Z. G., Rashid K. Abu Al-Rub, "A plasticity and anisotropic damage model for plain concrete", International Journal of Plasticity 23 (2007) p. 1874-1900
5. Composite Structures, Lectures from the National Technical University of Athens
6. Dassault Systems, Abaqus CAE
7. Dassault Systems, Abaqus Guide
8. Eurocode 2 – Part 4 "Design of concrete structures – Design of fastenings for use in concrete"
9. FIB CEB FIP, bulletin 70, "Code type models for concrete behaviour", November 2013
10. Grassl P., Xenos D., Nyström U., Rempling R. and Gylltoft K. (2013), "CDPM2: A damage – plasticity approach to modelling the failure of concrete", arXiv: 13076998v1
11. Guowang M., Bo Gao, Zhou J.M Guodong C., Zhang Q. (2016) "Experimental investigation of the mechanical behavior of the steel fiber reinforced concrete tunnel segment", Construction and Building Materials 126 (2016) 98-107
12. HALFEN Guide
13. HALFEN HTA CE Channels
14. J. Shafaie, A. Hosseini, M. S. Marefat (2009), "3D finite element modelling of bond-slip between rebar and concrete in pull-out test", 3rd International Conference on Concrete & Development, p. 403-413
15. Konertz D., Mahrehonltz C. and Mark P. (2019), "Verification of a Load Distribution Model for Anchor Channels in the Experimental Lab, Proceedings: Concrete 2019 – Concrete in Practise – Progress through Knowledge, Sydney
16. Lubliner J., Oliver J., Oller S. and Onate E. (1989), "A plastic – damage model for concrete", Solids Structures Vo. 25, No 3, p. 229-326
17. Mahrenholtz C., Sharma A. (2019). «Qualification and design of anchor channels with channel bolts according to the new EN1992-4 and ACI 318», International Federation for Structural Concrete 2019
18. Matsuoka S., Masuda A., Takeda Y. and Doi S., "Analytical model for concrete structures influenced by crack initiation and propagation", Concrete librart of JSCE No. 35, June 2000
19. P. Kmiecik, M. Kaminski (2011), "Modelling of reinforced concrete structures and composite structures with concrete strength degradation taken into consideration", Archives of civil and mechanical engineering, Vol. XI, No. 3
20. R. Eligehausen, R. Mallée and J. F. Silva (2006). «Anchorage in Concrete Construction», Ernst & Sohn GmbH & Co. KG.
21. Spyridis P., "Analysis of lateral openings in tunnel linings", Master Thesis, University of Natural Resources and Applied Life Sciences, Vienna 2013
22. Spyridis P., Design of fastenings for use in concrete Eurocode 2 – part 4, Lectures from Technical University of Dortmund
23. Szczecina Michal and Winnicki Andrezej (2015), "Calibration of the CDP model parameters in Abaqus", The 2015 World Congress on Advances in Structural Engineering and Mechanics (ASEM15), Kore